PAVLOVIAN CONDITIONED ODOUR MEMORY IN THE *NRXN1*$^{+/-}$ MOUSE MODEL OF AUTISM SPECTRUM DISORDER AND MODULATION ON DOPAMINE CIRCUITRY

by

Jessica Frances Garden

Submitted in partial fulfilment of the requirements

for the degree of Master of Science

at

Dalhousie University

Halifax, Nova Scotia

August 2023

Dalhousie University is located in Mi'kma'ki, the ancestral and unceded territory of the Mi'kmaq. We are all Treaty people.

©Copyright by Jessica Frances Garden, 2023

TABLE OF CONTENTS

LIST OF TABLES

LIST OF FIGURES

ABSTRACT

Individuals with autism spectrum disorders (ASD) are impaired not only in social behaviors but also in higher-order sensory (such as olfaction) processes that influence cognitive abilities and behaviours. Neurexin-1 (*Nrxn1*) expression controls NEUREXIN-1 (NRXN1) levels, a presynaptic cell adhesion protein that binds postsynaptic ligands, and controls the balance of excitatory and inhibitory transmission, a commonly altered mechanism in autism. Here we asked the question of whether olfactory learning ability correlates with dopamine (DA) signalling in the olfactory system and memory strength in Nrxn1 deficient mice. Male and female *Nrxn1*$^{+/-}$ and WT (*Nrxn1*$^{+/+}$; C57BL/6J) mice at 90-130 days of age were conditioned to dig in an odour pot to receive a sugar reward over 8 trials in a 1-day Pavlovian conditioning protocol. Short- and long-term memory was tested, then DA transporter (DAT) and DA receptor 1 and 2 (DRD1, DRD2) gene expression was measured in the olfactory bulb, olfactory tubercle, and hippocampus of conditioned and unconditioned mice. The Pavlovian conditioned mice showed more digging in the odour pot than naïve mice during learning and memory trials, indicating digging behaviour reflects olfactory learning and memory. Olfactory bulb *DRD1* and hippocampus *DAT* and *DRD2* expression was lower in the 7-day than the 24-hour memory test, while olfactory tubercle *DAT* relative expression was higher in the 7-day than the 24-hour test, indicating region-specific gene expression was dependent on when the memory test was performed. Sugar consumption was positively correlated with *DRD2* expression in the olfactory bulb and olfactory tubercle but negatively correlated with *DRD2* expression in the hippocampus of conditioned mice. Overall, olfactory learning and memory was not impaired in the *Nrxn1*$^{+/-}$ mice in the 1-day Pavlovian conditioning odour paradigm. Interestingly, however, the region-specific changes in DA receptor expression appeared to be associated with DA activity in response to sugar consumption, odour presentation, and episodic olfactory memories, which needs further study.

LIST OF ABBREVIATIONS AND SYMBOLS USED

α: alpha

β: beta

Δ: delta

ρ: rho

%: percent

^{o}C: Degrees centigrade

AOB: accessory olfactory bulb

AON: anterior olfactory nucleus

ASD: Autism Spectrum Disorder

ATP: adenosine triphosphate

BTBR: Black and Tan BRachyury $T^{+}Itpr3^{tf}$/J

Ca^{2+}: calcium

CaMKII: calcium–calmodulin (CaM)-dependent protein kinase II

cAMP: cyclic adenosine monophosphate

Cas9: CRISPR-associated protein 9

cDNA: complementary DNA

cKO: conditional knock out

cm: centimeter

CNTNAP: contactin associated protein

CPu: caudate-putamen

Cq: quantification cycle

CRISPR: Clustered regularly interspaced short palindromic repeats

CS: conditioned stimulus

DA: dopamine

DAG: diacylglycerol

DAT: dopamine transporter

DNA: deoxyribonucleic acid

DRD1: dopamine receptor D1

DRD2: dopamine receptor D2

E: primer efficiency

g: grams

GOI: gene of interest

HET: heterozygous

HIPP: hippocampus

IP_3: inositol trisphosphate

IPC: interplate calibrator

LEC: lateral entorhinal cortex

LRRTMs: leucine-rich repeat transmembrane neuronal proteins

m: slope

mg: milligram

mL: millilitre

mm: millimeter

MOB: main olfactory bulb

NAc: nucleus accumbens

NLGN: neuroligin

nm: nanometer

NRT: no reverse transcriptase control

NRXN: neurexin

NTC: no template control

OB: olfactory bulb

OE: olfactory epithelium

OT: olfactory tubercle

p: probability

PCR: Polymerase Chain Reaction

PFC: prefrontal cortex

PIR: piriform cortex

PKA: protein kinase A

PKC: protein kinase C

R^2: coefficient of determination

REF: reference gene

RNA: ribonucleic acid

RT-qPCR: Reverse Transcription quantitative PCR

s: seconds

SE: Standard Error

SHANK: SH3 and multiple ankyrin repeat domains

SNc: substantia nigra pars compacta

SS: splice site

ssDNA: single-stranded DNA

Tsc1: TSC Complex Subunit 1

VTA: ventral tegmental area

WT: wildtype

µg: microgram

µL: microlitre

µM: micromolar

ACKNOWLEDGMENTS

I would like to extend my heartfelt appreciation and thanks to my supervisors, Dr. Ian Weaver and Dr. Richard Brown for their guidance, encouragement, and mentorship throughout my master's degree. I have greatly appreciated the opportunity to work with them both, and I have become a stronger researcher and better student as a result.

I would also like to thank the members of my examination committee, Dr. Tara Perrot, and Dr. Shelley Adamo. They have provided me with invaluable feedback throughout my master's degree and offered gracious support.

I would like to thank Kyle Roddick for his immense help and support over the last 2 years. Also, to the other members of the Brown lab, including Val Burdeyny, Oliver Schnare, Ana Faustova, and Paige Croney for their help and company on long testing days.

I am so grateful to have been surrounded by many wonderful and encouraging graduate students, including Libby, Nicole, Brodie, Elizabeth, Alex, and Sam.

I also want to thank the animal care team, especially Andrea, for all of their hard work in taking care of the animals in the facility.

Additionally, I was supported by a Nova Scotia Graduate Student Master's scholarship and a Dalhousie Faculty of Medicine Graduate Studentship for Medical Neuroscience Research. The research I completed was funded by NSERC discovery grants to R.E. Brown and I.C.G. Weaver.

And finally, I would like to thank my husband Bailey for his unwavering support in everything that I do. And our dog Goose, who has provided many laughs and needed study breaks throughout this journey.

CHAPTER 1: INTRODUCTION

1.1 Autism Spectrum Disorder

Autism Spectrum Disorder (ASD) is one of the most common neurodevelopmental disorders, affecting approximately 1% of children world-wide (Baird et al., 2006). This life-long disorder predominately affects males, with a reported male: female ratio ranging from 1.33:1 to 15.7:1 (Autism and Developmental Disabilities Monitoring Network Surveillance Year 2008 Principal Investigators & Centers for Disease Control and Prevention, 2012; Fombonne, 2009), and is commonly co-morbid with intellectual disability and/or major psychosis, including schizophrenia (Chien et al., 2021; Matson & Shoemaker, 2009; Mpaka et al., 2016). The *Diagnostic and Statistical Manual of Mental Disorders, 5th Edition, Text-Revised Edition* (*DSM-5-TR*) defines ASD as including several areas of persistent deficits in social communication and interaction as well as restricted repetitive behaviours and interests (APA, 2022). Individuals with ASD also show impaired higher-order sensory (such as olfaction) and cognitive processes, in which sensory processing dysfunctions influence some cognitive abilities and behaviors (Dawson et al., 2002; Ebrahimi-Fakhari & Sahin, 2015; Luo et al., 2018). Clinical presentation and underlying pathophysiology of ASD is highly heterogeneous, posing a complex challenge for diagnosis and therapeutic treatments (Jeste & Geschwind, 2014).

ASD has a strong genetic component, with heritability estimates ranging from 50% – 90% (Nordenbæk et al., 2014; Sandin et al., 2014; Sandin et al., 2017). In some rare cases, spontaneous (i.e., de novo mutations) mutations have also been identified that were not inherited from the parents (Miles, 2011). However, a majority (70%) of ASD cases are idiopathic

with an unknown genetic cause (Devlin & Scherer, 2012), leading to the suggestion that gene x environment interactions may play a role in the etiology of ASD (Cheroni et al., 2020). Nonetheless, whole exome sequencing has shown that ~5% of cases are caused by single gene mutations (De Rubeis et al., 2014) and ~10% of cases are caused by copy number variations (CNV) that disrupt normal gene expression and function in ASD (Abrahams & Geschwind, 2008; Rosenfeld et al., 2010).

An imbalance between excitatory and inhibitory synaptic transmission is a hallmark of ASD (Gao & Penzes, 2015) and genetic analyses strongly implicate three biological pathways: chromatin remodeling, transcriptional regulation, and synaptic function (De Rubeis et al., 2014; Devlin & Scherer, 2012). Indeed, many of the ASD risk genes identified so far encode for pre- and post-synaptic cell adhesion proteins including SHANK (Durand et al., 2007), CNTNAP (Alarcón et al., 2008; Bakkaloglu et al., 2008), neuroligin (NLGN) (Jamain et al., 2003), and NRXN (Kim et al., 2008), which form transsynaptic complexes critical for maintaining the balance between excitatory and inhibitory transmission (E/I balance) between neurons. Recent studies on the neural basis of ASD have focused on the association between altered dopamine (DA) neuron connectivity and olfactory dysfunction as an early indicator of cognitive impairment (Mandic-Maravic et al., 2022).

A variety of mouse models of ASD have been used to help characterize the observable characteristics (phenotypes) associated with candidate ASD risk genes, including learning and memory impairments (Southwick et al., 2011). For example, mice with mutations in *Shank3*, *Cntnap2*, and *Tsc1* show deficits in visual spatial mapping and fear conditioning paradigms (Moy et al., 2007), while Black and Tan Brachyury $T^{+}Itpr3^{tf}/J$ (BTBR) mice show deficits in reversal

learning (Moy et al., 2007). Furthermore, mice carrying *Nrxn1* gene disruptions show electrophysiological and behavioral changes consistent with cognitive impairments (Etherton et al., 2009) and demonstrate an essential role for NRXNs in DA neuron synaptic transmission and autism-related phenotypes (Ducrot et al., 2021).

Together, these findings raise the question of whether olfactory learning ability correlates with DA signalling in the olfactory system and odour memory strength in a mouse model of ASD. In the present study we used a Pavlovian conditioned odour task in which male and female *Nrxn1* knockdown mice received a single day of odourous conditioned stimuli presentations and were then tested for memory 24 hours and 7 days later and analyzed for DA receptor expression in the olfactory system.

1.2 Olfactory System

The olfactory system is responsible for the important functions of odour discrimination, odour detection, and olfactory memory. Olfaction is essential in humans for exploratory behaviors, appetite regulation, and social interactions (Fine & Riera, 2019; Sarafoleanu et al., 2009), while rodents rely heavily on their sense of smell for avoiding predators, locating food, finding mates, and establishing social hierarchies (Takahashi, 2014; Wesson, 2013). Olfaction is the primary sensory system for rodents, enabling them to learn olfactory-stimulus reward associations better than associations with auditory or visual stimuli (Nigrosh et al., 1975). This makes olfactory stimuli a meaningful sensory modality to employ when investigating cognitive functions in rodents, such as short- and long-term odour memory.

Odours are detected by odourant receptors on olfactory sensory neurons of the olfactory epithelium (OE). Each olfactory sensory neuron in the OE expresses a single olfactory receptor out of the approximately 1000 possible odourant receptor genes in the mouse genome (Buck & Axel, 1991), and projects directly to a single glomerulus in the olfactory bulb expressing the same olfactory receptor (Mombaerts, 2006; Treloar et al., 2002). Glomeruli are present on the surface of the olfactory bulb and are innervated by inhibitory interneurons as well as excitatory projection neurons: mitral and tufted cells, located in the mitral cell layer and the external plexiform layer, respectively (Figure 1B). Mitral and tufted cells synapse with granule cells located in the granule cell layer, where projections to higher-order areas of the brain including the piriform cortex and the olfactory tubercle (OT) can occur (Shipley & Ennis, 1996). The olfactory cortex, where complex olfactory signals are processed, is composed of brain regions that receive synaptic inputs from OB projection neurons including the piriform cortex, olfactory tubercle, cortical amygdala, anterior olfactory nucleus, and the entorhinal cortex (Figure 1A) (Neville & Haberly, 2004).

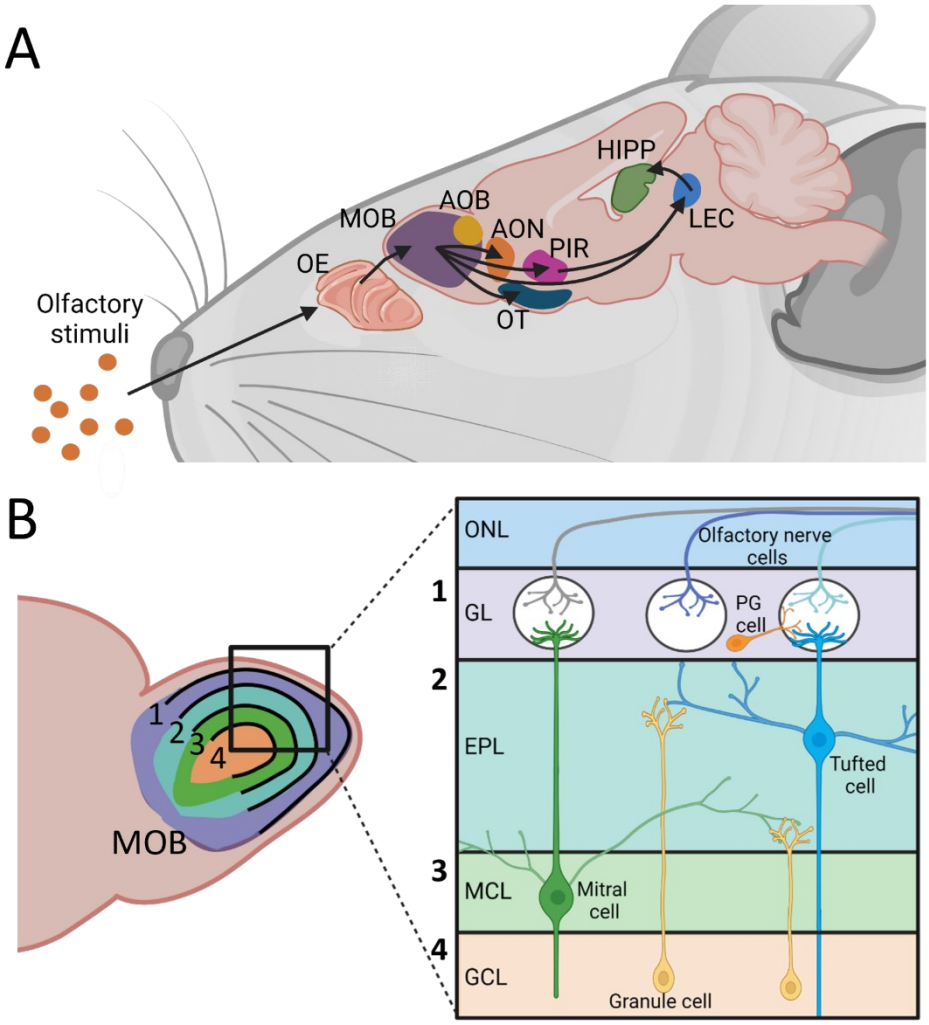

Figure 1. Mouse olfactory system. **(A)** Schematic of basic mouse olfactory circuits. Olfactory sensory neurons present in the olfactory epithelium (OE) project to main olfactory bulb (MOB) which then sends projections to the anterior olfactory nucleus (AON), olfactory tubercle (OT), piriform cortex (PIR), and the lateral entorhinal cortex (LEC). The PIR also projects to the LEC, and the LEC projects to the hippocampus (HIPP). **(B)** Main olfactory bulb basic neural circuit. Olfactory nerve cells run in the olfactory nerve layer (ONL) before projecting to the glomeruli in the glomerular layer (GL). The somata of tufted cells are located in the external plexiform layer (EPL) with primary dendrites extending to a single glomerulus. The somata of mitral cells are present in the mitral cell layer (MCL) with primary dendrites projecting to a single glomerulus. Olfactory sensory neurons form axodendritic synapses with mitral, tufted, and periglomerular (PG) cells. Mitral and tufted secondary dendrites form dendrodendritic synapses with granule cells in the EPL. Somata of granule cells are found in the granule cell layer (GCL). Adapted from Imamura et al., 2020. Created with BioRender.com

The olfactory bulb plays a central role in processing olfactory information. The OB has a large population of DA neurons (Cave & Baker, 2009), which are crucial for refining odour resolution, decreasing odour noise, and increasing odour discrimination (Ennis et al., 2001; Wilson & Sullivan, 1995). D2 neurons are the most abundant DA receptor type found in the OB and are localized in the granular and glomerular layers (Coronas et al., 1997; Koster et al., 1999).

The importance of the olfactory tubercle in odour-induced motivation-based behaviors has recently been identified (DiBenedictis et al., 2015; Murofushi et al., 2018; Yamaguchi, 2017). The OT is a part of the ventral striatum and the nucleus accumbens, two regions which both receive significant dopaminergic input from the ventral tegmental area (Ikemoto, 2007). The OT is also a component of the olfactory cortex, and thus receives inputs from the olfactory bulb as well as from other parts of the olfactory cortex (Zhang et al., 2017) as D1 and D2 neurons in the medial region of the OT are preferentially innervated by olfactory areas (Zhang et al., 2017). The OT is made up of three main neuron types: medium spiny neurons, dwarf cells, and granule cells. Spiny neurons in the OT express either DA receptor D1 or D2 (Yung et al., 1995), while dwarf cells express D1 and not D2, and granule cells weakly express D1 (Murata et al., 2015). There are distinct regions of the OT that respond differently to conditioned odour cues. Odour cues associated with a sugar reinforcement induce *c-Fos* expression in D1 neurons of the cortex-like region of the anteromedial domain of the OT, while odour cues associated with aversive stimulus induce *c-Fos* expression in D2 neurons of anteromedial and lateral OT domains (Murata et al., 2015) (Figure 2). D1-type neurons in the olfactory tubercle have also been found to represent odour valence (i.e., how attractive or aversive an odour is to an animal) while D2-type

neurons have been found to be selective for odour identity rather than valence (Martiros et al., 2022).

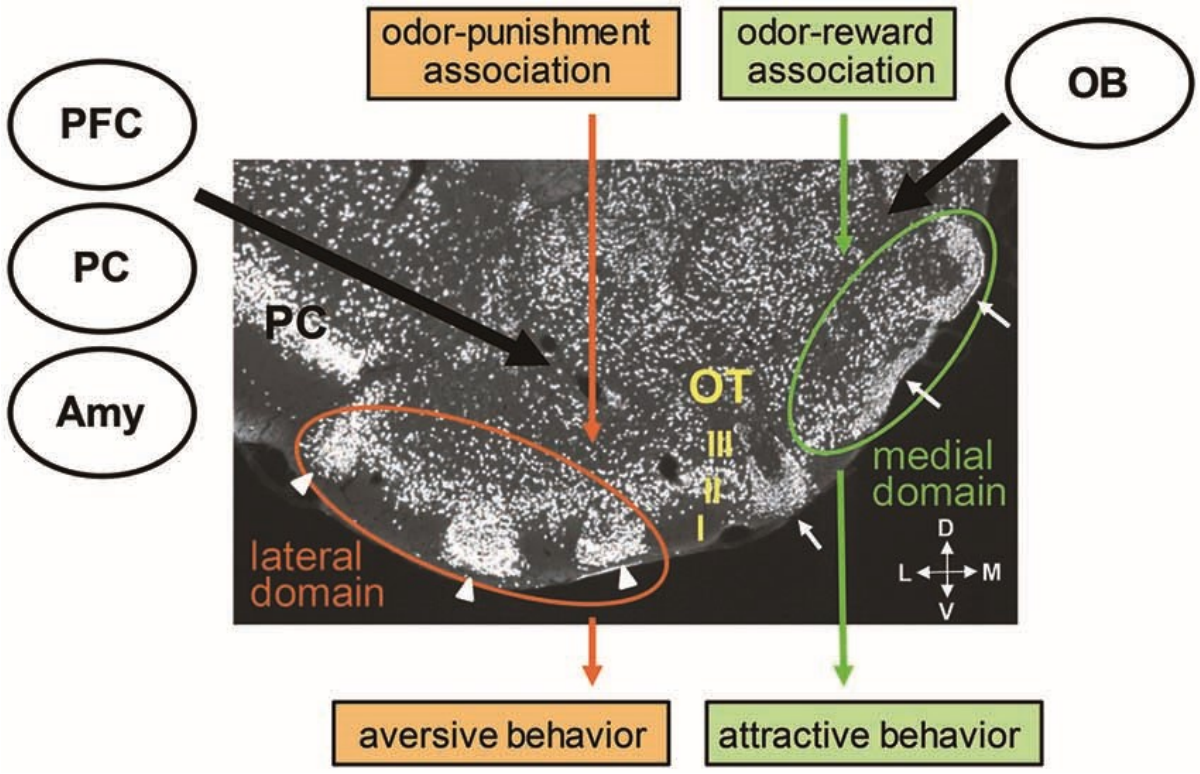

Figure 2. Olfactory tubercle architecture outlining distinct domains that represent distinct odour motivated behaviors. Coronal section of OT. From Yamaguchi, 2017.

While olfaction as a sensory modality is primarily shaped by bottom-up input originating from the olfactory bulb, top-down modulation also occurs through strong connections from higher cortical and limbic structures, such as the hippocampus (HIPP) (Aqrabawi et al., 2016; Martin et al., 2007). Unlike other sensory modalities, the olfactory system in mammals does not pass through the thalamus in order to reach cortical areas (Mouly & Sullivan, 2010). Instead, neurons from the olfactory bulb project directly to cortical structures, such as the amygdala and hippocampus, which are important in emotion and memory. More precisely, the olfactory bulb

and piriform cortex directly project to the lateral entorhinal cortex through the lateral olfactory tract, where the lateral entorhinal cortex then projects to the hippocampus (Figure 1A).

Generally, long-term memory consolidation is thought to rely on bidirectional interactions between sensory and limbic regions. In fact, only two synapses separate the olfactory bulb from the dentate gyrus of the hippocampus (Vanderwolf, 1992) through the lateral perforant path and the lateral entorhinal cortex. The hippocampus has been shown to support odour-discrimination learning, with involvement and cooperation between both the dorsal and ventral hippocampus during olfactory learning (Martin et al., 2007). Thus, investigating various regions of the olfactory system, including initial sensory processing areas such as the olfactory bulb and olfactory tubercle, while also considering a higher-level cortical area involved in olfactory memory, like the hippocampus, will provide a wide picture of how DA modulation differs at various brain regions throughout the olfactory pathway.

Olfactory dysfunction is associated with disorders like schizophrenia (Moberg & Turetsky, 2003), bipolar disorder (Hardy et al., 2012), Alzheimer's disease, and Parkinson's (Rahayel et al., 2012). Interestingly, evidence also suggests that individuals with ASD may display impaired sensitivity to olfactory stimuli and impaired odour detection (Kumazaki et al., 2016; Xu et al., 2020). Atypical responsiveness to olfactory stimuli and odor detection deficits have been identified as a strong predictor of social impairment in children with ASD (Kumazaki et al., 2016), which makes investigating the olfactory function in mouse models of ASD an important avenue to define.

1.3 Dopamine Pathways

The DA system is critical in central nervous system functions including motor control, sleep, reward, and cognition (Klein et al., 2019). DA plays a crucial role in the reinforcement and motivation of behavior and for establishing memories of cue-reward associations, such as during Pavlovian conditioning (Dalley et al., 2005). Recent studies have implicated reward-processing deficits and altered DA mesolimbic circuitry in ASD patients (Dichter et al., 2012; Mandic-Maravic et al., 2022). DA is important in motor function, reward, and motivation, which are all affected in ASD; however, the neuropathology and etiology of such deficits remains unknown.

Five DA receptors have been identified, each belonging to the G protein-coupled receptor family, which can be further classified into subgroups: the D1-like receptors (D1 and D5) and the D2-like receptors (D2-D4). Dopaminergic neurons primarily originate from midbrain structures including the substantia nigra pars compacta (SNc) and the ventral tegmental area (VTA) (Luo & Huang, 2016). The nigrostriatal pathway is composed of DA neurons projecting from the SNc to the dorsal striatum (Figure 3) and is involved in regulating voluntary movement (Moore & Bloom, 1978; Ungerstedt, 1971). The mesocorticolimbic pathway is composed of DA neurons projecting from the VTA to the nucleus accumbens, limbic systems, the olfactory tubercle, and the frontal cortex (Figure 3) (Moore & Bloom, 1978; Ungerstedt, 1971) and is involved in the regulation of reward, motivation, and memory, which can all be affected in autism (Bromberg-Martin et al., 2010).

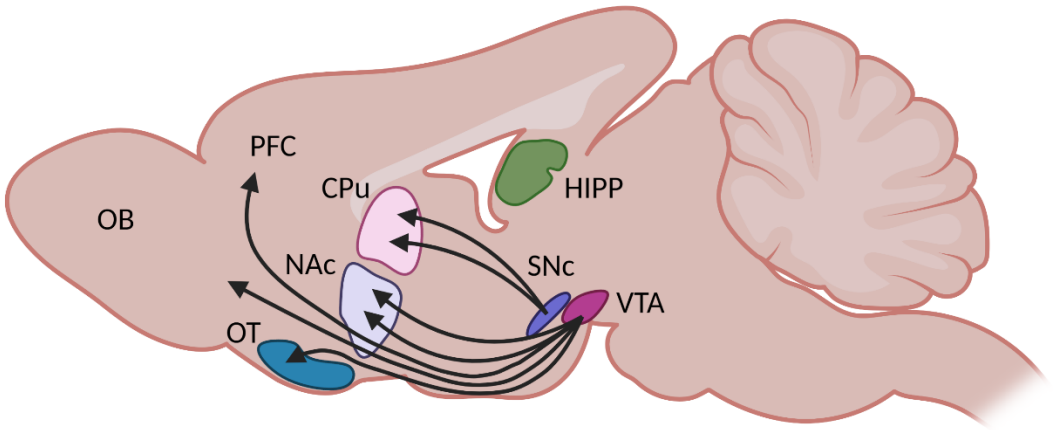

Figure 3. Simple diagram of mesocorticolimbic and nigrostriatal DA pathways. Midbrain DA neuron clusters in the substantia nigra pars compacta (SNc) project to the caudate/putamen (CPu). DA neuron clusters in ventral tegmental area (VTA) project to the nucleus accumbens (NAc), the olfactory tubercle (OT), and the prefrontal cortex (PFC). Adapted from Luo & Huang, 2016. Created with BioRender.com

The DA transporter (DAT) is a plasma membrane protein that is selectively expressed in dopaminergic neurons and regulates DA neurotransmission by transporting extracellular DA back into the intracellular space (Bu et al., 2021). It is well known that DA signaling is not limited to a single synaptic location, as DA receptors are predominantly extrasynaptic (Hersch et al., 1995; Sesack et al., 1994; Yung et al., 1995). Thus, DA spills over from its initial release site into the extrasynaptic space, acting on receptors to modulate movement, learning, and motivation (Bu et al., 2021). Synaptic DA is tightly regulated by DAT, allowing for the fine-tuned phasic DA signaling needed for salience coding (Fiorillo et al., 2013) and reward prediction error signal coding (Bayer & Glimcher, 2005); both of which are required for reward processing, behavioral learning, and synaptic plasticity (Pessiglione et al., 2006; Schultz, 2016). In fact, deletion of the *DAT* gene results in high striatal concentrations of extracellular DA, decreased DA tissue levels

(Jones et al., 1998; Leo et al., 2018), and reduced levels of D1 and D2 receptors (Giros et al., 1996). *DAT* KO mice also demonstrate impaired working memory (Savchenko et al., 2022), cognitive deficits in sensorimotor tasks (Leo et al., 2018), and deficits in olfactory discrimination (Tillerson et al., 2006).

The DA receptor D1 (DRD1) is the most abundant DA receptor in the rodent and human brain, with broad expression throughout brain regions including the dorsal striatum, ventral striatum, olfactory bulb, cortex, thalamus, amygdala, hippocampus, hypothalamus, and the substantia nigra (Hall et al., 1994; Mansour et al., 1990; Mishra et al., 2018). D1 receptors function in processes including memory, attention, locomotion and impulse control while the DA receptor D2 (DRD2) is important for locomotion, sleep, memory, and learning (Mishra et al., 2018). DRD2 is localized in the striatum, VTA, olfactory bulb, and the cerebral cortex (Mishra et al., 2018). D1 and D2 receptors have opposing functions. D1-like receptors activate adenylyl cyclase by coupling to $G\alpha_s$ subunits of G proteins which increases cAMP production and increases phosphorylation activity by protein kinase A (PKA) as a result (Figure 4). D2-like receptors have an opposite function, where they inhibit the adenylyl cyclase-cAMP-PKA pathway by coupling to $G\alpha_i$ subunits, thus reducing PKA activity (Figure 4) (Missale et al., 1998). D1-like and D2-like receptors are also capable of forming heteromeric complexes. D1-D2 heterodimers couple with $G\alpha_q$ subunits to activated phospholipase C (PLC) (Figure 4). PLC activation results in production of diacylglylcerol (DAG) and inositol triphosphate (IP_3). DAG then activates protein kinase C (PKC), while IP_3 activation causes intracellular Ca^{2+} mobilization (Osinga et al., 2017). DA modulation plays an important role in controlling odour detection thresholds, discrimination, and odour learning. D1 and D2 receptors have opposing influences

on odour discrimination learning. For example, administration of the D2 receptor agonist quinpirole causes decreases in odour detection performance in rats, while administration of the D1 receptor agonist SKF 28393 results in enhanced odour detection in rats (Doty & Risser, 1989; Escanilla et al., 2009).

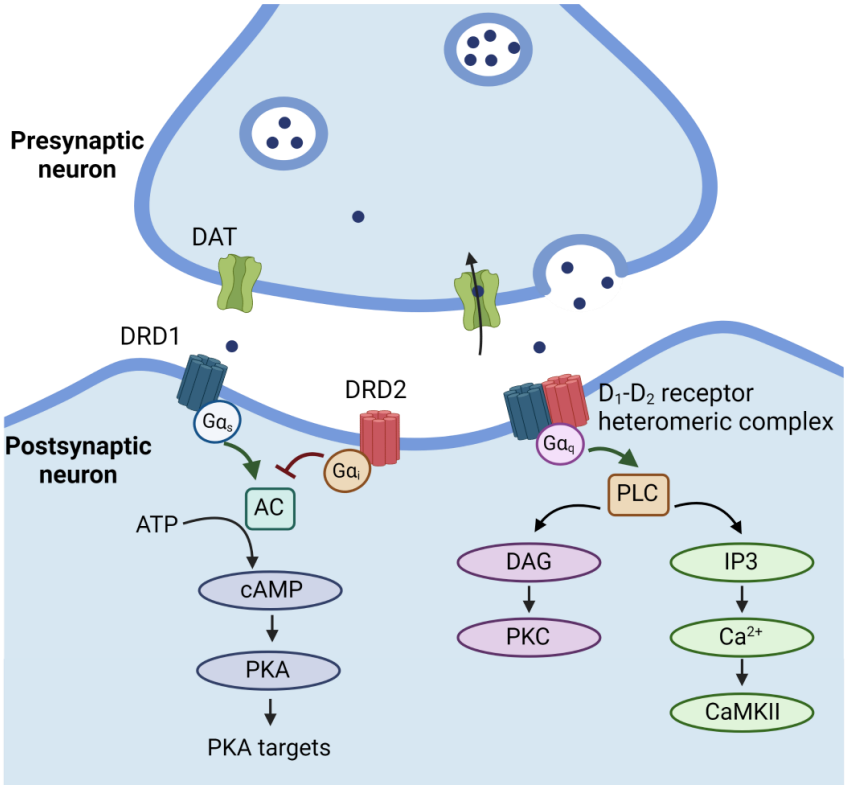

Figure 4. Signalling networks regulated by DA through D1-like receptors, D2-like receptors, and D1-D2 heteromeric complexes. Adapted from Osinga et al., 2017. Created with Biorender.com

A recent study has identified that *Nrxn* plays a role in DA neuron connectivity. While *Nrxn* deletion did not impair development or structure of DA neuron terminals, it did impair DA transmission via reduced DA reuptake, and decreased DA transporter levels (Ducrot et al., 2021). Interestingly, *Nrxn* deletion resulted in increased GABA release from DA neurons. This exciting finding is the first direct evidence to support the role of *Nrxns* as regulators of DA

circuitry and DA-mediated functions. The role of dopaminergic dysfunction in ASD, and specifically related to *Nrxn* has not been deeply investigated. Similarly, the BTBR mouse model of ASD shows reduced D2-mediated neurotransmission (Squillace et al., 2014), but much more work is to be done on understanding dopaminergic dysfunction in various mouse models of ASD.

1.4 Neurexin

Effective neurotransmission requires alignment between presynaptic and postsynaptic cells, which is regulated by synaptic cell-adhesion molecules, such as NRXNs. NRXNs were originally discovered as receptors for α-latroxin; a toxin originating from the venom of black widow spiders, that binds presynaptic nerve terminals, resulting in neurotransmitter release (Ushkaryov et al., 1992). NRXNs along with their postsynaptic binding partners are among the most well-studied synaptic organization proteins. Through complex alternative splicing (Schreiner et al, 2014; Südhof, 2017) and interactions with diverse trans-synaptic binding partners, including neuroligins, leucine-rich repeat transmembrane neuronal proteins (LRRTMs), and dystroglycans (Siddiqui et al., 2010: Sugita et al., 2001), NRXNs are important contributors to synaptic organization.

There are three *Nrxn* genes (*Nrxn1*, *Nrxn2*, *Nrxn3*) that are each highly conserved between species. Each *Nrxn* gene has three independent promotors, resulting in three protein isoforms: a larger NRXN-α protein, a NRXN-β protein (Ushkaryov et al., 1992), and a recently identified smaller NRXN-γ protein (Sterky et al., 2017). The NRXN-α isoform results in a protein containing an N-terminal signal peptide, six laminin/neurexin/sex-hormone binding globulin (LNS) domains,

followed by three epidermal growth factor (EGF)-like repeats, a carbohydrate-binding region, a transmembrane domain, and a short cytoplasmic section with a PDZ binding domain (Figure 5). The promoter for the NRXN-β isoform produces a protein containing the same sequence as the NRXN-α isoform, starting at the sixth LNS domain, and without the EGF-like repeats interspersed throughout (Figure 5). The *NRXN-γ* isoform consists of only the carbohydrate binding region, the transmembrane domain, and a C-terminal PDZ binding domain (Figure 5). Given the distinct structure of the NRXN isoforms, they each bind to neuroligins and LRRTMs with differential affinities and can have distinct functions (Boucard et al., 2005; Siddiqui et al., 2010).

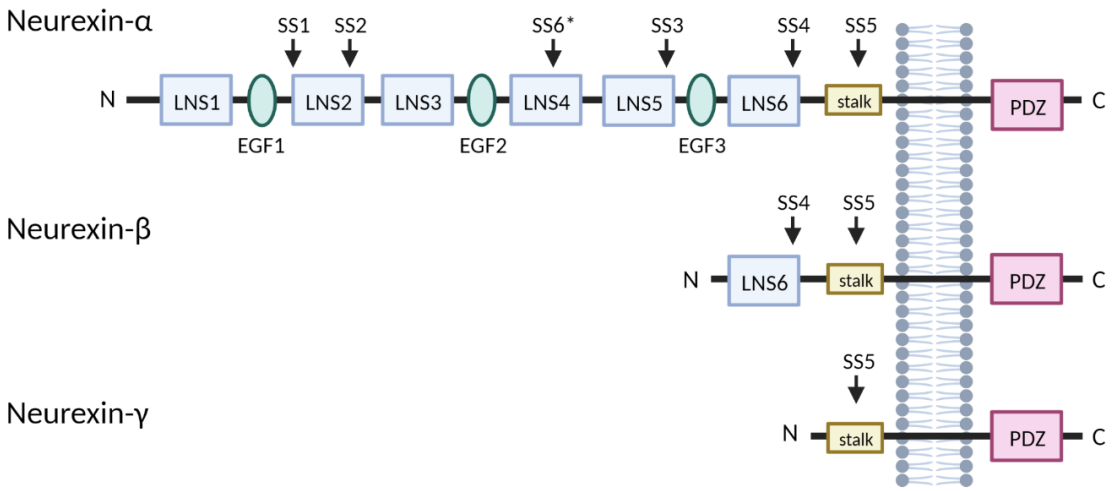

Figure 5. NRXN-α, NRXN-β, and NRXN-γ domain organization. The organization of the NRXN-α isoform contains N-terminal signal peptide, six laminin/neurexin/sex-hormone binding globulin (LNS) domains, three epidermal growth factor (EGF)-like repeats, a carbohydrate-binding region (stalk), a transmembrane domain, and a C-terminal PDZ binding domain. The NRXN-β isoform lacks EGF-like repeats interspersed throughout and contains one LNS domain, a carbohydrate-binding region (stalk), a transmembrane domain, and a C-terminal PDZ binding domain. The NRXN-γ isoform consists of only the carbohydrate binding region (stalk), a transmembrane domain, and a C-terminal PDZ binding domain. Sites of alternative splice site insertions are identified (SS1-6). SS6* is not found in neurexin-2. Adapted from Tromp et al., 2021. Created with BioRender.com.

The neurexin family also undergoes extensive alternative splicing (Tabuchi & Südhof, 2002), producing over 1000 potential distinct NRXN isoforms (Ullrich et al., 1995), making the *Nrxn* gene a very complicated gene to study in both humans and animal models. *Nrxn1* is highly associated with neurodevelopmental and neuropsychiatric disorders (Béna et al., 2013) and is the specific gene of focus for the current study. *Nrxn1* is a high-risk gene for ASD, accounting for an estimated 0.4% of cases, making it an important candidate gene to further study in the context of ASD. Heterozygous exonic *Nrxn1* deletions play a role in the pathology of neurodevelopmental disorders including ASD (Béna et al., 2013; Lowther et al., 2017); thus, fully understanding the function of NRXN is an important step in deepening our understanding of neurodevelopmental disorders, and the neuropathologies leading to such disorders.

1.4.1 Neurexin Mouse Models

Various *Nrxn* mouse models have been generated in order to further elucidate the function of neurexin in neuropathologies, physiological processes, and specific behaviors. The first *Nrxn* loss of function mouse models were generated by Missler et al. (2003), who produced a variety of *Nrxn*-α KO mice (single, double, and triple *Nrxn1-α*/*Nrxn2-α*/*Nrxn3-α* knockout mice) to determine the result of *Nrxn*-α loss of function mutations. However, the ablation of *Nrxn*-α resulted in significantly impaired survival. Double and triple KO mice were alive at birth, but most triple KO mice died on the first day and most double KO mice died within the first week (Missler et al., 2003). While triple *Nrxn-α* KO mice had marked impairments in synaptic transmission, the mice did not show a significant decrease in the number of excitatory synapses and only a moderate decrease in the number of inhibitory synapses (Missler et al., 2003). These findings support the concept that neurexins are not required for synapse formation, but play an

essential role in synaptic function, including Ca^{2+}-dependent neurotransmitter release (Dudanova et al., 2007; Missler et al., 2003).

Etherton et al. (2009) produced a *Nrxn1-α* homozygous KO mouse model (SV129/C57BL/6 hybrid background) which show reduced excitatory synaptic strength in the hippocampus, a brain region involved in learning and memory. Behaviorally, the *Nrxn1-α* KO mice had decreased prepulse inhibition, increases in grooming, nest-building impairments, and improvements in motor learning (Etherton et al., 2009). However, tasks involving social behaviors and spatial learning were normal in the *Nrxn1-α* KO mice (Etherton et al., 2009). In another study, heterozygous *Nrxn1-α* mice were shown to have impaired social memory (Dachtler et al., 2015). A conditional knockout of *Nrxn-β* in hippocampal CA1-regions showed impaired contextual fear memory (Anderson et al., 2015). Even with continued expression of *Nrxn-α*, the conditional knockout of *Nrxn-β* was found to greatly decrease neurotransmitter release in excitatory synapses of cultured cortical neurons (Anderson et al., 2015). These findings suggest that while both the *Nrxn-α* and *-β* isoforms are important individually, *Nrxn-β* knockout is sufficient to impair neurotransmitter release and effect behaviour.

Nrxn3-α/β conditional KO mice generated by Aoto and colleagues (2015) demonstrated increased latency to find buried food compared to controls, supporting the importance of *Nrxn3-α/β* in inhibitory synaptic transmission in the olfactory bulb (Aoto et al., 2015). Additionally, *Nrxn3-α/β* was found to be essential for normal AMPA receptor levels in hippocampal excitatory synapses and for controlling inhibitory neurotransmitter release in olfactory bulb neurons (Aoto et al., 2015). A limitation of knockout models that affect both α and β isoforms of the *Nrxn3* gene is the lethality of the knockout. Most *Nrxn3-α/β* conditional

KO mice died at birth (Aoto et al., 2015), making behavioural assays in adult mice difficult in this type of model.

The *Nrxn1-α/β/γ* knockdown mouse model produced by Lu and colleagues (2023) is the *Nrxn* mouse model that is the focus of this study. Characterizing behaviour of *Nrxn1-α/β/γ* knockdown mice is a distinct contribution from previous behavioural studies using mice with *Nrxn1* knockdowns that only affect the NRXN-α or NRXN-β isoform. As this is a newly developed *Nrxn1* knockdown mouse model that affects all *Nrxn1* isoforms, it is important that the behaviour of the strain is extensively investigated, to know of any potential cognitive deficits in a candidate mouse model of autism spectrum disorder, since this disorder is defined by its behavioural phenotype.

Limited work has investigated the olfactory function and memory in *Nrxn* KO and knockdown models. One study that characterized a *Nrxn1-α* KO mouse model assessed the latency for mice to find buried food and found that there were no significant effects of genotype; however, female mice in general tended to take longer to find buried food (Grayton et al., 2013), indicating that there were no differences in olfactory processing between *Nrxn1-α* KO and WT mice. Interestingly, a *Nlgn* knockdown mouse model was found to have impaired olfactory function (Radyushkin et al., 2009). NLGN is one of the main binding partners of NRXN, making this finding relevant to our interest in NRXN. In a buried food task with only olfactory cues, *Nlgn* KO mice had significantly higher food-finding latencies than WT controls; however, in food-finding tests with visible food, the *Nlgn* KO mice performed identically to WT controls (Radyushkin et al., 2009). Additionally, *Nrxn3* in mice has been shown to be essential for normal release probability of olfactory bulb inhibitory synapses (Aoto et al., 2015) and specifically,

Nrxn3-α has been found to play a crucial role in inhibitory synapses of dissociated OB cell cultures and the granule cell to mitral cell synapse in vivo (Trotter et al., 2023). Despite the important of *Nrxn* in the synapses involved in olfactory pathways, and evidence of potential olfactory disruptions in *Nrxn* and *Nlgn* KO mouse models, olfactory memory has not yet been assessed in the *Nrxn1-α/β/γ* $^{+/-}$ mouse model. The physiological and behavioural changes in Nrxn mouse models are summarized in Table 1.

Table 1. Summary of behaviour and physiological changes in *Nrxn* mouse models

Model	**Behaviour Observations**	**Physiological Observations**	**Source**
Triple *Nrxn-α* KO	Most died on PD1 Breathing difficulty	↓: synaptic transmission Moderate ↓ in number of inhibitory synapses Normal: number of excitatory synapses	Missler et al., 2003
Double *Nrxn-α* KO	Most died within 1 week Breathing difficulty	↓: Ca^{2+} currents, spontaneous neurotransmitter release, and synaptic transmission that correlate with number of deleted *α Nrxns.*	Missler et al., 2003
Single *Nrxn-α* KO	Single *Nrxn3-α* KO mice had impaired survival	↓: Ca^{2+} currents, spontaneous neurotransmitter release, and synaptic transmission that correlate with number of deleted *α Nrxns.*	Missler et al., 2003
Nrxn1-α KO	↓: Prepulse inhibition, nest-building ↑: Grooming, motor learning Normal: spatial learning, social behaviour	Impaired hippocampal excitatory synaptic strength	Etherton et al., 2009

Model	Behaviour Observations	Physiological Observations	Source
Nrxn1-α KO	↓: social approach, social investigation, locomotion in novel environments ↑: aggressive behaviour in male *Nrxn1-α* KO mice		Grayton et al., 2013
Nrxn1-α HET	↓: social memory		Dachtler et al., 2015
Nrxn2-α HET	↓: long-term object discrimination		Dachtler et al., 2015
Triple *Nrxn-β* cKO	↓: contextual fear memory		Anderson et al., 2015
Nrxn3-α/β cKO	Most mice died at birth ↑: latency to find buried food	↓: AMPA receptor input-output relationship in the hippocampus ↓: Olfactory bulb inhibitory synaptic transmission	Aoto et al., 2015

1.5 Present Research

NRXN molecules are crucial components of the molecular machinery that control synaptic transmission, stability, and allow neural networks to process signals involved in processes such as olfactory memory. Alterations in *Nrxn* expression can lead to impairments in neural networks that link olfactory processing (olfactory bulb and olfactory tubercle) to brain regions involved in regulating learning and memory (hippocampus). Such impairments have been implicated in ASD as well as other neurodevelopmental and neuropsychiatric disorders; however, the specific effects of *Nrxn* deficiency in the brain on the development of short- and long-term olfactory

memory remains rudimentary. The current research set out to establish a novel odour-conditioning paradigm to investigate olfactory learning and memory in a *Nrxn1*$^{+/-}$ model of ASD, while also investigating the dopaminergic neural substrates of olfactory learning and memory, including *DAT*, *DRD1*, and *DRD2*, holding the potential for greater clinical relevance in disorders such as ASD. Thus, the current study will utilize olfactory learning to aid in clarifying the nature of olfactory processes impaired in autism spectrum disorder by determining if there are modulations in dopaminergic gene expression in the olfactory bulb, olfactory tubercle, and hippocampus of *Nrxn1*$^{+/-}$ and WT mice that have been trained in a Pavlovian odour conditioning paradigm.

1.6 Main Objectives

The main goal of this study was to characterize the region-specific expression and regulation of *Nrxn1* in brain tissue and identify how it relates to mechanisms underlying odour memory in a mouse model of autism spectrum disorder. Overall, I was interested in understanding how *Nrxn1* gene disruption renders changes in the olfactory system.

The main objectives include:

I. Measure olfactory learning and memory in *Nrxn1*$^{+/-}$ mice and WT controls utilizing a novel Pavlovian odour conditioning paradigm.

II. Characterize *DAT*, *DRD1*, and *DRD2* expression in the olfactory bulb, olfactory tubercle, and hippocampus tissue of male and female *Nrxn1*$^{+/-}$ and wildtype control mice after competition of olfactory memory tests.

III. Assess the relationship between *DAT*, *DRD1*, and *DRD2* expression and performance in the Pavlovian odour conditioning paradigm.

CHAPTER 2: MATERIALS AND METHODS

2.1 Subjects

A total of 75 male and female *Nrxn1*$^{+/-}$ and *Nrxn1*$^{+/+}$ (WT) control mice on a C57BL/6J background were included in the study. Mice used in this study were obtained from the in-house breeding colony at Dalhousie, with original *Nrxn1*$^{+/-}$ and *Nrxn1*$^{+/+}$ breeders provided by Anne Marie Craig (Centre for Brain Health and Department of Psychiatry, University of British Colombia). The original *Nrxn1*$^{-/-}$ knockout models were custom generated by The Jackson Laboratory. A 140bp deletion mutation, beginning in the intron upstream of *Nrxn1* exon 22a, and terminating at the last residue of *Nrxn1* exon 22a, was introduced using the CRISPR-Cas9 system. Mouse embryos were injected with Cas9 mRNA, guide RNA against *Nrxn1* exon 22, and donor ssDNA oligonucleotide with the targeted mutation (Lu et al., 2023). The 140bp deletion results in reduced expression of all three *Nrxn1* isoforms. Mouse genotyping was performed via Polymerase Chain Reaction (PCR) and protein loss was confirmed with western blot (Lu, 2023). *Nrxn1*$^{-/-}$ mice were bred with *Nrxn1*$^{+/+}$ mice to produce pups with a heterozygous *Nrxn1*$^{+/-}$ genotype.

Pups were weaned at 21 days of age and housed in same-sex groups of 2-4 mice per cage prior to separation for testing. Mice were kept on a reversed 12:12 hour light/dark cycle and provided with food (LabDiet® Prolab® RHM 3500) and water *ad libitum*. Mice ranged from the age of 90-130 days at the start of testing. Mice were housed in transparent polyethylene cages (35 x 12 x 12 cm) containing pine chip bedding, Enviro-dri® nesting material, and a polyvinyl chloride tube for enrichment. Mice were ear punched and genotyped for *Nrxn1* using

Polymerase Chain Reaction (PCR) by Dr. Chris Sinal (Department of Pharmacology, Dalhousie University) (Figure 6). All of the test procedures outlined were approved by the Dalhousie Committee on Animal Care (Protocol #19-073).

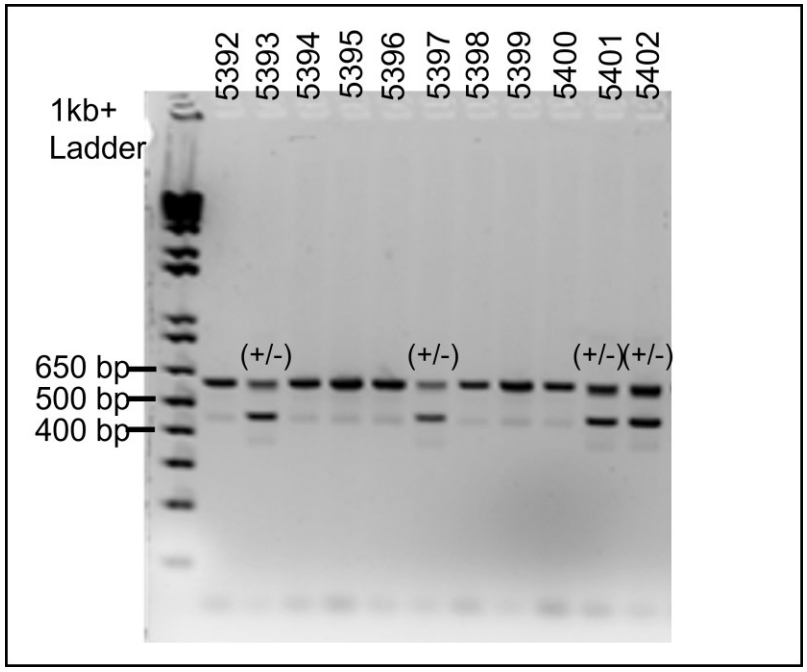

Figure 6. Agarose gel electrophoresis of genotyping PCR product provided by Dr. Chris Sinal (Department of Pharmacology, Dalhousie University). *Nrxn1*$^{+/-}$ mice are denoted by (+/-). The lower band at 456bp indicates a *Nrxn1* allele with the 142bp deletion. The upper band at 596bp represents the unaltered *Nrxn1* allele. Forward primer sequence: 5'-GCA GCC TCA CAC AGT AGC TT-3'. Reverse primer sequence: 5'-GGC CTA AGG TAG CTC TCA CA-3'.

2.2 Apparatus for Pavlovian Odour Conditioning Paradigm

Mice were trained and tested in transparent polyethylene cages (35 x 12 x 12 cm) identical to their home cages, with an odour pot placed in the center of the front third of the cage, and a stainless-steel hopper covering the cage (Figure 7). To construct each odour pot, 0.05 mL of pure lemon extract (Club House, McCormick Canada) was syringed onto a 55 mm filter paper using 1 mL syringe, and the filter paper was placed in the bottom of a plastic cup

(2.5 cm height and 6.3 cm diameter). A plastic petri dish lid (1.5 cm height and 5.3 cm diameter) with 12 small 1.5 mm holes was placed in the plastic cup, covering the filter paper (Figure 7A) The plastic petri dish lids acted as a barrier between the bedding and the odour filter paper. Pine chip bedding (Beta Chip, NEPCO) was placed on top of the petri dish lid to the level of the odour pot. If the odour stimulus was paired with sugar reinforcement, 8 grains of sugar (~ 8 mg each) were buried in the pine chips.

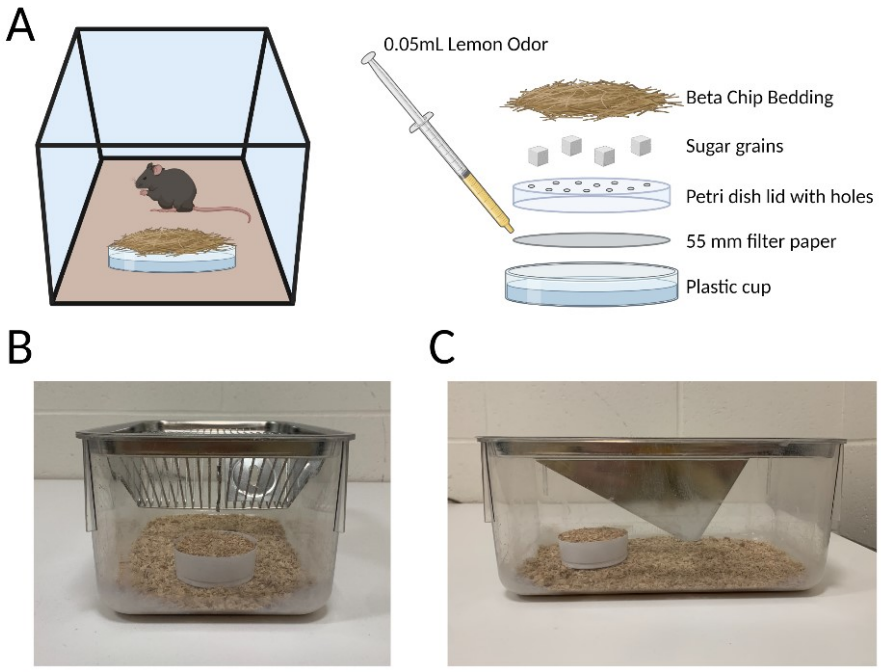

Figure 7. Pavlovian odour conditioning apparatus design. **(A)** Diagram of odour pot design used in training and testing. **(B)** Front-facing view of the training/testing cage with an odour pot and a metal hopper covering the cage. **(C)** Side view of the training/testing cage with an odour pot and a metal hopper covering the cage. Created with BioRender.com.

2.3 Pavlovian Odour Conditioning Paradigm Procedures

2.3.1 Training

Methods were adapted from the Simple Pavlovian Conditioning Odour Paradigm developed by Schellinck et al. (2001) and researchers were blinded to genotype throughout the study. In the current adapted protocol, mice were trained over eight five-minute trials on one day. Mice were weighed daily during testing, and were food deprived 24-hours prior to training. Eight pieces of sugar (~ 8 mg each) were provided to mice in the conditioned group at the time of food deprivation in order reduce potential neophobia (Sweatt, 2010) during training. Mice were weighed in their housing rooms and brought into a novel training room where they immediately began training. Mice were divided into conditioned and unconditioned groups, where mice in the conditioned group received a sugar reward for digging in the odour pot, while mice in the unconditioned group were exposed to the odour pot with no reward. During training, mice were moved from their home cage to a training cage which commenced the five-minute trial. During each trial, digging behaviour in the odour pot was observed and a Panasonic video camera (Panasonic HC-V180) was used to record behaviour for later scoring. After a trial was finished, mice were removed from the training cages and placed back in their home cages. Before the commencement of the next trial, the number of sugar grains consumed for mice in the conditioned group was counted and recorded, the odour pot was emptied, cleaned, a new filter paper with fresh lemon extract was added, and new sugar was buried in the pine chip bedding. Odour pots were also cleaned and refreshed after each trial for mice in the unconditioned group. Each inter-trial interval lasted between 5-10 minutes. This procedure was repeated for all eight five-minute training sessions. Mice in the 24-hour memory group

were maintained on food deprivation between the training day and the 24-hour test and were provided with LabDiet® Prolab® rodent chow (~3.5g each) such that they maintained 80-85% of their free feeding weight. Mice in the 7-day memory group were given free access to food after the completion of training but underwent another food deprivation period 24-hours prior to the 7-day test.

2.3.2 Memory Testing

Both conditioned and unconditioned mice were tested in either a 24-hour or 7-day memory test following training. On the memory testing day, mice were tested in a different room than they were trained in, to avoid contextual memory clues. Mice were weighed prior to testing and immediately moved from their housing room to the testing room. The testing apparatus was identical to the testing setup, but the odour pot had no sugar in it. The memory tests lasted for 10 minutes, and behaviour was recorded for later scoring.

Digging behaviour was later quantified from videos using the Behavioural Observation Research Interactive Software (BORIS) (Friard & Gamba, 2016). Digging was defined as a mouse moving the pine chip bedding with their paws or nose. The measures collected were the total digging duration(s), average digging duration(s), onset of digging(s), number of digging bouts, and the number of sugar grains consumed per trial.

2.4 Tissue Collection and Sectioning

Immediately after the 24-hour or 7-day memory test, mice in each respective group were sacrificed and tissues collected. Cages were covered with a lab coat to reduce visual stimuli and stress during transport and the mice were transported to a room where sacrifice

and perfusion would take place. The mice were restrained in dorsal recumbency and injected with 0.10 - 0.15mL of Euthanyl (Bimeda-MTC Animal Health Inc., Cambridge, ON, CA) intraperitoneally. Movement was monitored and the toe pinch reflex was checked to ensure a surgical anesthetic plane was reached. Mice were perfused with 10% PBS for 2 minutes until the blood ran clear. After decapitation and skull removal, the brain was carefully removed and placed in a 1.5mL microcentrifuge tube, and frozen on dry ice before being moved to a -80^{o}C freezer for storage.

From each brain, the olfactory bulb, olfactory tubercule, hypothalamus, prefrontal cortex, cerebellum, and hippocampus were sectioned and collected. Each brain region was subdivided into three sections and the tissue sections were weighed, labelled, and stored at -80^{o}C for future use. Only the olfactory bulb, olfactory tubercle, and hippocampus were used in the current study.

2.5 RNA extraction

RNA was extracted from the olfactory bulb, olfactory tubercle, and hippocampal sections of each mouse using the RNeasy® Plus Mini Kit (Cat. #74136, Qiagen, Valencia, CA, USA) and the RNeasy® Micro Kit (Cat. #74034, Qiagen, Valencia, CA, USA) as per the manufacturer's protocol. The RNeasy Micro kit was used to extract RNA from half of the olfactory tubercle samples, as RNA yields from this brain region were particularly low (< 4 mg). Olfactory bulb and hippocampal samples were eluted in 50µL of RNase-free water while olfactory tubercle samples were eluted in 30µL of RNase-free water. The eluted RNA concentration and quality was immediately measured using a Take3 micro-volume plate with an Epoch Microplate

Spectrophotometer (Biotek Instruments, Inc., Winooski, VT, USA). 2µL of each sample was pipetted onto the Take3 micro-volume plate and 2µL of RNase-free water was used as a blank control. RNA purity was assessed using the 260/280 nm ratio, with a 260/280 nm ratio > 2.0 indicating pure RNA. RNA samples were subsequently stored at -80^{o}C until use.

2.6 Complimentary DNA conversion

RNA was reverse-transcribed into single-strand complimentary DNA (cDNA) using the C1000 Touch™ Thermal Cycler (Bio-Rad Laboratories, Inc., Hercules, CA, USA). cDNA synthesis was completed using the iScript™ Reverse Transcription Supermix for RT-qPCR (Cat. #1708841, Bio-Rad Laboratories, Inc., Hercules, CA, USA) or the iScript™ cDNA Synthesis Kit (Cat. #1708891, Bio-Rad Laboratories, Inc., Hercules, CA, USA). For each sample, a reaction volume of 20µL was prepared in 200µL PCR strip tubes, following the respective manufacturer's protocol. The RNA template volume varied per sample, with RNA input ranging from 650ng - 1µg total RNA template depending on the concentration of RNA extracted, to ensure sufficient sample for all required RT-qPCR plates. All reactions were run according to the temperature cycling protocol outlined in Table 2. In each cDNA conversion run, a no template control (NTC) and a no reverse-transcriptase control (NRT) were run following the same temperature cycling protocol in order to assess potential genomic DNA contamination within the reagents or the RNA template. After the cDNA conversion reaction was complete, 2µL of cDNA from each sample was pipetted into a 1.5µL microcentrifuge tube to generate pooled cDNA for each brain region of interest (olfactory bulb, olfactory tubercle, hippocampus). All cDNA was stored at -30^{o}C until used.

Table 2. Reverse transcription temperature cycling protocol for the C1000 Touch™ Thermal Cycler (Bio-Rad Laboratories, Inc., Hercules, CA, USA)

Step	Time (minutes)	Temperature (^{o}C)
Priming	5	25
Reverse Transcription	20	46
Reverse Transcriptase inactivation	1	95

2.7 Reverse Transcription Quantitative Polymerase Chain Reaction (RT-qPCR)

Each RT-qPCR primer set, including primers for four target genes; *DAT*, *DRD1*, *DRD2*, and *Slc6a2* (norepinephrine transporter), and five reference genes: *CycA*, *HPRT1*, *GAPDH*, *RN18S1*, and *RPL13A* (Table 3), were first optimized and validated. A survey of the literature was completed to select candidate reference genes that have been shown to be stable in the brain regions of interest in mice and encompassed different functional classes (i.e., cellular metabolism, transcription, translation). To optimize each primer set, a representative sample of pooled cDNA was prepared to be run on a 96-well plate with a thermal gradient of annealing temperatures ranging between 55^{o}C-65^{o}C. Pooled cDNA samples were run in duplicate technical replicates for each annealing temperature, which varied by row on the CFX96 qPCR Instrument (Bio-Rad Laboratories, Inc., Hercules, CA, USA). For primer optimization, the temperature cycling protocol was the same as outlined in Table 4, except for the 55^{o}C-65^{o}C thermal gradient that occurred during the annealing step. Melt curve analysis was completed to ensure that only one product had been amplified. The optimal annealing temperatures were decided for each primer set based on a quantitative cycle (Cq) value that landed between 15-30,

clean and distinct melt peak profiles, and consistent Cq values between technical replicates. *RPL13A* had very low expression (Cq > 38) in all brain regions of interest across all tested annealing temperatures, and thus was removed from consideration as a reference gene candidate. *Slc6a2* had very low expression in the hippocampus, with Cq values greater than 36 and many wells without any amplification. As a result, *Slc6a2* was removed from the list of target genes was not used for further quantification. The optimal annealing temperatures were found to be 57^{o}C for *Slc6a3* (*DAT*), 59^{o}C for *DRD1*, and 61^{o}C for *DRD2*, *CycA*, *HPRT1*, *GAPDH*, and *RN18S1*. For each primer at the optimal annealing temperature, a melt curve with a single peak was produced, indicating annealing specificity and absence of primer dimers.

Table 3. Primer sequences used in RT-qPCR reactions.

Gene	**Forward Primer (5'-3')**	**Reverse Primer (5'-3')**
Slc6a3 (DAT)	CAC CTC CAT CAG AGT CGT GG	GCA GAA CAA TGA CCA GCA CC
Slc6a2	GCA CCT CCA TTC TGT TTG CGG T	GCT CAC GAA CTT CCA ACA CAG C
DRD1	AGA TGA CTC CGA AGG CAG CCT T	GCC ATG TAG GTT TTG CCT TGT GC
DRD2	CGT GTC CTT CAC CAT CTC TTG C	TAG ACC AGC AGG GTG ACG ATG A
CycA	CAT CCT AAA GCA TAC AGG TCC TG	TCC ATG GCT TCC ACAAT
HPRT1	TTG GGC TTA CCT CAC TGC TTT C	ATC GCT AAT CAC GAC GCT GG
GAPDH	GTT GTC TCC TGC GAC TTC A	GGT GGT CCA GGG TTT CTT A
RN18S1	CCT GGA TAC CGC AGC TAG GA	GCG GCG CAA TAC GAA TGC CCC
RPL13A	ACA AGAAAA AGC GGA TGG TG	TTC CGG TAA TGG ATC TTT GC

Table 4. RT-qPCR temperature cycling protocol.

Step	**Time**	**Temperature (°C)**
Activation	2 min	95
Denaturation	5s	95
Annealing/Extension	30s	57 for *Slc6a3 (DAT)*
		59 for *DRD1*
		61 for *DRD2*, *CycA*, and *HPRT1*
Melt-curve	0.5s/increase in 1°C	65-95

To determine the dynamic range of each reaction, a serial dilution of pooled cDNA was prepared by starting with an undiluted pooled cDNA sample and performing a tenfold serial dilution covering 5 logs of dynamic range. Standard curve RT-qPCR runs were run in duplicate, including appropriate controls (NT, NRT, and negative controls). Standard curves were utilized to calculate the PCR efficiency (E) of each primer pair using the following equation where *m* represents slope:

$$E = 10^{\left[-\frac{1}{m}\right]} - 1$$

Standard curves were considered acceptable if the PCR efficiency was between 90-110% and if the R^2 was greater or equal to 0.98 (Figure 8). In cases where standard curves for a primer pair did not follow these guidelines, the runs were first repeated to ensure accuracy. If the standard curve values still were outside of the mentioned parameters after the repeated run, different primer pairs were selected for the chosen gene and the process was repeated.

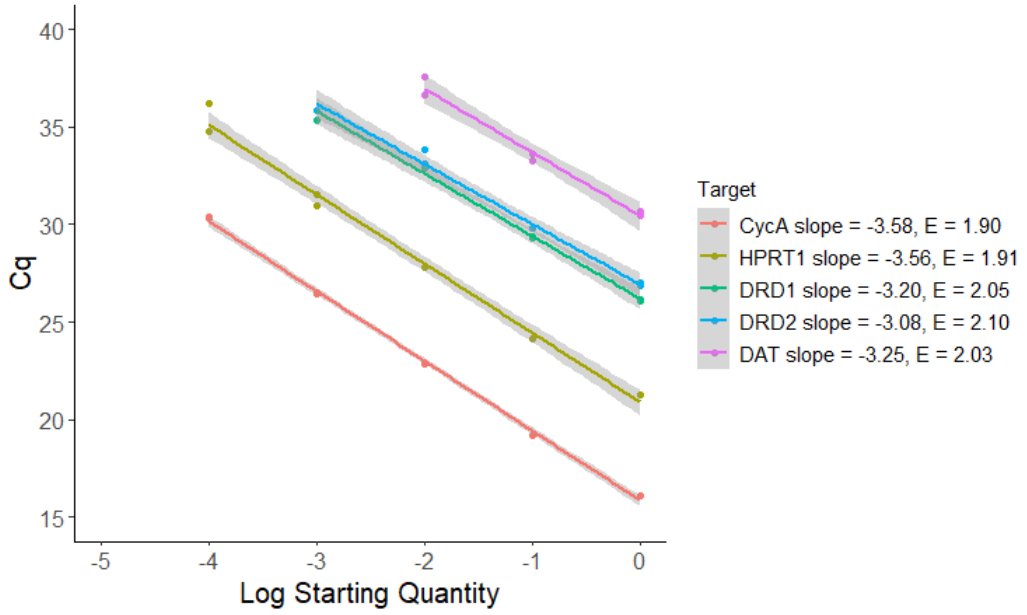

Figure 8. PCR efficiencies of reference genes (*CycA*, *HPRT1*) and target genes (*DRD1*, *DRD2*, *DAT*).

To determine the optimal reference genes, the stability of a series of candidate reference genes (*CycA*, *GAPDH*, *HPRT1*, and *RN18S1*) was assessed. Each candidate reference gene primer pair was run with a representative group of samples (4 samples per biological group). The stability of each gene was assessed using GeNorm and Normfinder. *CycA* and *HPRT1* were found to be the most stably expressed across treatments and were selected as the optimal reference genes.

For each RT-qPCR plate run using *CycA*, *HPRT1*, *DRD1*, or *DRD2*, master mix was made by adding 5µL of SsoAdvanced Universal SYBR® Green Supermix (Cat. #1725274), 0.5µL of 10µM forward primer, 0.5µL of 10µM reverse primer, 2µL of PCR-grade H_2O. For each plate run with *DAT*, the master mix was made by adding 5µL of SsoAdvanced Universal SYBR® Green Supermix (Cat. #1725274), 0.5µL of BIORAD PrimePCR™ Template for SYBR® Green Assay: Slc6a3, Mouse (Cat. 10025637), and 2.5µL PCR-grade H_2O. Each reaction in the 96-well plate had a total

volume of 10µL, including 8µL of Master Mix and 2µL of cDNA. All samples were run in duplicate technical replicates. When technical replicates varied by 0.3 Cq or more, the samples were run again in triplicate, and the mean of the two technical replicates within 0.2 Cq of each other were used for analysis. If repeated samples were not within 0.2 Cq of each other, they were removed from the analysis.

RT-qPCR plates were organized by gene, so as many samples as possible were included in a single plate and one gene was targeted per plate. With a total of 65 samples for each brain region, a single gene run spanned across two 96-well plates, not including any repeats to be completed later. In order to make valid comparisons between samples spanning multiple plates, an interplate calibrator (IPC) was included on each plate, to adjust for run-to-run variation. The IPC was pooled cDNA from the respective brain region (olfactory bulb, olfactory tubercle, or hippocampus) and *CycA* was the target selected for the IPC. IPCs were included in every run and were run in triplicate.

RT-qPCR plates were prepared on ice, with 8µL of Master Mix added to each well in the 96-well plate first, followed by 2µL of cDNA. Each plate was run with a NT, NRT, and a negative control prepared in duplicate. For the control wells, Master Mix was added first, followed by 2µL of the respective control. After plates were fully loaded, the plates were sealed with Microseal® 'B' Film Seals (Cat. #MSB1001), spun down with a VWR PCR plate centrifuge, and placed into the CFX96 qPCR Instrument (Bio-Rad Laboratories, Inc., Hercules, CA, USA) to be run according to the optimized temperature cycling protocol (Table 4).

Data was corrected for the variation between runs using the following equation:

$$Cq_i^{corrected} = Cq_i^{uncorrected} - Cq_i^{IPC} + \frac{1}{no.plates} \sum_{i=1}^{no.plates} Cq_i^{IPC}$$

For gene runs that spanned multiple plates, the Cq_i^{IPC} was subtracted from the $Cq_i^{uncorrected}$ and the average of the IPC Cq values ($\frac{1}{no.plates}\sum_{i=1}^{no.plates} Cq_i^{IPC}$) for a given gene and brain region was added. After correcting for run-to-run variation, the mean of the $Cq_i^{corrected}$ duplicate technical replicates were calculated for each sample.

Relative gene expression was calculated using a modified Pfaffl equation (Hellemans et al., 2007; Vandesompele et al., 2002) since the original Pfaffl equation does not account for the use of multiple reference genes (Pfaffl, 2001). The $2^{-\Delta\Delta CT}$ method was not used because this approach heavily relies on the assumption of 100% PCR amplification efficiencies for all genes (Livak & Schmittgen, 2001).

$$Relative\ gene\ expression = \frac{(E_{GOI})^{\Delta Cq\ GOI}}{GeoMean[(E_{REF})^{\Delta Cq\ REF}]}$$

The ΔCq for the gene of interest (GOI) was calculated by subtracting the mean $Cq^{corrected}$ for each sample from the mean Cq of the calibrator (ΔCq = Calibrator Cq – Sample Cq). The calibrator selected was the group of unconditioned WT mice tested in the 24-hour memory test. A control average was calculated from the samples in this control group and then subtracted from the $Cq^{corrected}$ of each sample. The final results are thus presented as relative to the control average Cq values. Next, the relative quantity (RQ) values were calculated ($RQ = E^{\Delta Cq}$) where E represents the PCR efficiency. The geometric mean of the reference gene RQs were then

calculated, and relative expression was calculated by dividing the RQ of the target by the reference gene RQ geometric mean.

2.8 Statistical Analysis

Throughout the study and during analysis, researchers were blinded to genotype. For each data set, standardized residuals were plotted in a Q-Q plot to visually assess normality. The Shapiro-Wilk test was also run to assess normality of data and Levene's test was used to assess homogeneity of variance. In cases where the assumptions of normality and/or homogeneity of variance was violated, non-parametric tests were run. All data was found to violate the assumptions, so non-parametric tests were used throughout. When directly comparing two independent groups, the Mann-Whitney U test was completed to assess whether population means differed significantly. When comparing more than two independent groups, the Kruskal-Wallis test was completed. If the Kruskal-Wallis test indicated significance (defined as $p < 0.05$), the test was followed up with Dunn's-Test post hoc using a Bonferroni correction. Correlations were run using the Spearman's rank correlation test. In cases where boxplots showed potential meaningful differences between groups, but had not been statistically significant, a sample size calculation was completed. The calculation included a 15% adjustment for non-parametric tests, to assess how many samples would be required per group for significance ($p < 0.05$) with a power of 0.8. All statistical analyses and graphs were completed with R (R version 4.1.2 (2021-11-01) -- "Bird Hippie") (R Core Team, 2023).

CHAPTER 3: RESULTS

3.1 Pavlovian Odour Conditioning

During training, mice in the conditioned group dug significantly more than mice in the unconditioned group ($W = 294.5$, $p < 0.001$; Figure 9A). A Kruskal-Wallis test revealed significant differences between digging among the four groups ($H(3) = 20.99$ $p < 0.001$) so a Dunn's post hoc was performed to identify potential interactions between genotype and training condition. Unconditioned *Nrxn1*$^{+/-}$ mice dug significantly less than conditioned *Nrxn1*$^{+/-}$ mice ($p < 0.001$; Figure 9B) and conditioned WT mice ($p = 0.048$; Figure 9B). Unconditioned WT mice dug significantly less than conditioned *Nrxn1*$^{+/-}$ mice in training ($p = 0.003$; Figure 9B). These results indicate that there is a main effect of training condition on the mean digging duration during training, but no significant interaction between training and genotype.

In the 24-hour memory test, the same trend was observed, as mice in the conditioned group dug significantly more than mice in the unconditioned group ($W=112$, $p = 0.01$; Figure 9C), indicating a main effect of training on digging duration. While a Kruskal-Wallis test indicated significant difference between groups ($H(3) = 8.18$, $p = 0.04$), there were no interactions between genotype and training condition for mean digging duration in the 24-hour test according to the post hoc ($p >= 0.059$; Figure 9D).

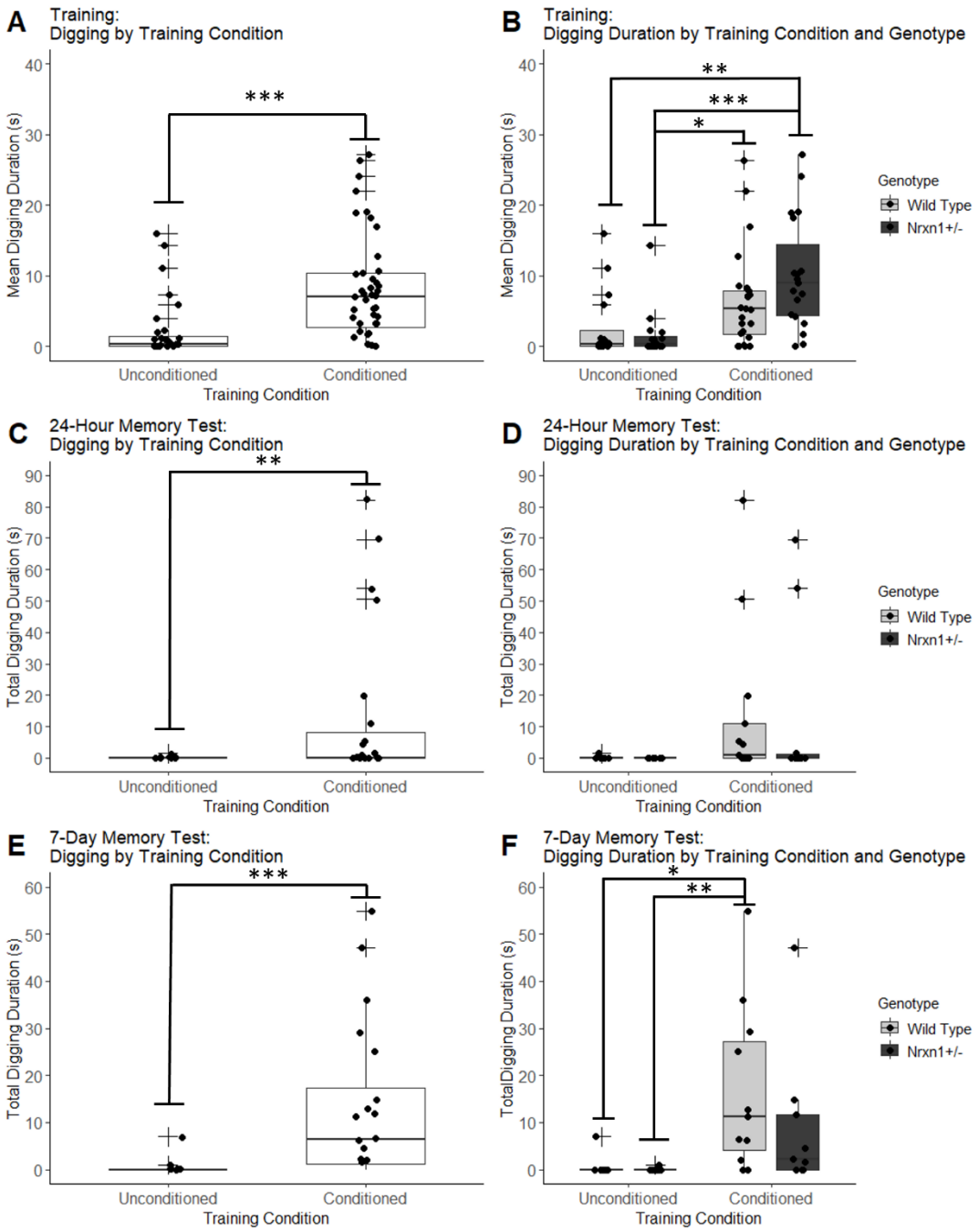

Figure 9. Total digging duration during training, 24-hour memory test, and 7-day memory test. Time digging (s) by training condition during **(A)** the training phase (N = 32-43 per group), **(C)** the 24-hour memory test (N = 16-23 per group) and **(E)** the 7-day memory test (N = 16-20 per group). Time digging (s) by training condition and genotype during **(B)** the training phase (N = 16-24 per group), **(D)** the 24-hour memory test (N = 8-13 per group), and **(F)** the 7-day memory test (N = 8-11 per group). (*$p < 0.05$; **$p < 0.01$; ***$p < 0.001$). Boxplots represent the median, quartiles one and three form the box edges, and whiskers extend to the maximum and minimum values within 1.5 times the inter-quartile range. Individual data points are represented by black points and outliers are represented by crosses.

In the 7-day memory test, conditioned mice dug significantly more than unconditioned mice (W = 51, p < 0.001; Figure 9E). A Kruskal-Wallis test (H(3) = 15.23, p = 0.0016) with a Dunn's post hoc revealed that conditioned WT mice dug significantly more than unconditioned WT mice (p = 0.013) and unconditioned *Nrxn1*$^{+/-}$ mice (p = 0.0066; Figure 9F).

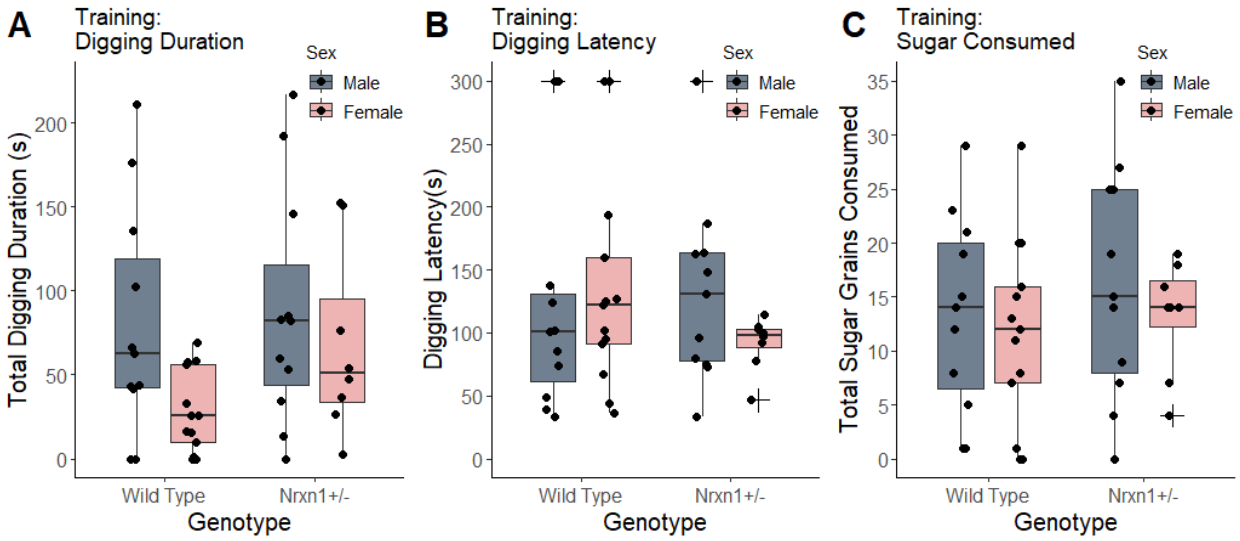

Figure 10. Training behaviour of conditioned mice by genotype and sex. **(A)** Time spent digging (s) during the training trials of conditioned mice by genotype and sex. **(B)** Digging latency (s) during the training trials of conditioned mice by genotype and sex. **(C)** Total sugar grains consumed during the training trials of conditioned mice by genotype and sex. N= 16-19 per group. Boxplots represent the median, quartiles one and three form the box edges, and whiskers extend to the maximum and minimum values within 1.5 times the inter-quartile range. Individual data points are represented by black points and outliers are represented by crosses.

To compare how well the conditioned mice performed during the training phase, the mean digging duration, digging latency, and sugar grains consumed during training were quantified and compared between genotype and sex groups (Figure 10). Within the conditioned mice, there were no significant genotype or sex differences in mean digging duration (H(3) = 2.6, p = 0.46; Figure 10A), digging latency (H(3) = 0.33, p = 0.95: Figure 10B), or sugar consumption

(H(3) = 1.25, p = 0.74; Figure 10C), indicating that *Nrxn1*$^{+/-}$ and WT, male and female mice performed equivalently in training.

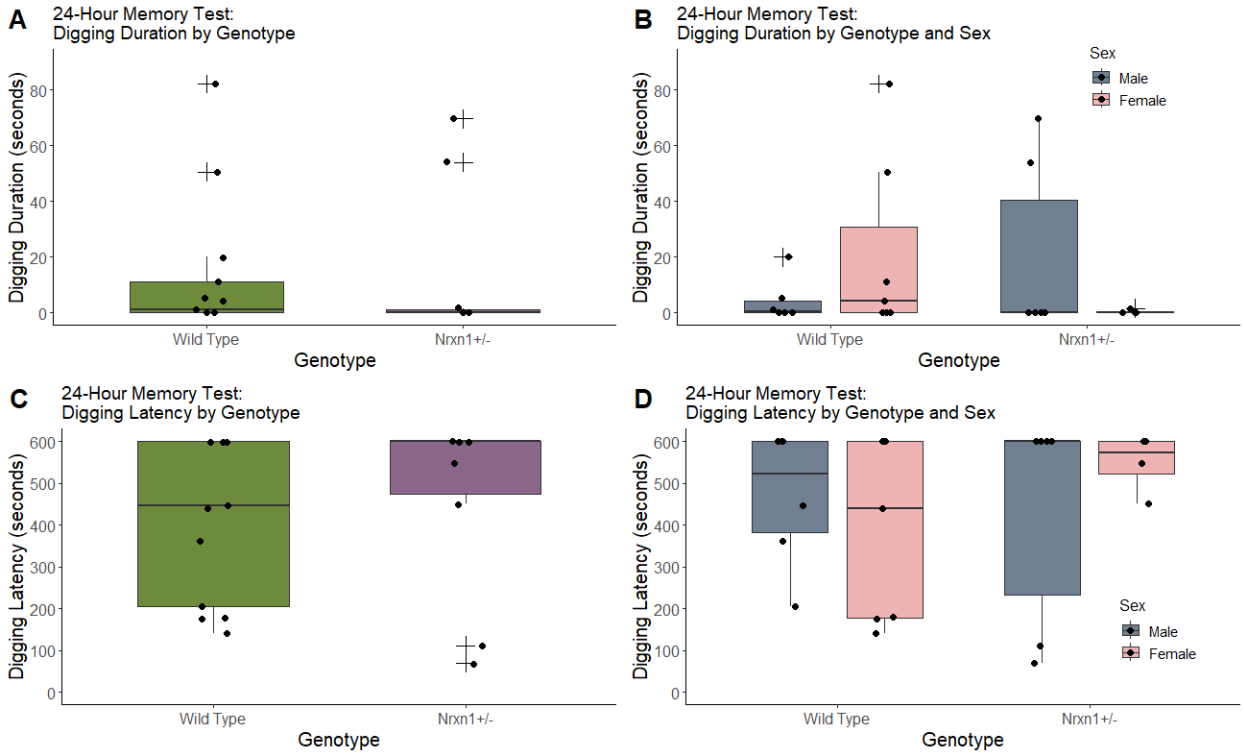

Figure 11. Digging duration and latency in the 24-hour memory test for conditioned mice. **(A)** Digging duration presented between genotypes, N = 10-13 per group. **(B)** Digging duration (s) presented between genotypes and sexes, N = 4-7 per group. **(C)** Digging latency (s) presented between genotypes, N = 10-13 per group. **(D)** Digging latency presented between genotypes and sexes, N = 4-7 per group. Boxplots represent the median, quartiles one and three form the box edges, and whiskers extend to the maximum and minimum values within 1.5 times the inter-quartile range. Individual data points are represented by black points and outliers are represented by crosses.

To compare the memory test performance of conditioned mice in the 24-hour test, the mean digging duration and digging latency were quantified between genotypes (Figures 11A, C) and genotype-sex groups (Figures 11B, D). In the 24-hour memory test, there were no significant genotype (W = 78, p = 0.39) or sex differences (H(3) = 1.7, p = 0.64) in digging duration. There were also no differences in digging latency between genotypes (W = 56, p =

0.57; Figure 11C) or between genotype x sex groups (H(3) = 0.91, p = 0.8; Figure 11D). Overall, digging duration was very low across all groups, as overall WT mice had low median digging duration (Median = 1.0, IQR = 11.0) while *Nrxn1*$^{+/-}$ mice had an even lower median digging duration (Median = 0, IQR = 1.12).

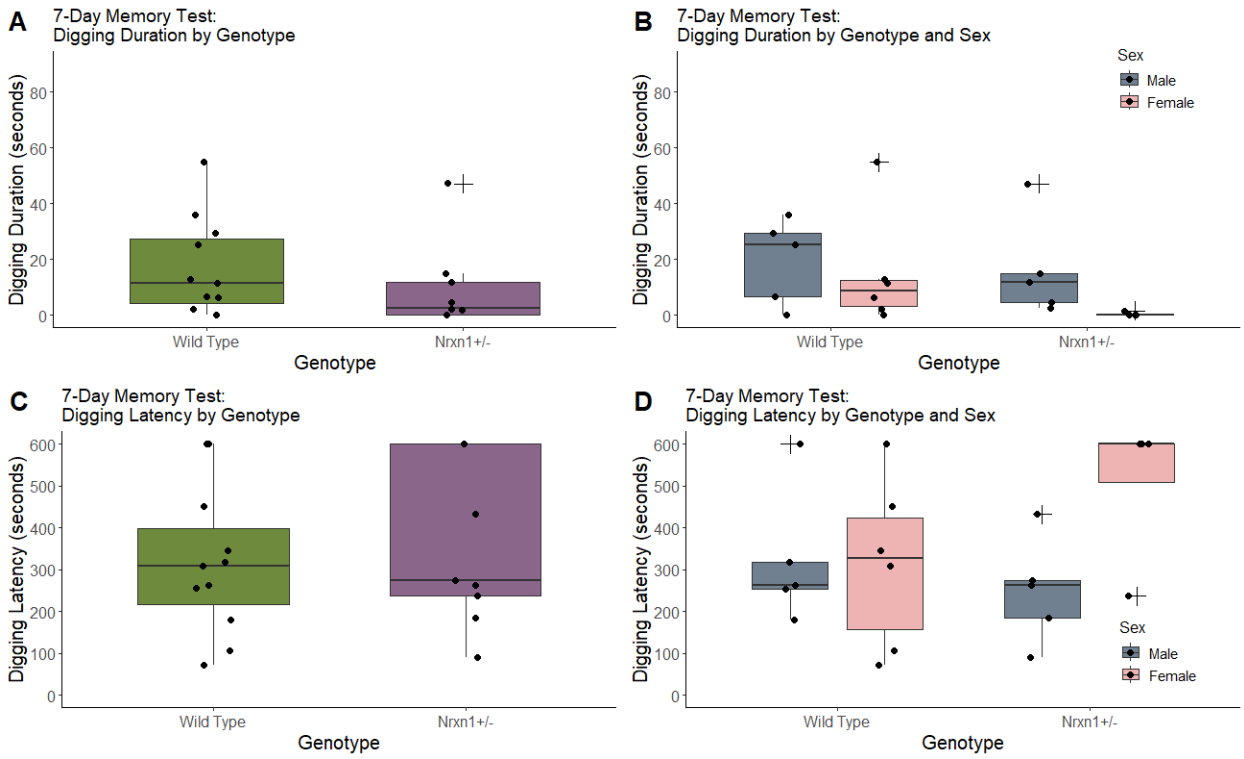

Figure 12. Digging duration and latency in the 7-day memory test for conditioned mice. **(A)** Digging duration presented between genotypes, N = 9-11 per group. **(B)** Digging duration (s) presented between genotypes and sexes, N = 4-6 per group. **(C)** Digging latency (s) presented between genotypes, N = 9-11 per group. **(D)** Digging latency presented between genotypes and sexes, N = 4-6 per group. Boxplots represent the median, quartiles one and three form the box edges, and whiskers extend to the maximum and minimum values within 1.5 times the inter-quartile range. Individual data points are represented by black points and outliers are represented by crosses.

To compare the memory test performance of conditioned mice in the 7-day memory test, the total digging duration and digging latency were quantified between genotypes (Figures 12A, C) and genotype-sex groups (Figures 12B, D). While *Nrxn1*$^{+/-}$ mice did have a lower median digging duration (Median = 2.26, IQR = 11.8) than WT mice (Median = 11.3, IQR = 23.1), the slight difference between these groups was not significant ($W = 65$, $p = 0.25$; Figure 12A). There were also no significant genotype differences in digging latency in the 7-day memory test ($W = 44$, $p = 0.7$; Figure 12C). In the 7-day memory test, we did not find any significant genotype by sex interactions for digging duration ($H(3) = 7.0$, $p = 0.07$; Figure 12B) or digging latency ($H(3) = 3.35$, $p = 0.34$; Figure 12D).

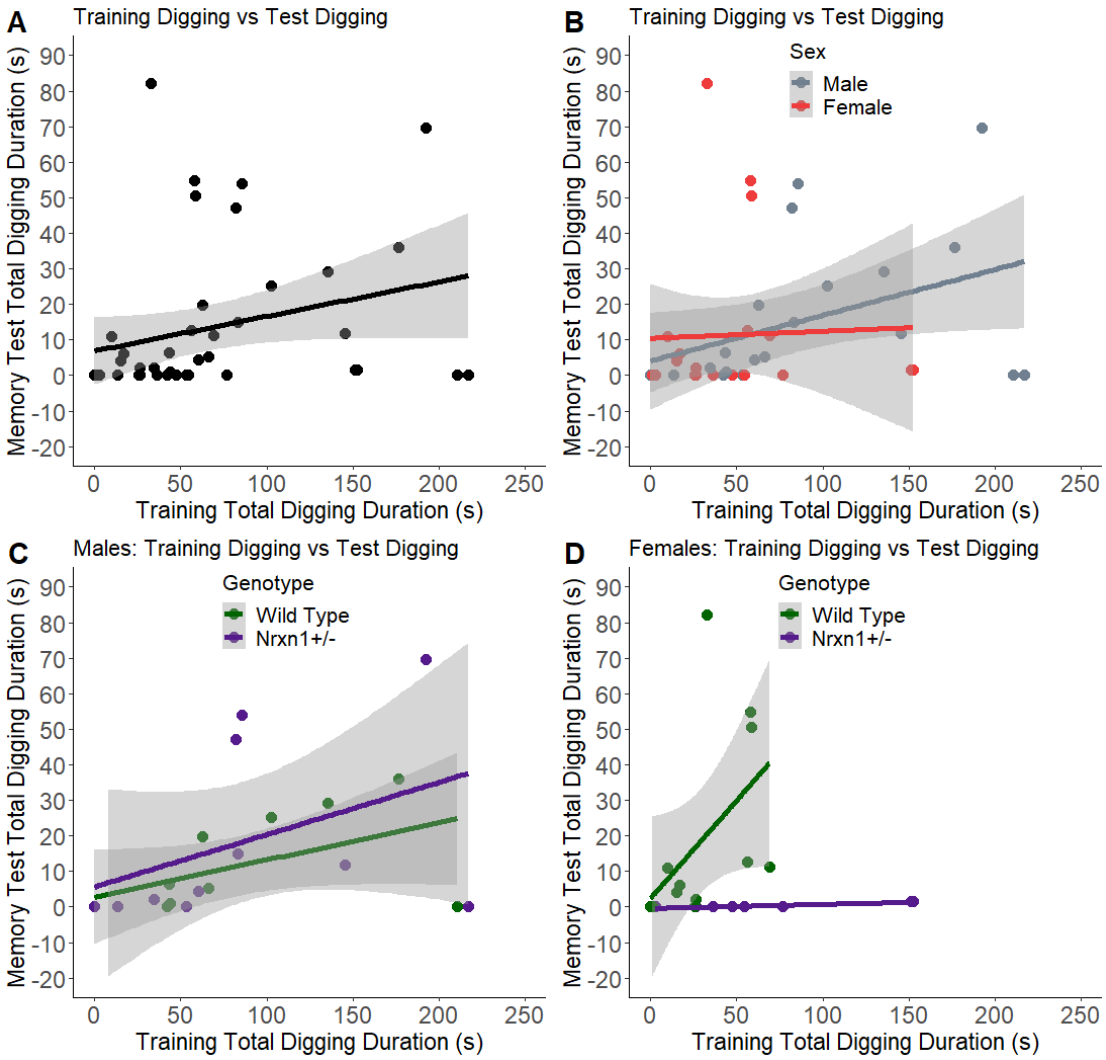

Figure 13. Correlations between total training digging duration (s) during training and total memory test digging duration (s). **(A)** All conditioned mice, ρ(41) = 0.48, p = 0.001, N = 43, **(B)** conditioned mice factored by sex; males, ρ(20) = 0.53, p = 0.012, N = 22; females, ρ(19) = 0.33, p = 0.144, N = 21, **(C)** conditioned male mice factored by genotype; male WT, ρ(9) = 0.57, p = 0.065, N = 11; male *Nrxn1*$^{+/-}$, ρ(9) = 0.53, p = 0.093 N = 11, and **(D)** conditioned female mice factored by genotype; female WT, ρ(11) = 0.77, p = 0.002, N = 13; female *Nrxn1*$^{+/-}$, ρ(6) = 0.76, p = 0.027, N = 8.

To measure the strength and direction of the association between ranked total training digging and ranked total memory test digging in conditioned mice, a Spearman's rank correlation was completed. Collapsed across groups, total training digging duration was moderately positively correlated with memory test digging in conditioned mice ρ(41) = 0.476, p

= 0.001 (Figure 13A). To further assess what was driving this correlation, male and female mice were plotted separately (Figure 13B). There was a significant positive correlation between training digging and test digging in males, ρ(20) = 0.53, p = 0.011, while there was no significant correlation between training and testing digging in females, ρ(19) = 0.33, p = 0.144 (Figure 13B). When looking specifically at males, both male WT (ρ(9) = 0.57, p = 0.065) and male *Nrxn1*$^{+/-}$ mice (ρ(9) = 0.53, p-value = 0.093) had positive correlations approaching significance (Figure 13C). When measuring the relationship between training and testing digging in conditioned females by genotype, it was found that the female WT mice had a positive correlation between variables, ρ(11) = 0.76, p = 0.002 (Figure 13D). Interestingly, contrary to visual indicators, female *Nrxn1*$^{+/-}$ mice also had a positive correlation between total training digging and test digging, ρ(6) = 0.76, p = 0.027 (Figure 13D). However, it is important to note that in the Spearman's correlation test, original data points are ranked for each variable, and rankings are assessed for correlations. In female *Nrxn1*$^{+/-}$ mice, 6/8 mice did not demonstrate any digging in the memory test (0 seconds) and the remaining two mice that did demonstrate digging, dug for a total of 1.498 - 1.50 seconds. These two mice with the highest ranked test digging also had the highest ranked training digging durations, resulting in the strong positive correlation coefficient. However, even though the Spearman's correlation has indicated a significant positive correlation between training digging and testing digging in female *Nrxn1*$^{+/-}$ mice, we can assume this correlation is not meaningful because of the negligible digging duration totals.

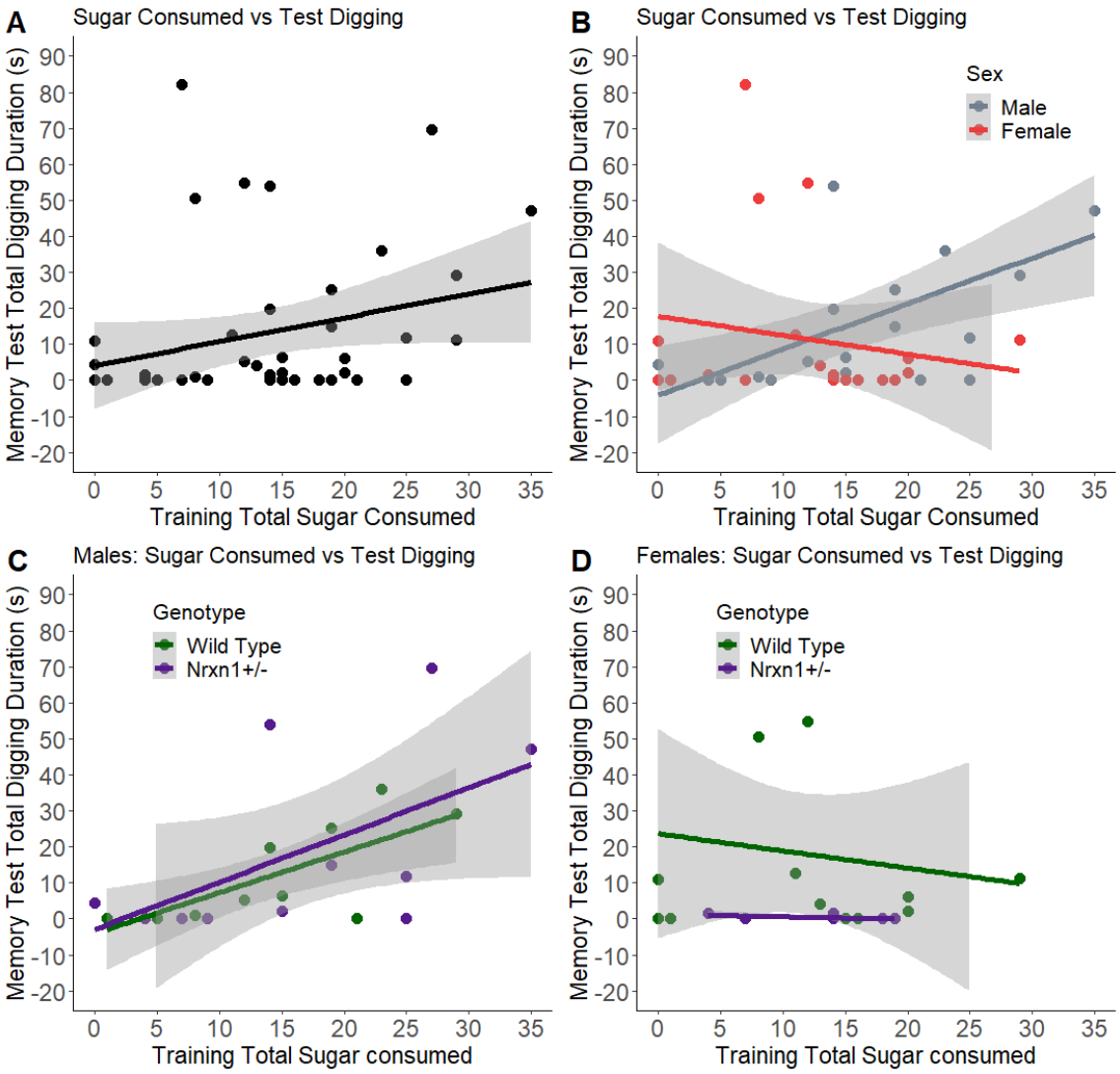

Figure 14. Correlations between total sugar consumed during training and total memory test digging duration (s). **(A)** All conditioned mice, ρ(41) = 0.30, p = 0.05. N = 43, **(B)** conditioned mice factored by sex; males, ρ(20) = 0.62, p = 0.002, N = 22; females, ρ(19) = -0.12, p = 0.607, N = 21, **(C)** conditioned male mice factored by genotype; male WT, ρ(9) = 0.75, p = 0.0078, N = 11; male *Nrxn1*$^{+/-}$, ρ(9) = 0.54, p = 0.084, N = 11, and **(D)** conditioned female mice factored by genotype; female WT, ρ(11) = -0.07, p = 0.82, N = 13; female *Nrxn1*$^{+/-}$, ρ(6) = -0.46, p = 0.248, N = 8.

Spearman's correlations were also used to assess the relationship between total sugar consumed during training and test digging in conditioned mice. Collapsed across groups, conditioned mice did not demonstrate a strong correlation between sugar consumption and memory test digging, ρ(41) = 0.301, p = 0.05 (Figure 14A). However, conditioned male mice had

a positive correlation between sugar consumption and memory test digging, ρ(20) = 0.62, p = 0.002, while conditioned female mice had no correlation, ρ(19) = -0.12, p = 0.607) (Figure 14B). When further investigating the sexes by genotype, we found that WT males had a significant positive correlation between sugar consumption and test digging, ρ(9) = 0.75, p = 0.0078; while *Nrxn1*$^{+/-}$ males did not have a significant positive correlation, ρ(9) = 0.54, p = 0.084, although the relationship is approaching significance (Figure 14C). Neither female WT (ρ(11)= -0.068, p = 0.824), nor female *Nrxn1*$^{+/-}$ mice (ρ(6) = -0.46, p = 0.248) had meaningful relationships between sugar consumed and test digging (Figure 14D).

3.2 *DAT*, *DRD1*, and *DRD2* RNA expression

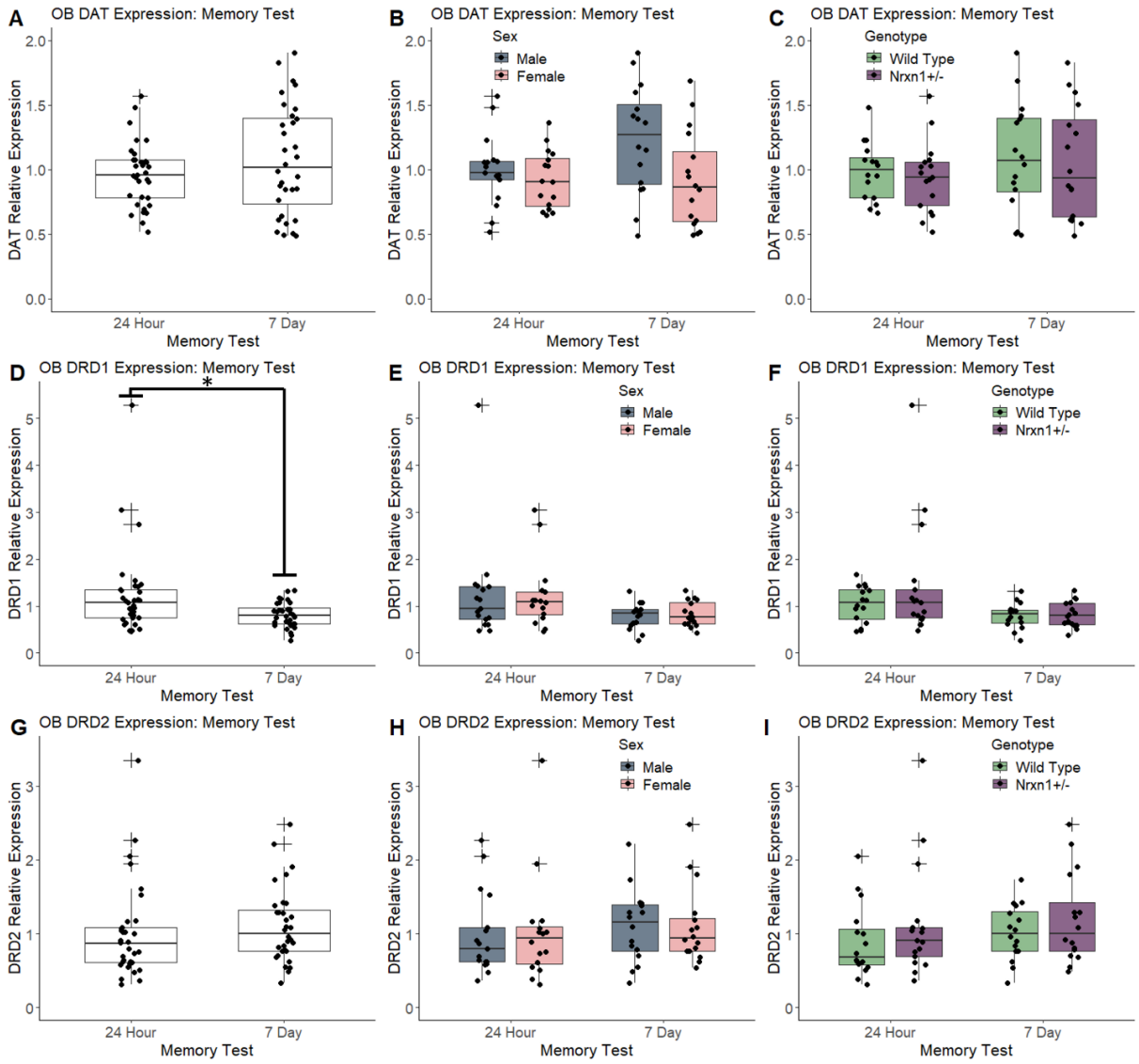

Figure 15. DA target gene expression in the olfactory bulb. **(A)** Olfactory bulb *DAT* relative expression by memory test, N = 32-33 per group, **(B)** by memory test and sex, N = 16-17 per group, **(C)** by memory test and genotype, N = 16-17 per group. **(D)** Olfactory bulb *DRD1* relative expression by memory test, N = 32-33 per group, **(E)** by memory test and sex, N = 16-17 per group, **(F)** by memory test and genotype, N = 16-17 per group. **(G)** Olfactory bulb *DRD2* relative expression by memory test, N = 32-33 per group, **(H)** by memory test and sex, N = 16-17 per group, **(I)** by memory test and genotype, N = 16-17 per group. (*$p < 0.05$; **$p < 0.01$; ***$p < 0.001$). Boxplots represent the median, quartiles one and three form the box edges, and whiskers extend to the maximum and minimum values within 1.5 times the inter-quartile range. Individual data points are represented by black points and outliers are represented by crosses.

Relative expression of *DAT*, *DRD1*, and *DRD2* in the olfactory bulb was compared between memory groups for all mice (conditioned and unconditioned), as there were no significant differences between conditioned and unconditioned mice (Supplementary Figure 1). Olfactory bulb relative *DRD1* expression differed significantly between mice in the 24-hour memory test and in the 7-day memory test, with mice in the 24-hour test having increased *DRD1* relative expression compared to mice in the 7-day test ($W = 714$, $p = 0.014$; Figure 15D). Breaking up 24-hour and 7-day memory test groups into either sex (Figure 15E) or genotype subgroups (Figure 15F) revealed that there were not any memory group by sex or memory group by genotype interactions ($p >= 0.08$). The same analyses were completed to assess OB relative expression of *DAT* (Figure 15A-C) and *DRD2* (Figure 15G-I), however, there were no significant interactions between memory test groups, sex, or genotype ($p >= 0.1$). Visual observation indicated potential sex group differences in OB DAT relative expression in the 7-day memory test group (Figure 15B) with 7-day males having a greater median OB DAT expression (Median = 1.27, IQR = 0.624) than 7-day females (Median = 0.917, IQR = 0.442). Given there were no differences found between these sex groups based on the Kruskal-Wallis test, a sample size calculation was completed to determine the necessary sample size required for significance with a 0.8 power value. This analysis revealed that 26 samples would be required per group to reach significance but an additional 15% was added to account for the non-parametric nature of the data, resulting in a required sample size of 30. The current sample size was 16-17 per group.

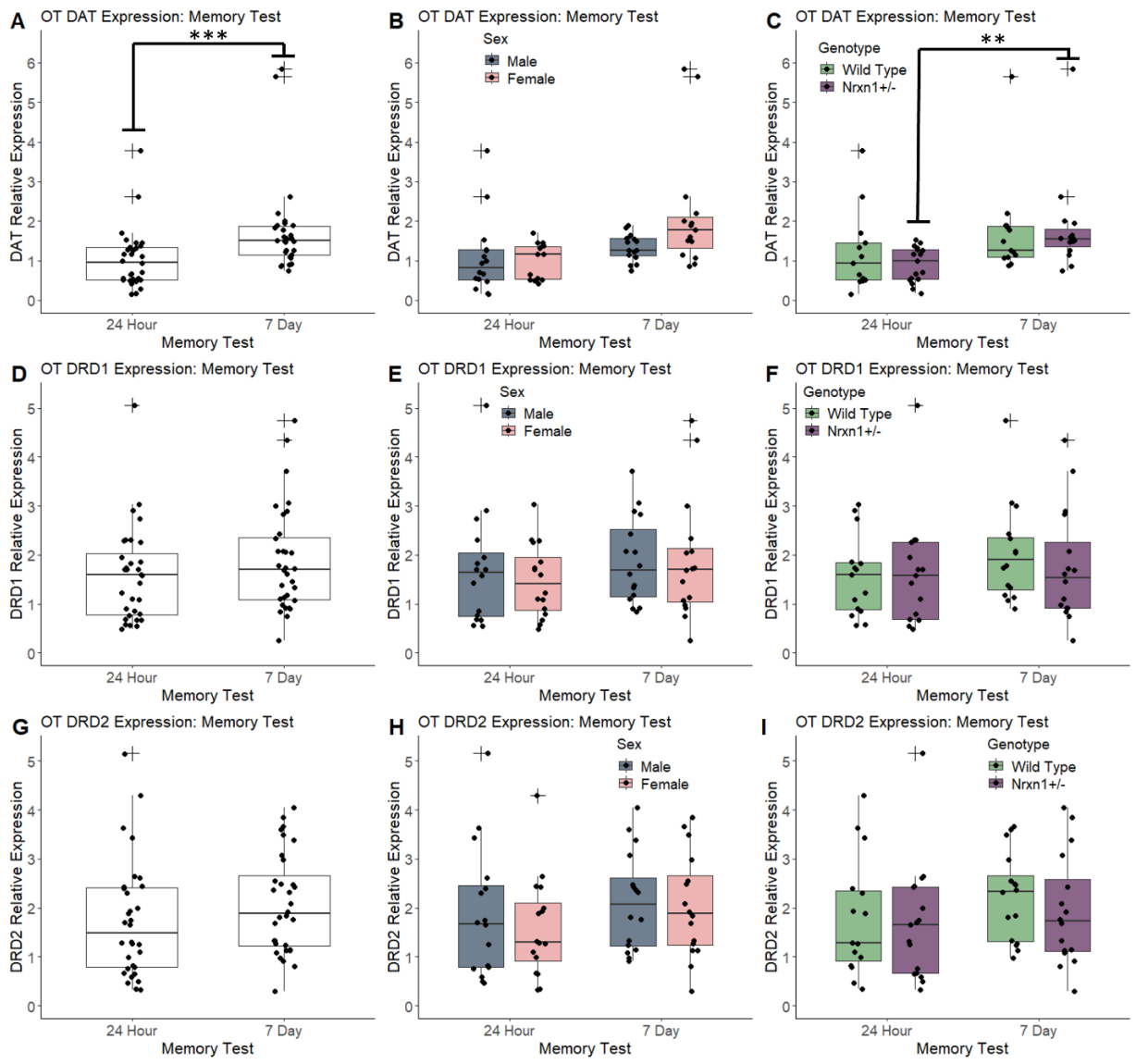

Figure 16. DA target gene expression in the olfactory tubercle. **(A)** Olfactory tubercle *DAT* relative expression by memory test, N = 30 per group, **(B)** By memory test and sex, N = 14-16 per group, **(C)** By memory test and genotype, N = 13-17 per group. **(D)** Olfactory tubercle *DRD1* relative expression by memory test, N = 32 per group, **(E)** by memory test and sex, N = 16 per group, **(F)** by memory test and genotype, N = 15-17 per group. **(G)** Olfactory tubercle *DRD2* relative expression by memory test, N = 32 per group, **(H)** by memory test and sex, N = 16 per group, **(I)** by memory test and genotype, N = 15-17 per group. (*$p < 0.05$; **$p < 0.01$; ***$p < 0.001$). Boxplots represent the median, quartiles one and three form the box edges, and whiskers extend to the maximum and minimum values within 1.5 times the inter-quartile range. Individual data points are represented by black points and outliers are represented by crosses.

Relative expression of *DAT*, *DRD1*, and *DRD2* in the olfactory tubercle were compared between memory groups for all mice. Differences in expression of OT DA target genes between conditioned and unconditioned mice were analyzed and not significant (Supplementary Figure 2). Relative expression of *DAT* in the olfactory tubercle of mice in the 24-hour test group was significantly lower than that of mice in the 7-day memory group ($W = 211$, $p < 0.001$; Figure 16A). A Kruskal-Wallis test revealed differences in relative OT *DAT* expression between memory x genotype groups ($H(3) = 13.4$, $p = 0.003$) and post hoc analysis of memory group by genotype interactions revealed that *Nrxn1*$^{+/-}$ mice in the 24-hour test had significantly lower *DAT* relative expression than *Nrxn1*$^{+/-}$ mice in the 7-day test ($p = 0.007$; Figure 16C). The same analyses were completed to assess relative expression of *DRD1* (Figure 16D-F) and *DRD2* (Figure 16G-I) in the olfactory tubercle, however, no main effects of memory test ($p >= 0.12$), nor significant interactions between memory test groups and sex ($p >= 0.47$), or memory test groups and genotypes were observed ($p >= 0.31$). A sample size calculation was completed for OT DAT relative expression between males (Median = 1.25, IQR = 0.624) and females (Median = 1.77, IQR = 0.442) in the 7-day memory test group (Figure 16B). The sample size calculation with an added 15% for non-parametric data revealed that 33 mice would be required in each group to reach significance of $p < 0.05$ with a 0.8 power.

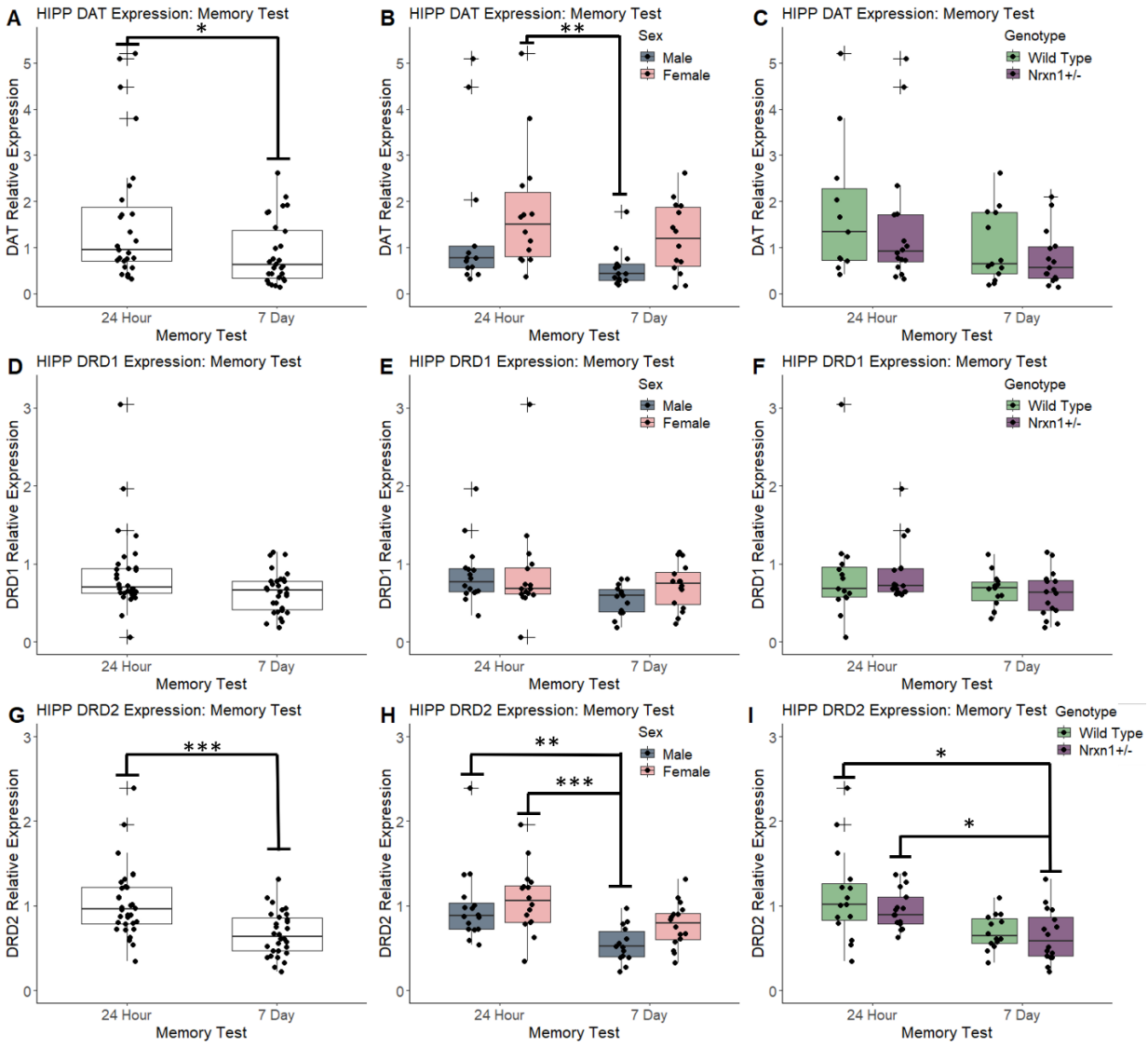

Figure 17. DA target gene expression in the hippocampus. **(A)** Hippocampus *DAT* relative expression by memory test, N = 27-28 per group, **(B)** by memory test and sex, N = 13-15 per group, **(C)** by memory test and genotype, N = 11-16 per group. **(D)** Hippocampus *DRD1* relative expression by memory test, N = 30-32 per group, **(E)** by memory test and sex, N = 14-16 per group, **(F)** by memory test and genotype, N = 15-16 per group. **(G)** Hippocampus *DRD2* relative expression by memory test, **(H)** by memory test and sex, N = 14-16 per group, **(I)** By memory test and genotype, N = 15-17 per group. (*$p < 0.05$; **$p < 0.01$; ***$p < 0.001$). Boxplots represent the median, quartiles one and three form the box edges, and whiskers extend to the maximum and minimum values within 1.5 times the inter-quartile range. Individual data points are represented by black points and outliers are represented by crosses.

Relative expression of *DAT*, *DRD1*, and *DRD2* in the hippocampus were compared between memory groups for all mice. Differences in expression of HIPP DA target genes between conditioned and unconditioned mice were analyzed and not significant (Supplementary Figure 3). Mice in the 24-hour group had significantly higher relative *DAT* expression compared to mice in the 7-day group, W = 511, p = 0.025 (Figure 17A). Memory group by sex analysis revealed that there were significant differences in expression (H(3) = 13.8, p = 0.005) between groups, and a Dunn's post hoc showed that female mice in the 24-hour memory test had higher relative *DAT* expression compared to male mice in the 7-day memory test (p = 0.0028; Figure 17B). When analysing *DRD1* expression in the hippocampus, we observed that the difference in relative *DRD1* expression between memory test groups was not significant, but did approach significance (W = 609, p = 0.07; Figure 17D) and there were no interactions observed between sex or genotype (p >= 0.06). When analyzing relative *DRD2* expression in the hippocampus, we found that mice tested in the 24-hour memory test had significantly higher relative *DRD2* expression than mice tested in the 7-day memory test, W = 751, p < 0.001 (Figure 17G). Comparing memory test x sex subgroups revealed significant group differences, (H(3) = 19.49, p < 0.001) and a post hoc showed that male mice in the 24-hour test had significantly higher *DRD2* relative expression than males in the 7-day test (p = 0.0043) and female mice in the 24-hour test also had significantly higher *DRD2* relative expression compared to 7-day memory test males (p < 0.001; Figure 17H). Memory test x genotype subgroup analysis revealed significant group differences (H(3) = 14.84, p = 0.002) and a Dunn post hoc showed that *Nrxn1*$^{+/-}$ mice in the 24-hour test had significantly higher relative *DRD2* expression than *Nrxn1*$^{+/-}$ mice in the 7-day test (p = 0.033; Figure 17I), while wild-type mice in the 24-hour test

also had higher relative *DRD2* expression than *Nrxn1*$^{+/-}$ mice in the 7-day test ($p = 0.013$; Figure 17I). A sample size calculation was completed for HIPP relative DAT expression between males and females in both the 24-hour and 7-day memory test groups (Figure 17B). In the 24-hour test, males had a median DAT relative expression of 0.769 (IQR = 0.465) and females had a median relative expression on 1.5 (IQR = 0.505). The sample size for significance denoted at $p < 0.05$, a power value of 0.8, and with a correction for non-parametric data, would need to be 255 mice per group. For the 7-day memory test, median HIPP DAT expression differed between males (Median = 0.434, IQR = 0.624) and females (Median = 1.20, IQR = 0.442). The required sample size was calculated to be 18, and the current sample sizes were 13-15 mice per group. A sample size calculation was also completed for HIPP relative DRD2 expression between males (Median = 0.518, IQR = 0.624) and females (Median = 0.796, IQR = 0.442) in the 7-day memory test (Figure 17H). The calculation revealed that the required sample size per group would be 21.

To quantify if training was associated with gene expression, correlations between sugar consumed during training and relative expression of DAT, DRD1, and DRD2 were plotted for the brain regions of interest (Figure 18). Spearman's rank correlation was used to assess the relationship between sugar consumption and gene expression based on ranks. There was a moderate positive correlation between total sugar consumption during training and DRD2 relative expression in the olfactory bulb $\rho(30) = 0.37$, $p = 0.032$ (Figure 18C) as well as between DRD2 relative expression in the olfactory tubercle $\rho(30) = 0.34$, $p = 0.05$ (Figure 18F). Additionally, we found a moderate negative correlation between total sugar consumed and *DRD2* relative expression in the hippocampus, $\rho(30) = -0.426$, $p = 0.017$ (Figure 18I).

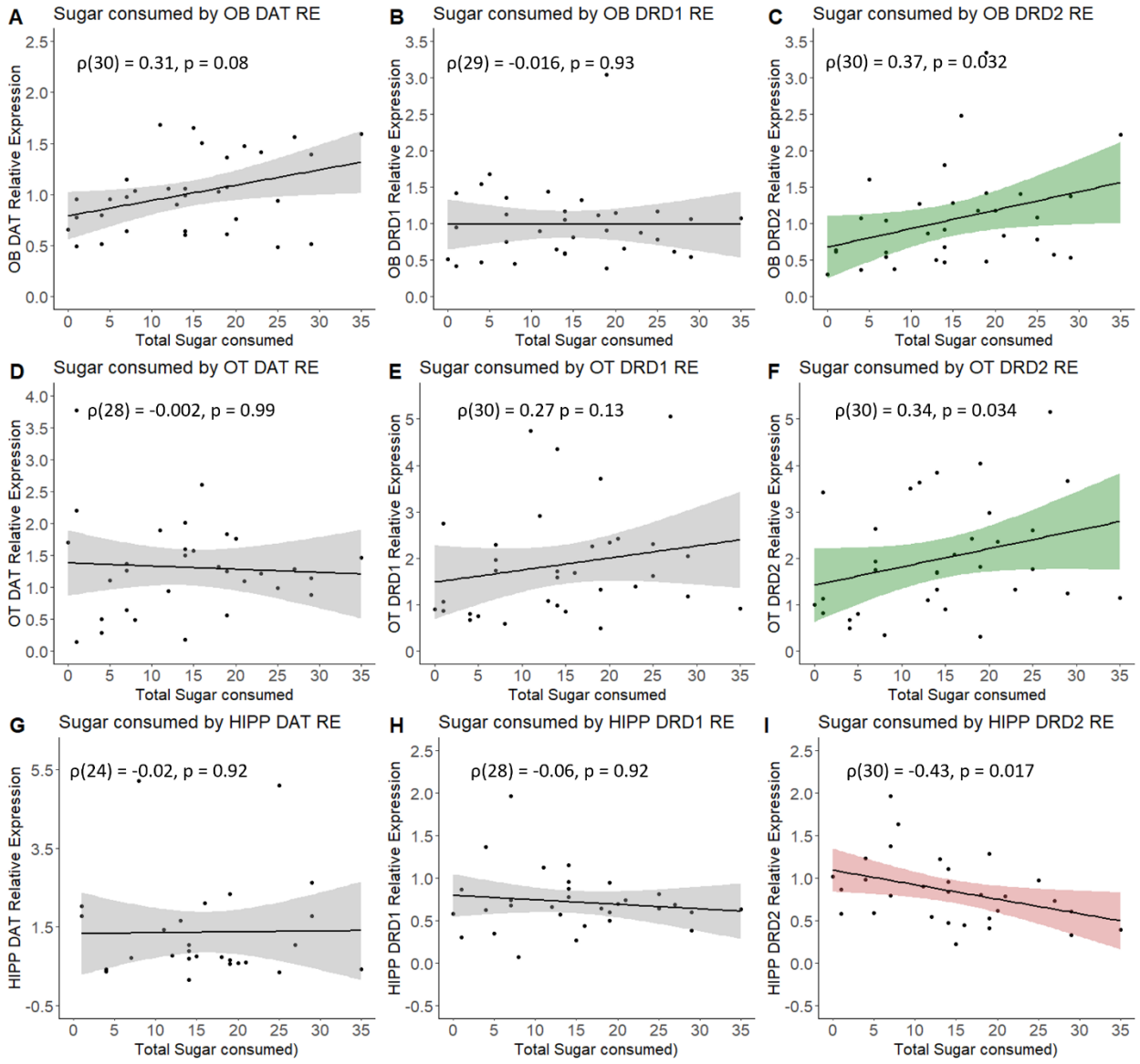

Figure 18. Correlations between total sugar grains consumed during training and relative gene expression of *DAT*, *DRD1*, and *DRD2* in the olfactory bulb, olfactory tubercle, and hippocampus of conditioned mice. N = 26-32 per group.

To further investigate the relationship between sugar consumption and gene expression, we divided the conditioned mice into 4 groups, male WT, male *Nrxn1*$^{+/-}$, female WT, and female *Nrxn1*$^{+/-}$ mice, and repeated the same correlation analysis (Figure 19,20,21). First, the relationship between sugar consumption and target gene expression in the olfactory bulb was

compared (Figure 19). Within these defined sex x genotype groups, male WT mice had a positive correlation between sugar consumption and relative DAT expression, $\rho(6) = 0.9$, $p = 0.002$ (Figure 19A) in the olfactory bulb. Additionally, female *Nrxn1*$^{+/-}$ mice had a significant positive correlation between sugar eaten and relative *DAT* expression in the olfactory bulb, $\rho(6) = 0.71$, $p = 0.049$ (Figure 19L). Similar analysis was completed within the olfactory tubercle (Figure 20); however, there were not any genotype x sex groups that showed a significant correlation between sugar consumption and target gene expression. Comparison of the relationship between sugar and target gene expression in the hippocampus (Figure 21) showed that only female *Nrxn1*$^{+/-}$ mice had a positive correlation between sugar consumption and *DAT* relative expression, $\rho(6) = 0.71$, $p = 0.049$ (Figure 21D).

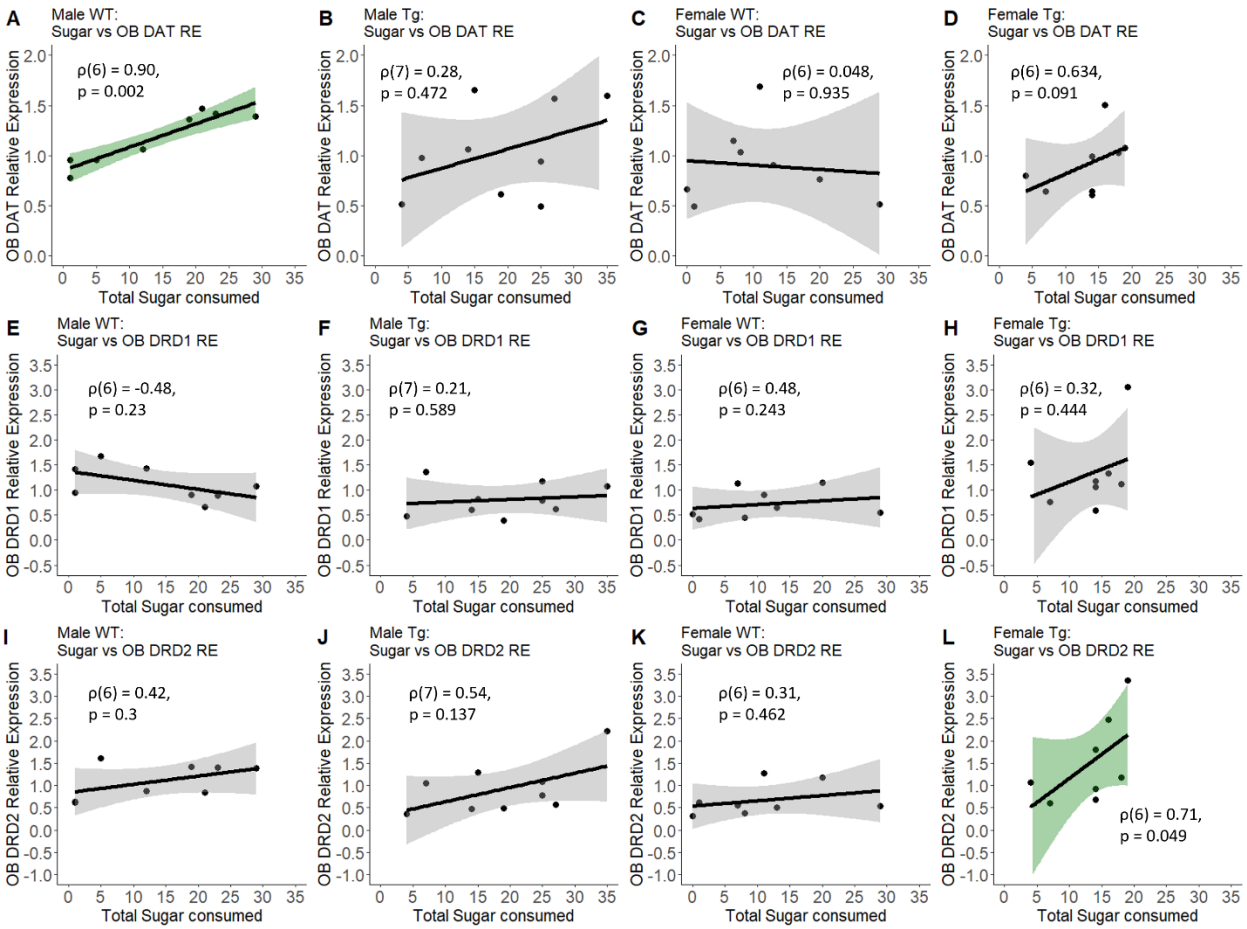

Figure 19. Correlations between total sugar consumed during training and relative gene expression of *DAT*, *DRD1*, and *DRD2* in the olfactory bulb of conditioned mice. N = 8-9 per group.

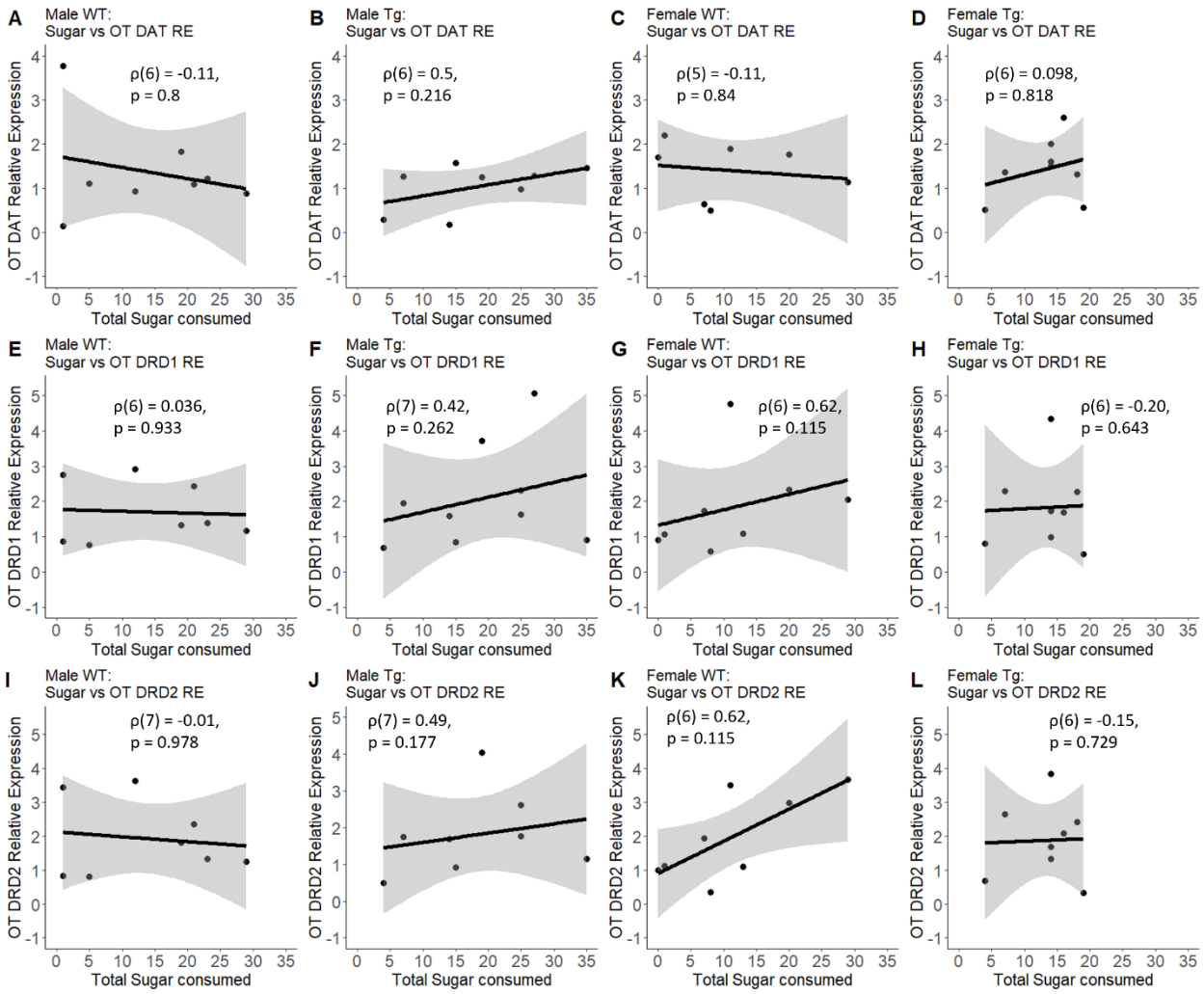

Figure 20. Correlations between total sugar consumed during training and relative gene expression of *DAT*, *DRD1*, and *DRD2* in the olfactory tubercle of conditioned mice. N = 6-9 per group.

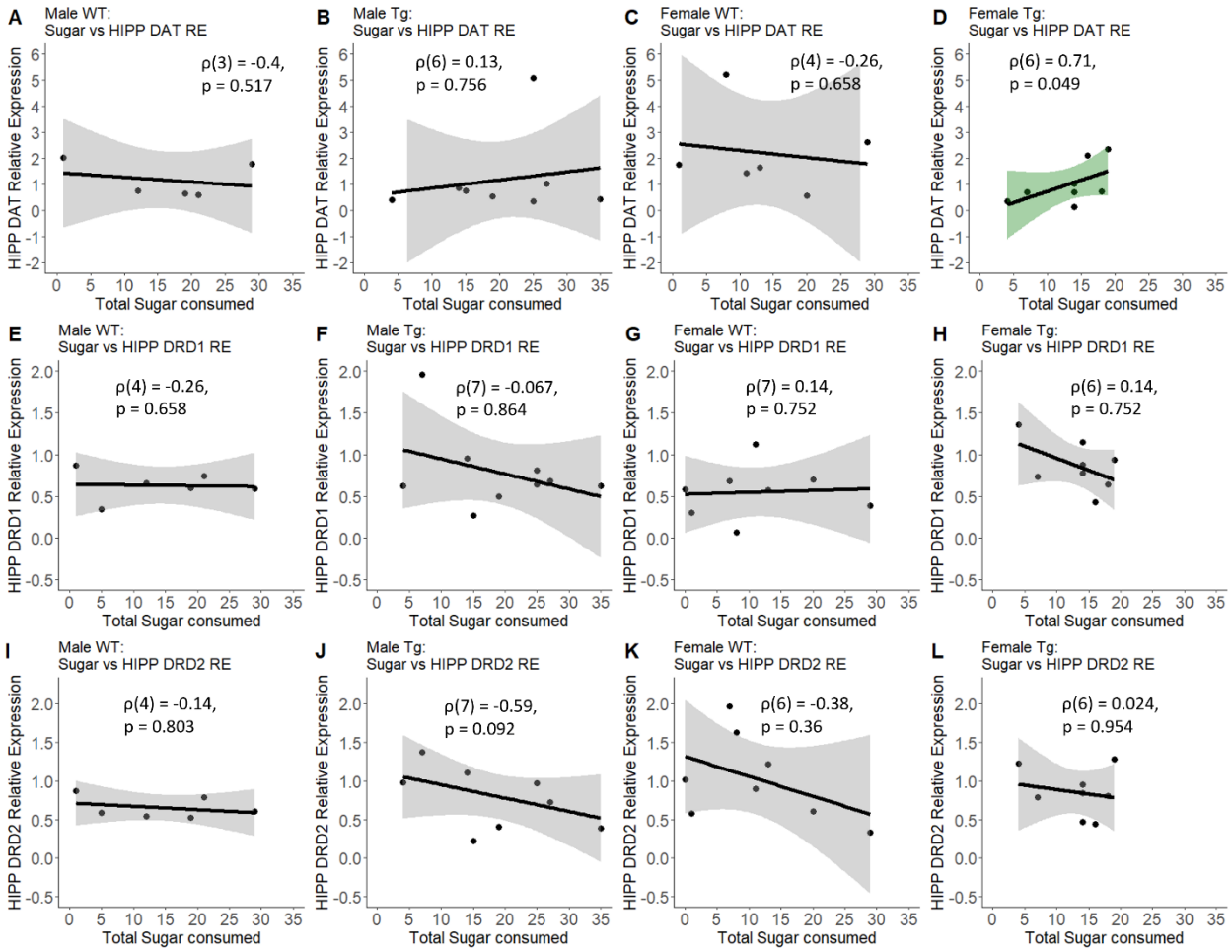

Figure 21. Correlations between total sugar consumed during training and relative gene expression of *DAT*, *DRD1*, and *DRD2* in the hippocampus of conditioned mice. N = 5-9 per group.

We found no significant correlations between the amount of time spent digging during training and expression of *DAT*, *DRD1*, and *DRD2* in the olfactory bulb, olfactory tubercle, and hippocampus of conditioned and unconditioned mice (Figure 22).

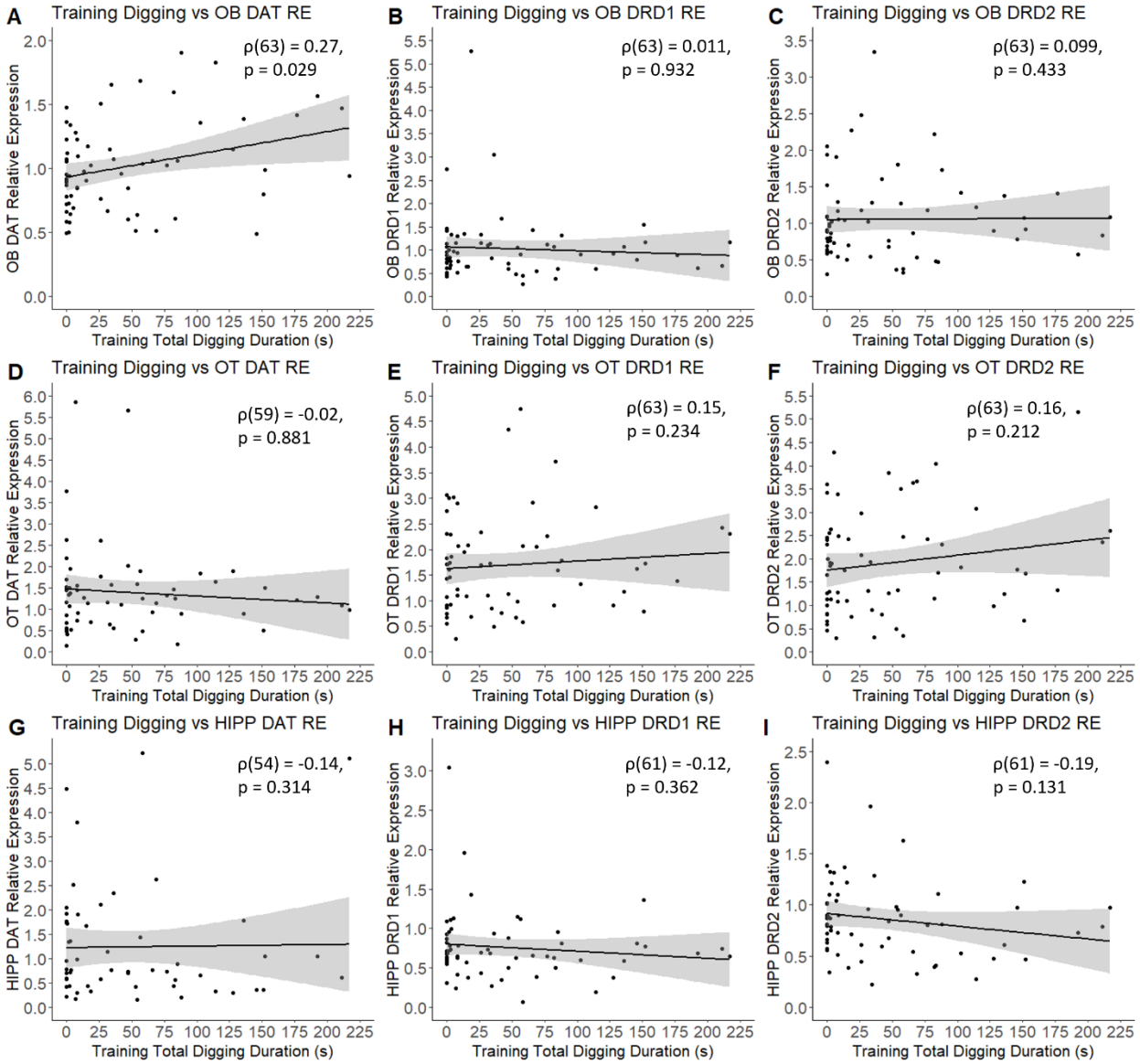

Figure 22. Correlations between total training digging duration (s) and relative gene expression of *DAT*, *DRD1*, and *DRD2* in the olfactory bulb, olfactory tubercle, and hippocampus of conditioned and unconditioned mice. N = 56- 65 per group.

CHAPTER 4: DISCUSSION

The purpose of this study was to assess if the *Nrxn1*$^{+/-}$ mouse model of autism spectrum disorder had impaired olfactory learning and memory based on a novel Pavlovian conditioning paradigm, and to what extent if any short term versus long term memory was impaired. We measured the gene expression of important DA circuitry targets including *DAT*, *DRD1*, and *DRD2* in the olfactory bulb, olfactory tubercle, and hippocampus of conditioned and unconditioned *Nrxn1*$^{+/-}$ and WT mice to assess if olfactory learning and memory capability correlated with DA molecular markers in the olfactory system.

4.1 Pavlovian Odour Conditioning

4.1.1 Training

During the training phase, conditioned mice consistently exhibited more digging in the odour pot than unconditioned mice (Figure 9A), suggesting that the observed digging behaviour during training was indicative of the mice searching for the sugar reward. Conditioned mice also dug in the odour pot significantly more than unconditioned mice during the 24-hour memory test (Figure 9C) and the 7-day memory test (Figure 9E); with mice in the unconditioned group exhibiting extremely minimal digging during memory tests. These results suggest that the digging behaviour observed in the conditioned group during the memory tests represents the learning and memory of the olfactory digging task.

We found no significant differences in the quality of training between genotypes or sexes as assessed by total digging duration during the eight training trials, mean digging latency,

and total sugar consumed during the training phase (Figure 10). These findings suggest that the training performance was similar for *Nrxn1*$^{+/-}$ and WT mice.

During the training phase, the mean latency to start digging in order to find the sugar reward during the 8 training trials was measured and analysed. Latency to find buried food has not yet been assessed in a *Nrxn1-α/β/γ* knockdown mouse model; however, this has previously been measured in a *Nrxn3-α/β* KO mouse model (Aoto et al., 2015), a *Nrxn1* KO mouse model (Grayton et al., 2013), and a *Nlgn* KO mouse model (Radyushkin et al., 2009). Both *Nrxn3-α/β* KO mice and *Nlgn* KO mice demonstrated increased latency to find buried food in comparison to controls, indicating potential olfactory deficits in these models (Aoto et al., 2015; Radyushkin et al., 2009); however, *Nrxn1* KO mice did not have increased latency to find food compared to controls (Grayton et al., 2013). We found no significant differences in digging latency between genotypes (Figure 10B), suggesting that *Nrxn1*$^{+/-}$ mice do not have an olfactory processing deficit. This result aligns with the results of Grayton and colleagues (2013) and suggests that *Nrxn1* may not be essential in olfactory detection; however, the literature indicates that reductions in other *Nrxn* genes and *Nrxn* binding partners (i.e., *Nrxn3* and *Nlgn*) may in fact contribute to olfactory deficits (Aoto et al., 2015; Radyushkin et al., 2009). Although an established buried food protocol (Yang & Crawley, 2009) was not used in the study, the total amount of sugar consumed and mean digging latency during the training was similar for *Nrxn1*$^{+/-}$ and WT mice. Based on these results, the *Nrxn1*$^{+/-}$ mice did not show olfactory deficits, but further studies analyzing latency to find buried food with an established buried food protocol should be completed to allow for more robust comparison of food finding behaviour in *Nrxn1*$^{+/-}$ to the previous literature.

4.1.2 Memory Tests

When examining the digging behaviour between *Nrxn1*$^{+/-}$ and WT mice in the 24-hour and 7-day memory test, both the latency to dig and digging duration were measured. Interestingly, no significant differences in total digging duration were observed between genotypes, and there were no significant differences between sexes. Both WT and *Nrxn1*$^{+/-}$ mice had very low levels of digging in the 24-hour and 7-day memory tests (Figure 11A, 12A). This could indicate that the training phase was insufficient for the mice to robustly learn and remember the task. The low digging level of WT mice in the current studies raises concerns, as the WT group is our control group, and previous studies using a similar olfactory learning task have shown robust odour learning and memory in WT mice of varying background strains (O'Leary et al., 2020; Schellinck et al., 2001). Specifically, a study by O'Leary and colleagues (2020) utilized a conditioned odour preference task in order to study olfactory memory between a transgenic model of Alzheimer's disease and WT control mice (C57BL/6J x SJL/J). The training protocol in this study, originally described by Schellinck and colleagues (2001), consisted of 4 training trials over 4 days, where mice were presented with two odours, one paired with sugar (CS+) and one without sugar (CS-). The odour conditioning paradigm utilized in the current study differs from the protocol described in O'Leary et al. (2020) and Schellinck et al. (2001) in several ways. A notable difference between the protocols is that in Schellinck et al. (2001), the paradigm describes an olfactory discrimination task, which utilizes two odours and assesses the ability for mice to discriminate between the conditioned odour and the unconditioned odour. The current study adapted this protocol so that mice were only exposed to a CS+ odour, and there was a separate group of mice that were unconditioned; i.e., were

exposed to an odour pot lacking sugar. Because mouse brain tissue was collected after the olfactory memory test, the altered protocol was chosen to assess the molecular effects of the olfactory learning and memory paradigm, without including additional inhibitory signals that would occur in mice exposed to a CS- odour. Thus, the current Pavlovian odour conditioning paradigm was selected in order to simplify the experimental design and assess how conditioning to a single odour altered DA gene expression in the brain. However, the low levels of digging in WT mice suggest that 8 training trials over 1 day, without the inclusion of a CS- odour, was not sufficient to reliably teach the mice the protocol.

4.1.3 Training and Memory Test Relationship

Given the large amount of individual variation observed between mice in the training and testing phases, the relationship between training and memory test digging was examined to determine if there were any meaningful differences between genotypes or sexes, while accounting for the large quantity of mice that exhibited low digging. Overall, training digging was positively correlated with memory test digging in conditioned mice (Figure 13), and this trend appears to be driven by the male mice, irrespective of genotype (Figure 13B, C). Similarly, when analysing the relationship between sugar consumption and memory test digging, males showed a significant positive correlation between sugar consumed and digging duration in memory tests, while no correlation was observed for female mice (Figure 14B). These results provide support for differential influence of a *Nrxn1* knockdown on male and female mice, as it appears that male mice who performed well in training, performed proportionally well in testing, while this was not the case for females. These results align with previous research indicating that *Nrxn1* knockdown and knockouts can differentially influence sexes. Grayton et al.

(2013) found that female *Nrxn1-α* KO mice had reduced locomotor activity compared to male *Nrxn1-α* KO mice, while male *Nrxn1-α* KO mice had increased aggression during a social investigation task. Such results show how alterations in *Nrxn1* gene expression can impact male and female mice differently, making the inclusion of sex analysis very important.

4.2 *DAT, DRD1*, and *DRD2* RNA Expression

4.2.1 *DAT* relative expression in the OB, OT, and HIPP

Overall, an intriguing pattern of relative *DAT* expression between the brain regions of interest was observed in this study. In the olfactory bulb, there were no differences in relative *DAT* expression between memory test groups, genotypes, or sexes (Figure 15A-C). However, alterations in relative *DAT* expression in both the olfactory tubercle and the hippocampus were observed between memory test groups.

Relative *DAT* expression was found to be enhanced in the olfactory tubercle of mice in the 7-day memory test compared to the 24-hour memory test (Figure 16A). Specifically, *Nrxn1*$^{+/-}$ mice in the 24-hour memory test had lower relative *DAT* expression than *Nrxn1*$^{+/-}$ mice in the 7-day test (Figure 16C). In combination, these results suggest that olfactory tubercle *DAT* expression is modified with a main effect of memory test time, and an interaction between memory test time and genotype. This interesting main effect of memory test suggests that expression of the DA transporter is enhanced when the mice were re-introduced to the odour and/or specific context they experienced during training, 7-days after, but not 24-hours after initial training. Additionally, given that there were no significant differences found between training groups, these results are applicable to both conditioned and unconditioned mice. Thus,

the increase in relative *DAT* expression cannot be the result of learning and recalling the memory to dig in the odour pot, but instead could potentially be associated with the exposure to the novel lemon odour, or the environment of the testing cage. In the current study it is difficult to determine how relative *DAT* expression in the OT changes from training to the 24-hour test, to the 7-day test. In future, mouse tissues should be collected before or immediately after training to measure and compare baseline levels of *DAT* expression, to determine if baseline OT *DAT* expression differs between genotypes or sexes prior to the introduction of an olfactory training paradigm.

DAT relative expression was found to be reduced in the hippocampus of mice in the 7-day memory test compared to mice in the 24-hour memory test. This difference was also observed in both conditioned and unconditioned mice, suggesting that the differential expression of *DAT* in the hippocampus was not a result of digging during the memory paradigm, given that mice in the unconditioned group exhibited extremely low levels of digging in the 24-hour (Figure 9C) and 7-day (Figure 9E) memory tests. We also found no significant differences in *DAT* expression between genotypes, but female mice in the 24-hour test had significantly higher expression than male mice in the 7-day test (Figure 17B), although this comparison between different factors is not meaningful. A sample size calculation was completed for males and females in the 7-day memory test group since visual data observation indicated a potential difference between sexes, with females having greater expression than males (Figure 17B). The calculation revealed that a total of 18 mice would be required per group to reach a significance value of 0.05 with a power of 0.8. Given that the current sample size was 13-15 per group, this calculation indicates that there may be a meaningful difference in DAT relative expression

between male and female mice in the 7-day memory group, but adding several more mice to each group could confirm this potential finding.

While it is known that DA neurons within the olfactory bulb are highly plastic and dependent on sensory input, modulation in *DAT* relative expression within the olfactory bulb was not observed. The observed increase in relative *DAT* expression in the olfactory tubercle and the decrease in relative *DAT* expression in the hippocampus of mice tested 7-days after initial odour exposure at training, may be related to the sensory input received by mice during the memory tests, since both conditioned and unconditioned mice were exposed to the lemon odour during memory testing. In fact, one study found that mice exposed to lemon essential oil vapour showed reduced anxiety in an elevated plus-mase, an open field task, and a forced swimming task, and also had significantly enhanced dopamine metabolism in the hippocampus (Komiya et al., 2006). Our findings further suggest that exposure to lemon odour may result in altered dopamine activity in olfactory system brain regions, but further work should be completed to identify the time course of DA activity after lemon exposure, and how multiple presentations of lemon odour may affect DA activity.

DAT is a crucial player in DA homeostasis, as it enables the transport of DA from the extracellular space back into presynaptic neurons. When DAT does not function properly, the buildup of cytosolic DA can become toxic to neurons (Mosharov et al., 2009); however, too much expression of *DAT* can also be harmful (Masoud et al., 2015). There is little research on the modulation of *DAT* expression in the olfactory tubercle and hippocampus, but the results suggest that these areas are distinctly modulated during a Pavlovian odour conditioning paradigm, in both conditioned and unconditioned mice.

Some studies have demonstrated that there is limited expression of DAT in the hippocampus (Kwon et al., 2008) and that DA clearance in the hippocampus is regulated by the norepinephrine transporter (*Slc6a2* gene) (Borgkvist et al., 2012). Based on this information from the literature, RT-qPCR was initially completed to measure expression of *Slc6a2* in the hippocampus of mice. The RT-qPCR results indicated very low *Slc6a2* expression, with Cq values beginning at approximately 36, and many samples showing no amplification. Due to the insufficient amplification, we pivoted our efforts to DAT instead, and sufficient DAT amplification in the hippocampus was observed. These findings contradict the literature regarding low expression of DAT in the hippocampus, as the results not only suggest that DAT is expressed in the hippocampus, but that expression can be affected by an olfactory learning paradigm. Studies assessing DAT in the hippocampus have mainly measured protein levels through radiolabelled RTI-55 and immunofluorescence (Borgkvist et al., 2012; Ciliax et al., 1999; Kwon et al., 2008); thus, completing ELISA assays on DAT protein levels in the hippocampus of mice could aid in better comparing our research to these mentioned studies.

In the hippocampus, DA binds to D1 receptors to promote formation of episodic memories and synaptic plasticity; however, the reduction of *DAT* expression in the hippocampus of mice after the 7-day memory test may indicate reduced requirement for DA transport, and thus, reduced dopaminergic signalling in the hippocampus at the 7-day memory test compared to the 24-hour memory test. It is possible that after the training phase; where both the unconditioned and conditioned mice would have encoded an episodic memory about the novel training environment and odour experience, *DAT* expression gradually decreases. This could provide support for why the relative *DAT* expression is reduced from the 24-hour test to the 7-

day test. However, more evidence would be required to support this idea, and the initial expression levels of hippocampal *DAT* would need to be assessed in mice who do not experience the training protocol and in mice directly after the training protocol.

4.2.2 *DRD1* relative expression in the OB, OT, and HIPP

A different expression pattern was observed in *DRD1* expression compared to *DAT*. *DRD1* relative expression decreased by memory group in the olfactory bulb (Figure 15D), while *DRD1* relative expression remained constant in both the olfactory tubercle (Figure 16D-F) and the hippocampus (Figure 17D-F) over time, genotype, and sex. Similar to the observations of *DAT* expression, the decrease in relative *DRD1* expression in the olfactory bulb was across both conditioned and unconditioned mice.

Recent research has indicated that experience-dependent changes in olfactory bulb DA neurons occur rapidly and involve changes in enzyme expression (Byrne et al., 2022), supporting the notion that sensory experiences have the ability to rapidly modulate expression of proteins like DA receptors in the olfactory bulb over time, as observed here. Specifically, modulation of *DRD1* expression in the olfactory bulb aligns with previous research suggesting the main neuromodulators of olfactory bulb dopaminergic neurons are DRD1 and DRD2, which work through opposing functions. DRD1 is important in odour detection in rodents (Doty et al., 1998; Doty & Risser, 1989; Escanilla et al., 2009), and downregulation of *DRD1* expression in the olfactory bulb of mice after the 7-day memory test could be representative of reduced odour salience in the 7-day test, compared to the 24-hour test.

4.2.3 *DRD2* relative expression in the OB, OT, and HIPP

DRD2 relative expression remained stable across time, between genotypes, and sexes in both the olfactory bulb (Figure 15G-I) and the olfactory tubercle (Figure 16G-I). However, we found reduced relative *DRD2* expression in the 7-day memory test compared to the 24-hour memory test in the hippocampus (Figure 17G). Additionally, both males and females in the 24-hour test had higher relative *DRD2* expression than males in the 7-day test, while both *Nrxn1*$^{+/-}$ and WT mice in the 24-hour test had higher expression than *Nrxn1*$^{+/-}$ mice in the 7-day test (Figure 17H, I). A sample size calculation was completed for DRD2 expression of males and females in the 7-day memory test group (Figure 17B). The calculation revealed that a total of 21 mice would be required per group to reach a significance value of 0.05 with a power of 0.8. Since the current sample size was 14-16 per group, this calculation indicates that there may be a meaningful difference in DRD2 relative expression between male and female mice in the 7-day memory group, but more mice should be added to confirm this.

Like *DRD1*, the function of *DRD2* in the hippocampus is to regulate neuron excitability and encode hippocampus-dependent memories (Dubovyk & Manahan-Vaughan, 2019). Similar to the reduced *DAT* expression in the hippocampus of mice after the 7-day memory test, the reduced relative expression of *DRD2* relative to the 24-hour memory test, may indicate reduced requirements of DA-dependent memory formation in the hippocampus. Since a whole week would have passed between the novel odour experienced in the training and the 7-day test, whereas only 24-hours would have passed between the training day and the short-term memory test, changes in *DRD2* expression brought upon by the training day could have

returned to baseline after 1 week. However, the measurement of baseline *DRD2* expression levels would also be important to assess in order to make this conclusion.

4.2.4 Correlations between *DAT*, *DRD1*, and *DRD2* relative expression and sugar consumption

Moderate positive correlations between *DRD2* relative expression and total sugar consumption in training were observed both in the olfactory bulb and the olfactory tubercle, whereas a moderate negative correlation between *DRD2* expression and total sugar consumption was observed in the hippocampus of conditioned mice (Figure 18). This overall effect of sugar consumption on *DRD2* relative expression is very interesting, but aligns with previous research, as it is well known that food rewards have substantial effects on the synaptic modifications of the mesolimbic DA circuit (Baik, 2013). Indeed, mice with a presynaptic D2 receptor KO have shown enhanced motivation for food rewards, potentially meaning that the loss of presynaptic inhibition by D2 autoreceptors could increase extracellular DA, increase stimulation of postsynaptic DA receptors, and lead to enhanced food motivation (Bello et al., 2011). Since D2 autoreceptors exert negative feedback that reduces DA firing, synthesis, and release (Bello et al., 2011), it is intriguing that *DRD2* expression increased with sugar consumption in the olfactory bulb and olfactory tubercle but decreased with increased sugar consumption in the hippocampus. However, the role of *DRD2* in food motivation is not clearly defined, as a different study found that D2 receptor KO mice have reduced food intake and body weights compared to littermate controls (Kim et al., 2010). Our results indicate that the specific *DRD2* expression changes modulated by food reward are distinct between brain regions.

When the conditioned mice were divided into sex x genotype groups to further assess the correlations between *DAT*, *DRD1*, and *DRD2* relative expression and total sugar

consumption, only male WT and female *Nrxn1*$^{+/-}$ mice had relationships between *DAT* relative expression and sugar consumption. Specifically, male WT mice had a strong positive correlation between *DAT* expression and sugar consumption in the olfactory bulb (Figure 19A), while female *Nrxn1*$^{+/-}$ mice had a strong positive correlation between *DAT* expression and sugar consumption in the hippocampus (Figure 21D). No significant correlations were found between reward consumed and *DRD1* expression in any of the genotype x sex groups. The only sex x genotype group that showed a correlation between *DRD2* expression and sugar consumption, was female *Nrxn1*$^{+/-}$ mice in the olfactory bulb, who had a strong positive correlation between these variables (Figure 19L).

By completing correlations within the sex x genotype groups, it becomes evident that the trends in *DRD2* expression observed with all conditioned mice, are not consistent within the smaller groups. In fact, the only group with an observed correlation between *DRD2* expression and sugar consumption is female *Nrxn1*$^{+/-}$ mice in the OB. The correlation between sugar consumption and expression of *DRD2* in the OB of female *Nrxn1*$^{+/-}$ mice (Figure 19L) does follow the same trend as the overall group correlation (Figure 18C). As well, the correlations observed in the male WT and female *Nrxn1*$^{+/-}$ groups are much stronger than those observed in the collapsed group, providing stronger evidence that sugar consumption is positively correlated with DAT expression in the OB of male WT mice and the HIPP of female *Nrxn1*$^{+/-}$ mice, and *DRD2* expression is positively correlated with sugar consumption in the OB of female *Nrxn1*$^{+/-}$ mice.

Interestingly, there was no significant correlations between total training digging and target gene expression (Figure 22), suggesting that gene expression changes were due to sugar consumption, rather than the digging duration during training.

4.3 Limitations

A primary limitation of this study was the quality of training that occurred in the Pavlovian odour conditioning paradigm. The initial protocol that was developed by Schellinck et al. (2001) was an olfactory discrimination task which included a total of 32 training trials over 4 days. In this protocol, mice were trained to associated one odour with a reward and another odour with no reward, then were tested on their ability to distinguish the different odours. An important difference between the initial paradigm created by Schellinck et al. (2001) and the current paradigm, is that the protocol utilized in this study did not test olfactory discrimination; instead, it tested only olfactory memory, since mice were taught only how to associate one odour with a sugar reward. Previous protocols completed within the Brown lab have demonstrated that mice were able to successfully learn the original odour discrimination task within 8 training trials over 1 day (Brown et al., in press), greatly reduced from the initial 32 trials over 4 days (Schellinck et al., 2001). Based on this data, I completed my adapted Pavlovian odour conditioning paradigm using the same reduced time frame. However, both WT and *Nrxn1*$^{+/-}$ mice in the current study showed low levels of digging, indicating that the training protocol may not have been sufficient to produce robust learning.

The current study was limited by the extensive individual variation observed in WT and *Nrxn1*$^{+/-}$ mice. The training protocol likely influenced the observed individual variation, and we predict that enhanced training would reduce the extensive variation in behaviour. However, the 1-day training protocol also may not have been ideal considering the estrous cycle of female mice, which lasts 4-5 days (Chari et al., 2020). In a 1-day training protocol, we cannot control for

any effects caused by hormonal fluctuations. However, recent studies have found that female C57BL/6J mice during estrous cycles show differences in social interaction tasks, but anxiety, working memory, or motor learning tasks were not influenced by estrous cycles (Chari et al., 2020; Lovick & Zangrossi, 2021). A longer training paradigm could help to control for any potential variations caused by estrous cycle and would also aid in reducing the extreme individual variation.

An additional limitation of the current study is the difficulty in dissociating the neural response activity of the lemon odour from the neural activity of the conditioned response to the lemon odour. We found that both conditioned and unconditioned mice showed alterations in DA target gene expression, suggesting that the results observed were not strictly due to the conditioned response to the lemon odour. However, the unconditioned mice were also exposed to the same contexts as the conditioned mice, so future studies could analyze a group of mice that are exposed to the lemon odour only, without the context of the Pavlovian odour conditioning paradigm. This distinction would help to further parse out if the exposure to the lemon order in particular is driving the observed DA target gene expression changes.

Another limitation associated with this study is that we assessed *DAT*, *DRD1*, and *DRD2* gene expression in full sections of the olfactory bulb, olfactory tubercle, and the hippocampus. That is to say, we did not differentiate distinct regions within these brain areas, such as the ventral and dorsal regions of the hippocampus. The functional differences between the dorsal and ventral hippocampal regions have mostly been identified in fear conditioning contexts (Richmond et al., 1999; Yoon & Otto, 2007). There also appears to be differences in the functioning of dorsal and ventral hippocampal subregions during odour learning, with results

suggesting as the learning process progresses towards reaching criterion, the hippocampus functions as a unit, while in earlier stages of olfactory learning, the two subregions may have separate functions (Martin et al., 2007). Given that many mice in the current study had relatively low learning, it is a possibility that the ventral and dorsal hippocampal subregions may have been functioning distinctly during the Pavlovian conditioning odour paradigm, since many mice did not attain high levels of digging during training.

Another limitation of this study is that we were unable to complete ELISA assays in order to quantify the protein levels of DAT, DRD1, and DRD2 in the olfactory bulb, olfactory tubercle, and the hippocampus. The inclusion of this data would have been beneficial in order to compare if relative RNA expression findings correlated with protein levels, to further support our findings. Unfortunately, time-constraints did not allow for this part of the project to be completed; however, future research to extend this study should measure protein levels in the olfactory bulb, olfactory tubercle, and the hippocampus, and compare protein levels with RNA expression.

As mouse brain tissue was not collected immediately after the completion of training, we are unable to compare the stability of *DAT*, *DRD1*, and *DRD2* expression between training, the 24-hour memory test, and the 7-day memory test. This data would be useful in further understanding how DA circuitry is modulated in *Nrxn1*$^{+/-}$ and WT mice throughout all stages of the Pavlovian conditioned odour paradigm and would provide more context regarding the differences we observed in DA target relative expression between the 24-hour and 7-day memory tests.

4.4 Concluding Remarks

Overall, we have shown that *Nrxn1*$^{+/-}$ mice do not demonstrate impaired olfactory learning or memory based on the 1-day Pavlovian odour conditioning paradigm, supporting the idea that *Nrxn1* expression may not be required in the functions of olfactory learning or memory in mice. The limitations discovered about the current Pavlovian odour conditioning paradigm provide us with important information regarding testing efficacy and open other exciting avenues of investigation to further refine conditioned olfactory memory paradigms.

Training behaviour of male mice was found to be positively correlated with memory test digging, while the training behaviour of female mice was not correlated with memory tests. These results indicate that male and female mice may have distinct learning and memory profiles in odour conditioned paradigms, and thus, further highlight how sex differences are important to investigate when characterizing *Nrxn1*$^{+/-}$ mouse models.

We found significant differences in DA target expression between memory tests and distinct relationships between sugar consumption during training and *DRD2* expression in the olfactory bulb, olfactory tubercle, and the hippocampus. However, no significant differences were found in DA target expression between *Nrxn1*$^{+/-}$ and WT mice, thus, the observed modulations are likely not mediated by *Nrxn1* as predicted.

Overall, the observed modulations in DA target circuitry appear to be mainly affected by time (24-hour test versus 7-day test); providing interesting information regarding time-dependent modulation of DA targets, and opening the door to further investigate how *DAT*, *DRD1*, and *DRD2* expression change at various time points throughout an odour conditioning

paradigm. As well, *DRD2* expression was moderately correlated with reward consumption in the training phase, and this relationship varied in different brain regions. Breakdown of sex x genotype groups revealed strong correlations between sugar consumption and hippocampal DAT expression, as well as olfactory bulb DRD2 expression specifically in female *Nrxn1*$^{+/-}$ mice. Further, male WT mice showed a strong positive correlation between relative hippocampal DAT expression and sugar consumption. These correlations provide evidence that DAT is involved in important hippocampal functions related to reward.

Overall, these results provide important insights into DA circuit regulation during an odour learning paradigm and demonstrate that observed effects do not appear to be mediated by *Nrxn1* expression based on this model. Instead, observed DA activity may instead be in response to odour presentation and episodic olfactory memories; an avenue that would need to be further studied in the future.

4.5 Future Directions

Based on the results and considering the limitations of the current study, one possibility for future investigation would be to refine the novel Pavlovian conditioning paradigm such that mice are trained to a particular criterion, or training time is increased to ensure robust acquisition of the task. This would ensure that the results obtained from memory tests are accurate and would decrease the large inter-individual variation between mice that was observed in the current study. Another interesting avenue to investigate would be to measure if *Nrxn1*$^{+/-}$ mice have deficits in an olfactory discrimination task (Schellinck et al., 2001) and if observed modulations in DA target receptors are similar, or different to what we observed in the

current study. Other tasks assessing olfactory function, such as a buried food task (Yang & Crawley, 2009), could be included to directly assess potential olfactory deficits of the *Nrxn1*$^{+/-}$ mice.

Future studies should assess the protein levels of DAT, DRD1, and DRD2 in the *Nrxn1*$^{+/-}$ mouse model in order to assess if the relationship observed in RNA expression in the current study is consistent with protein levels. Specifically, measuring hippocampal DAT protein levels would help to clarify the role of DAT in the hippocampus, and could enable better comparison between our study and previous studies indicating low hippocampal DAT levels (Borgkvist et al., 2012; Kwon et al., 2008).

Given the distinct anatomical and functional regions in the olfactory bulb, the olfactory tubercle, and the hippocampus (Martin et al., 2007; Mombaerts, 2006; Murata et al., 2015), further work to help distinguish potential differences in DA targets within brain regions should be completed. The protein expression of DAT, DRD1, and DRD2 can be assessed through immunofluorescence or immunohistochemistry protocols to differentiate how different cell types in these brain regions express DA target genes in the context of an olfactory learning paradigm.

Additionally, the current study selected a few DA targets, including *DAT*, *DRD1*, and *DRD2* to investigate in relation to *Nrxn1* depletion in the context of an olfactory learning and memory paradigm. However, we could gain a better idea of modulations in gene expression in the *Nrxn1*$^{+/-}$ mouse model by completing a whole exome gene array. This would allow for a more

robust assessment of *Nrxn1* gene regulation in the context of all gene expression and provide further future avenues to research.

BIBLIOGRAPHY

Abrahams, B. S., & Geschwind, D. H. (2008). Advances in autism genetics: On the threshold of a new neurobiology. *Nature Reviews Genetics*, *9*(5), Article 5. https://doi.org/10.1038/nrg2346

Alarcón, M., Abrahams, B. S., Stone, J. L., Duvall, J. A., Perederiy, J. V., Bomar, J. M., Sebat, J., Wigler, M., Martin, C. L., Ledbetter, D. H., Nelson, S. F., Cantor, R. M., & Geschwind, D. H. (2008). Linkage, Association, and Gene-Expression Analyses Identify CNTNAP2 as an Autism-Susceptibility Gene. *American Journal of Human Genetics*, *82*(1), 150–159. https://doi.org/10.1016/j.ajhg.2007.09.005

American Psychiatric Association. (2022). Diagnostic and statistical manual of mental disorders (5th ed., text rev.). https://doi.org/10.1176/appi.books.9780890425787

Anderson, G. R., Aoto, J., Tabuchi, K., Földy, C., Covy, J., Yee, A. X., Wu, D., Lee, S.-J., Chen, L., Malenka, R. C., & Südhof, T. C. (2015). β-Neurexins Control Neural Circuits by Regulating Synaptic Endocannabinoid Signaling. *Cell*, *162*(3), 593–606. https://doi.org/10.1016/j.cell.2015.06.056

Aoto, J., Földy, C., Ilcus, S. M. C., Tabuchi, K., & Südhof, T. C. (2015). Distinct circuit-dependent functions of presynaptic neurexin-3 at GABAergic and glutamatergic synapses. *Nature Neuroscience*, *18*(7), Article 7. https://doi.org/10.1038/nn.4037

Aqrabawi, A. J., Browne, C. J., Dargaei, Z., Garand, D., Khademullah, C. S., Woodin, M. A., & Kim, J. C. (2016). Top-down modulation of olfactory-guided behaviours by the anterior olfactory nucleus pars medialis and ventral hippocampus. *Nature Communications*, *7*(1), Article 1. https://doi.org/10.1038/ncomms13721

Autism and Developmental Disabilities Monitoring Network Surveillance Year 2008 Principal Investigators & Centers for Disease Control and Prevention. (2012). Prevalence of autism spectrum disorders—Autism and Developmental Disabilities Monitoring Network, 14 sites, United States, 2008. *Morbidity and Mortality Weekly Report. Surveillance Summaries (Washington, D.C.: 2002)*, *61*(3), 1–19. https://pubmed-ncbi-nlm-nih-gov.ezproxy.library.dal.ca/22456193/

Baik, J.-H. (2013). Dopamine Signaling in reward-related behaviors. *Frontiers in Neural Circuits*, *7*, 152. https://doi.org/10.3389/fncir.2013.00152

Baird, G., Simonoff, E., Pickles, A., Chandler, S., Loucas, T., Meldrum, D., & Charman, T. (2006). Prevalence of disorders of the autism spectrum in a population cohort of children in South Thames: The Special Needs and Autism Project (SNAP). *The Lancet*, *368*(9531), 210–215. https://doi.org/10.1016/S0140-6736(06)69041-7

Bakkaloglu, B., O'Roak, B. J., Louvi, A., Gupta, A. R., Abelson, J. F., Morgan, T. M., Chawarska, K., Klin, A., Ercan-Sencicek, A. G., Stillman, A. A., Tanriover, G., Abrahams, B. S., Duvall, J. A., Robbins, E. M., Geschwind, D. H., Biederer, T., Gunel, M., Lifton, R. P., & State, M. W. (2008). Molecular Cytogenetic Analysis and Resequencing of Contactin Associated Protein-Like 2 in Autism Spectrum Disorders. *American Journal of Human Genetics*, *82*(1), 165–173. https://doi.org/10.1016/j.ajhg.2007.09.017

Bayer, H. M., & Glimcher, P. W. (2005). Midbrain Dopamine Neurons Encode a Quantitative Reward Prediction Error Signal. *Neuron*, *47*(1), 129–141. https://doi.org/10.1016/j.neuron.2005.05.020

Bello, E. P., Mateo, Y., Gelman, D. M., Noaín, D., Shin, J. H., Low, M. J., Alvarez, V. A., Lovinger, D. M., & Rubinstein, M. (2011). Cocaine supersensitivity and enhanced motivation for reward in mice lacking dopamine D2 autoreceptors. *Nature Neuroscience*, *14*(8), 1033–1038. https://doi.org/10.1038/nn.2862

Béna, F., Bruno, D. L., Eriksson, M., van Ravenswaaij-Arts, C., Stark, Z., Dijkhuizen, T., Gerkes, E., Gimelli, S., Ganesamoorthy, D., Thuresson, A. C., Labalme, A., Till, M., Bilan, F., Pasquier, L., Kitzis, A., Dubourgm, C., Rossi, M., Bottani, A., Gagnebin, M., … Schoumans, J. (2013). Molecular and clinical characterization of 25 individuals with exonic deletions of NRXN1 and comprehensive review of the literature. *American Journal of Medical Genetics Part B: Neuropsychiatric Genetics*, *162*(4), 388–403. https://doi.org/10.1002/ajmg.b.32148

Borgkvist, A., Malmlöf, T., Feltmann, K., Lindskog, M., & Schilström, B. (2012). Dopamine in the hippocampus is cleared by the norepinephrine transporter. *The International Journal of Neuropsychopharmacology*, *15*(4), 531–540. https://doi.org/10.1017/S1461145711000812

Boucard, A. A., Chubykin, A. A., Comoletti, D., Taylor, P., & Südhof, T. C. (2005). A Splice Code for trans-Synaptic Cell Adhesion Mediated by Binding of Neuroligin 1 to α- and β-Neurexins. *Neuron*, *48*(2), 229–236. https://doi.org/10.1016/j.neuron.2005.08.026

Bromberg-Martin, E. S., Matsumoto, M., & Hikosaka, O. (2010). Dopamine in Motivational Control: Rewarding, Aversive, and Alerting. *Neuron*, *68*(5), 815–834. https://doi.org/10.1016/j.neuron.2010.11.022

Brown RE, Schnare OK Habib, E, & Kyle Roddick K. Development of a one-day test of olfactory learning and memory in mice. In: B. Schaal (editor) Chemical Signals in Vertebrates, 15. Springer Nature. In Press

Bu, M., Farrer, M. J., & Khoshbouei, H. (2021). Dynamic control of the dopamine transporter in neurotransmission and homeostasis. *Npj Parkinson's Disease*, *7*(1), Article 1. https://doi.org/10.1038/s41531-021-00161-2

Buck, L., & Axel, R. (1991). A novel multigene family may encode odorant receptors: A molecular basis for odor recognition. *Cell*, *65*(1), 175–187. https://doi.org/10.1016/0092-8674(91)90418-x

Byrne, D. J., Lipovsek, M., Crespo, A., & Grubb, M. S. (2022). Brief sensory deprivation triggers plasticity of dopamine-synthesising enzyme expression in genetically labelled olfactory bulb dopaminergic neurons. *European Journal of Neuroscience*, *56*(1), 3591–3612. https://doi.org/10.1111/ejn.15684

Cave, J. W., & Baker, H. (2009). Dopamine Systems in the Forebrain. In R. J. Pasterkamp, M. P. Smidt, & J. P. H. Burbach (Eds.), *Development and Engineering of Dopamine Neurons* (pp. 15–35). Springer. https://doi.org/10.1007/978-1-4419-0322-8_2

Chari, T., Griswold, S., Andrews, N. A., & Fagiolini, M. (2020). The Stage of the Estrus Cycle Is Critical for Interpretation of Female Mouse Social Interaction Behavior. *Frontiers in Behavioral Neuroscience*, *14*. https://doi.org/10.3389/fnbeh.2020.00113

Cheroni, C., Caporale, N., & Testa, G. (2020). Autism spectrum disorder at the crossroad between genes and environment: Contributions, convergences, and interactions in ASD developmental pathophysiology. *Molecular Autism*, *11*(1), 69. https://doi.org/10.1186/s13229-020-00370-1

Chien, Y.-L., Wu, C.-S., & Tsai, H.-J. (2021). The Comorbidity of Schizophrenia Spectrum and Mood Disorders in Autism Spectrum Disorder. *Autism Research*, *14*(3), 571–581. https://doi.org/10.1002/aur.2451

Ciliax, B. J., Drash, G. W., Staley, J. K., Haber, S., Mobley, C. J., Miller, G. W., Mufson, E. J., Mash, D. C., & Levey, A. I. (1999). Immunocytochemical localization of the dopamine transporter in human brain. *Journal of Comparative Neurology*, *409*(1), 38–56. https://doi.org/10.1002/(SICI)1096-9861(19990621)409:1<38::AID-CNE4>3.0.CO;2-1

Coronas, V., Srivastava, L. K., Liang, J. J., Jourdan, F., & Moyse, E. (1997). Identification and localization of dopamine receptor subtypes in rat olfactory mucosa and bulb: A combined in situ hybridization and ligand binding radioautographic approach. *Journal of Chemical Neuroanatomy*, *12*(4), 243–257. https://doi.org/10.1016/s0891-0618(97)00215-9

Dachtler, J., Ivorra, J. L., Rowland, T. E., Lever, C., Rodgers, R. J., & Clapcote, S. J. (2015). Heterozygous Deletion of α-Neurexin I or α-Neurexin II Results in Behaviors Relevant to Autism and Schizophrenia. *Behavioral Neuroscience*, *129*(6), 765–776. https://doi.org/10.1037/bne0000108

Dalley, J. W., Lääne, K., Theobald, D. E. H., Armstrong, H. C., Corlett, P. R., Chudasama, Y., & Robbins, T. W. (2005). Time-limited modulation of appetitive Pavlovian memory by D1 and NMDA receptors in the nucleus accumbens. *Proceedings of the National Academy of Sciences*, *102*(17), 6189–6194. https://doi.org/10.1073/pnas.0502080102

Dawson, G., Webb, S., Schellenberg, G. D., Dager, S., Friedman, S., Aylward, E., & Richards, T. (2002). Defining the broader phenotype of autism: Genetic, brain, and behavioral perspectives. *Development and Psychopathology*, *14*(3), 581–611. https://doi.org/10.1017/S0954579402003103

De Rubeis, S., He, X., Goldberg, A. P., Poultney, C. S., Samocha, K., Cicek, A. E., Kou, Y., Liu, L., Fromer, M., Walker, S., Singh, T., Klei, L., Kosmicki, J., Fu, S.-C., Aleksic, B., Biscaldi, M., Bolton, P. F., Brownfeld, J. M., Cai, J., … Buxbaum, J. D. (2014). Synaptic, transcriptional, and chromatin genes disrupted in autism. *Nature*, *515*(7526), 209–215. https://doi.org/10.1038/nature13772

Devlin, B., & Scherer, S. W. (2012). Genetic architecture in autism spectrum disorder. *Current Opinion in Genetics & Development*, *22*(3), 229–237. https://doi.org/10.1016/j.gde.2012.03.002

DiBenedictis, B. T., Olugbemi, A. O., Baum, M. J., & Cherry, J. A. (2015). DREADD-Induced Silencing of the Medial Olfactory Tubercle Disrupts the Preference of Female Mice for Opposite-Sex Chemosignals. *ENeuro*, *2*(5). https://doi.org/10.1523/ENEURO.0078-15.2015

Dichter, G. S., Damiano, C. A., & Allen, J. A. (2012). Reward circuitry dysfunction in psychiatric and neurodevelopmental disorders and genetic syndromes: Animal models and clinical findings. *Journal of Neurodevelopmental Disorders*, *4*(1), 19. https://doi.org/10.1186/1866-1955-4-19

Doty, R. L., & Risser, J. M. (1989). Influence of the D-2 dopamine receptor agonist quinpirole on the odor detection performance of rats before and after spiperone administration. *Psychopharmacology*, *98*(3), 310–315. https://doi.org/10.1007/BF00451680

Doty, R. L., Li, C., Bagla, R., Huang, W., Pfeiffer, C., Brosvic, G. M., & Risser, J. M. (1998). SKF 38393 enhances odor detection performance. *Psychopharmacology*, *136*(1), 75–82. https://doi.org/10.1007/s002130050541

Dubovyk, V., & Manahan-Vaughan, D. (2019). Gradient of Expression of Dopamine D2 Receptors Along the Dorso-Ventral Axis of the Hippocampus. *Frontiers in Synaptic Neuroscience*, *11*. https://doi.org/10.3389/fnsyn.2019.00028

Ducrot, C., Carvalho, G. de, Delignat-Lavaud, B., Delmas, C. V. L., Giguère, N., Mukherjee, S., Burke-Nanni, S., Bourque, M.-J., Parent, M., Chen, L. Y., & Trudeau, L.-É. (2021). *Neurexins Regulate GABA Co-release by Dopamine Neurons* (p. 2021.10.17.464666). bioRxiv. https://doi.org/10.1101/2021.10.17.464666

Dudanova, I., Tabuchi, K., Rohlmann, A., Südhof, T. C., & Missler, M. (2007). Deletion of α-neurexins does not cause a major impairment of axonal pathfinding or synapse formation. *Journal of Comparative Neurology*, *502*(2), 261–274. https://doi.org/10.1002/cne.21305

Durand, C. M., Betancur, C., Boeckers, T. M., Bockmann, J., Chaste, P., Fauchereau, F., Nygren, G., Rastam, M., Gillberg, I. C., Anckarsäter, H., Sponheim, E., Goubran-Botros, H., Delorme, R., Chabane, N., Mouren-Simeoni, M.-C., de Mas, P., Bieth, E., Rogé, B., Héron, D., … Bourgeron, T. (2007). Mutations in the gene encoding the synaptic scaffolding protein SHANK3 are associated with autism spectrum disorders. *Nature Genetics*, *39*(1), 25–27. https://doi.org/10.1038/ng1933

Ebrahimi-Fakhari, D., & Sahin, M. (2015). Autism and the synapse: Emerging mechanisms and mechanism-based therapies. *Current Opinion in Neurology*, *28*(2), 91–102. https://doi.org/10.1097/WCO.0000000000000186

Ennis, M., Zhou, F.-M., Ciombor, K. J., Aroniadou-Anderjaska, V., Hayar, A., Borrelli, E., Zimmer, L. A., Margolis, F., & Shipley, M. T. (2001). Dopamine D2 Receptor–Mediated Presynaptic Inhibition of Olfactory Nerve Terminals. *Journal of Neurophysiology*, *86*(6), 2986–2997. https://doi.org/10.1152/jn.2001.86.6.2986

Escanilla, O., Yuhas, C., Marzan, D., & Linster, C. (2009). Dopaminergic modulation of olfactory bulb processing affects odor discrimination learning in rats. *Behavioral Neuroscience*, *123*(4), 828–833. https://doi.org/10.1037/a0015855

Etherton, M. R., Blaiss, C. A., Powell, C. M., & Südhof, T. C. (2009). Mouse neurexin-1α deletion causes correlated electrophysiological and behavioral changes consistent with cognitive impairments. *Proceedings of the National Academy of Sciences of the United States of America*, *106*(42), 17998–18003. https://doi.org/10.1073/pnas.0910297106

Fine, L. G., & Riera, C. E. (2019). Sense of Smell as the Central Driver of Pavlovian Appetite Behavior in Mammals. *Frontiers in Physiology*, *10*, 1151. https://doi.org/10.3389/fphys.2019.01151

Fiorillo, C. D., Song, M. R., & Yun, S. R. (2013). Multiphasic Temporal Dynamics in Responses of Midbrain Dopamine Neurons to Appetitive and Aversive Stimuli. *The Journal of Neuroscience*, *33*(11), 4710–4725. https://doi.org/10.1523/JNEUROSCI.3883-12.2013

Fombonne, E. (2009). Epidemiology of Pervasive Developmental Disorders. *Pediatric Research*, *65*(6), Article 6. https://doi.org/10.1203/PDR.0b013e31819e7203

Friard, O., & Gamba, M. (2016). BORIS: a free, versatile open-source event-logging software for video/audio coding and live observations. *Methods in Ecology and Evolution*, *7*(11), 1325–1330. https://doi.org/10.1111/2041-210X.12584

Gao, R., & Penzes, P. (2015). Common Mechanisms of Excitatory and Inhibitory Imbalance in Schizophrenia and Autism Spectrum Disorders. *Current Molecular Medicine*, *15*(2), 146–167. https://doi.org/10.2174/1566524015666150303003028

Giros, B., Jaber, M., Jones, S. R., Wightman, R. M., & Caron, M. G. (1996). Hyperlocomotion and indifference to cocaine and amphetamine in mice lacking the dopamine transporter. *Nature*, *379*(6566), Article 6566. https://doi.org/10.1038/379606a0

Grayton, H. M., Missler, M., Collier, D. A., & Fernandes, C. (2013). Altered Social Behaviours in Neurexin 1α Knockout Mice Resemble Core Symptoms in Neurodevelopmental Disorders. *PLoS ONE*, *8*(6), e67114. https://doi.org/10.1371/journal.pone.0067114

Hall, H., Sedvall, G., Magnusson, O., Kopp, J., Halldin, C., & Farde, L. (1994). Distribution of D1- and D2-Dopamine Receptors, and Dopamine and Its Metabolites in the Human Brain. *Neuropsychopharmacology*, *11*(4), Article 4. https://doi.org/10.1038/sj.npp.1380111

Hardy, C., Rosedale, M., Messinger, J. W., Kleinhaus, K., Aujero, N., Silva, H., Goetz, R. R., Goetz, D., Harkavy-Friedman, J., & Malaspina, D. (2012). Olfactory acuity is associated with mood and function in a pilot study of stable bipolar disorder patients. *Bipolar Disorders*, *14*(1), 109–117. https://doi.org/10.1111/j.1399-5618.2012.00986.x

Hellemans, J., Mortier, G., De Paepe, A., Speleman, F., & Vandesompele, J. (2007). QBase relative quantification framework and software for management and automated analysis of real-time quantitative PCR data. *Genome Biology*, *8*(2), R19. https://doi.org/10.1186/gb-2007-8-2-r19

Hersch, S. M., Ciliax, B. J., Gutekunst, C. A., Rees, H. D., Heilman, C. J., Yung, K. K., Bolam, J. P., Ince, E., Yi, H., & Levey, A. I. (1995). Electron microscopic analysis of D1 and D2 dopamine receptor proteins in the dorsal striatum and their synaptic relationships with motor corticostriatal afferents. *Journal of Neuroscience*, *15*(7), 5222–5237. https://doi.org/10.1523/JNEUROSCI.15-07-05222.1995

Ikemoto, S. (2007). Dopamine reward circuitry: Two projection systems from the ventral midbrain to the nucleus accumbens–olfactory tubercle complex. *Brain Research Reviews*, *56*(1), 27–78. https://doi.org/10.1016/j.brainresrev.2007.05.004

Imamura, F., Ito, A., & LaFever, B. J. (2020). Subpopulations of Projection Neurons in the Olfactory Bulb. *Frontiers in Neural Circuits*, *14*. https://doi.org/10.3389/fncir.2020.561822

Jamain, S., Quach, H., Betancur, C., Råstam, M., Colineaux, C., Gillberg, I. C., Söderström, H., Giros, B., Leboyer, M., Gillberg, C., & Bourgeron, T. (2003). Mutations of the X-linked genes encoding neuroligins NLGN3 and NLGN4 are associated with autism. *Nature Genetics*, *34*(1), 27–29. https://doi.org/10.1038/ng1136

Jeste, S. S., & Geschwind, D. H. (2014). Disentangling the heterogeneity of autism spectrum disorder through genetic findings. *Nature Reviews. Neurology*, *10*(2), 74–81. https://doi.org/10.1038/nrneurol.2013.278

Jones, S. R., Gainetdinov, R. R., Jaber, M., Giros, B., Wightman, R. M., & Caron, M. G. (1998). Profound neuronal plasticity in response to inactivation of the dopamine transporter. *Proceedings of the National Academy of Sciences*, *95*(7), 4029–4034. https://doi.org/10.1073/pnas.95.7.4029

Kim, H.-G., Kishikawa, S., Higgins, A. W., Seong, I.-S., Donovan, D. J., Shen, Y., Lally, E., Weiss, L. A., Najm, J., Kutsche, K., Descartes, M., Holt, L., Braddock, S., Troxell, R., Kaplan, L., Volkmar, F., Klin, A., Tsatsanis, K., Harris, D. J., … Gusella, J. F. (2008). Disruption of Neurexin 1 Associated with Autism Spectrum Disorder. *American Journal of Human Genetics*, *82*(1), 199–207. https://doi.org/10.1016/j.ajhg.2007.09.011

Kim, K. S., Yoon, Y. R., Lee, H. J., Yoon, S., Kim, S.-Y., Shin, S. W., An, J. J., Kim, M.-S., Choi, S.-Y., Sun, W., & Baik, J.-H. (2010). Enhanced Hypothalamic Leptin Signaling in Mice Lacking Dopamine D2 Receptors. *Journal of Biological Chemistry*, *285*(12), 8905–8917. https://doi.org/10.1074/jbc.M109.079590

Klein, M. O., Battagello, D. S., Cardoso, A. R., Hauser, D. N., Bittencourt, J. C., & Correa, R. G. (2019). Dopamine: Functions, Signaling, and Association with Neurological Diseases. *Cellular and Molecular Neurobiology*, *39*(1), 31–59. https://doi.org/10.1007/s10571-018-0632-3

Komiya, M., Takeuchi, T., & Harada, E. (2006). Lemon oil vapor causes an anti-stress effect via modulating the 5-HT and DA activities in mice. *Behavioural Brain Research*, *172*(2), 240–249. https://doi.org/10.1016/j.bbr.2006.05.006

Koster, N. L., Norman, A. B., Richtand, N. M., Nickell, W. T., Puche, A. C., Pixley, S. K., & Shipley, M. T. (1999). Olfactory receptor neurons express D2 dopamine receptors. *The Journal of Comparative Neurology*, *411*(4), 666–673. https://doi.org/10.1002/(sici)1096-9861(19990906)411:4<666::aid-cne10>3.0.co;2-s

Kumazaki, H., Muramatsu, T., Fujisawa, T. X., Miyao, M., Matsuura, E., Okada, K., Kosaka, H., Tomoda, A., & Mimura, M. (2016). Assessment of olfactory detection thresholds in children with autism spectrum disorders using a pulse ejection system. *Molecular Autism*, *7*, 6. https://doi.org/10.1186/s13229-016-0071-2

Kwon, O. B., Paredes, D., Gonzalez, C. M., Neddens, J., Hernandez, L., Vullhorst, D., & Buonanno, A. (2008). Neuregulin-1 regulates LTP at CA1 hippocampal synapses through activation of dopamine D4 receptors. *Proceedings of the National Academy of Sciences*, *105*(40), 15587–15592. https://doi.org/10.1073/pnas.0805722105

Leekam, S. R., Nieto, C., Libby, S. J., Wing, L., & Gould, J. (2007). Describing the Sensory Abnormalities of Children and Adults with Autism. *Journal of Autism and Developmental Disorders*, *37*(5), 894–910. https://doi.org/10.1007/s10803-006-0218-7

Leo, D., Sukhanov, I., Zoratto, F., Illiano, P., Caffino, L., Sanna, F., Messa, G., Emanuele, M., Esposito, A., Dorofeikova, M., Budygin, E. A., Mus, L., Efimova, E. V., Niello, M., Espinoza, S., Sotnikova, T. D., Hoener, M. C., Laviola, G., Fumagalli, F., … Gainetdinov, R. R. (2018). Pronounced Hyperactivity, Cognitive Dysfunctions, and BDNF Dysregulation in Dopamine Transporter Knock-out Rats. *Journal of Neuroscience*, *38*(8), 1959–1972. https://doi.org/10.1523/JNEUROSCI.1931-17.2018

Livak, K. J., & Schmittgen, T. D. (2001). Analysis of Relative Gene Expression Data Using Real-Time Quantitative PCR and the 2−ΔΔCT Method. *Methods*, *25*(4), 402–408. https://doi.org/10.1006/meth.2001.1262

Lovick, T. A., & Zangrossi, H. (2021). Effect of Estrous Cycle on Behavior of Females in Rodent Tests of Anxiety. *Frontiers in Psychiatry*, *12*. https://doi.org/10.3389/fpsyt.2021.711065

Lowther, C., Speevak, M., Armour, C. M., Goh, E. S., Graham, G. E., Li, C., Zeesman, S., Nowaczyk, M. J. M., Schultz, L.-A., Morra, A., Nicolson, R., Bikangaga, P., Samdup, D., Zaazou, M., Boyd, K., Jung, J. H., Siu, V., Rajguru, M., Goobie, S., … Bassett, A. S. (2017). Molecular characterization of NRXN1 deletions from 19,263 clinical microarray cases identifies exons important for neurodevelopmental disease expression. *Genetics in Medicine : Official Journal of the American College of Medical Genetics*, *19*(1), 53–61. https://doi.org/10.1038/gim.2016.54

Lu, H. (2023). Modes of regulation for neurexin-1 function at hippocampal synapses [Unpublished doctoral dissertation]. University of British Columbia.

Lu, H., Zuo, L., Roddick, K. M., Zhang, P., Oku, S., Garden, J., Ge, Y., Bellefontaine, M., Delhaye, M., Brown, R. E., & Craig, A. M. (2023). Alternative splicing and heparan sulfation converge on neurexin-1 to control glutamatergic transmission and autism-related behaviors. *Cell Reports*, *42*(7), 112714. https://doi.org/10.1016/j.celrep.2023.112714

Luo, S. X., & Huang, E. J. (2016). Dopaminergic Neurons and Brain Reward Pathways. *The American Journal of Pathology*, *186*(3), 478–488. https://doi.org/10.1016/j.ajpath.2015.09.023

Luo, W., Zhang, C., Jiang, Y., & Brouwer, C. R. (2018). Systematic reconstruction of autism biology from massive genetic mutation profiles. *Science Advances*, *4*(4), e1701799. https://doi.org/10.1126/sciadv.1701799

Mandic-Maravic, V., Grujicic, R., Milutinovic, L., Munjiza-Jovanovic, A., & Pejovic-Milovancevic, M. (2022). Dopamine in Autism Spectrum Disorders—Focus on D2/D3 Partial Agonists and Their Possible Use in Treatment. *Frontiers in Psychiatry*, *12*, 787097. https://doi.org/10.3389/fpsyt.2021.787097

Mansour, A., Meador-Woodruff, J. H., Bunzow, J. R., Civelli, O., Akil, H., & Watson, S. J. (1990). Localization of dopamine D2 receptor mRNA and D1 and D2 receptor binding in the rat brain and pituitary: An in situ hybridization- receptor autoradiographic analysis. *Journal of Neuroscience*, *10*(8), 2587–2600. https://doi.org/10.1523/JNEUROSCI.10-08-02587.1990

Martin, C., Beshel, J., & Kay, L. M. (2007). An Olfacto-Hippocampal Network Is Dynamically Involved in Odor-Discrimination Learning. *Journal of Neurophysiology*, *98*(4), 2196–2205. https://doi.org/10.1152/jn.00524.2007

Martiros, N., Kapoor, V., Kim, S. E., & Murthy, V. N. (2022). Distinct representation of cue-outcome association by D1 and D2 neurons in the ventral striatum's olfactory tubercle. *ELife*, *11*, e75463. https://doi.org/10.7554/eLife.75463

Masoud, S., Vecchio, L., Bergeron, Y., Hossain, M., Nguyen, L., Bermejo, M., Kile, B., Sotnikova, T., Siesser, W., Gainetdinov, R., Wightman, R., Caron, M., Richardson, J., Miller, G., Ramsey, A., Cyr, M., & Salahpour, A. (2015). Increased expression of the dopamine transporter leads to loss of dopamine neurons, oxidative stress and L-DOPA reversible motor deficits. *Neurobiology of Disease*, *74*, 66–75. https://doi.org/10.1016/j.nbd.2014.10.016

Matson, J. L., & Shoemaker, M. (2009). Intellectual disability and its relationship to autism spectrum disorders. *Research in Developmental Disabilities*, *30*(6), 1107–1114. https://doi.org/10.1016/j.ridd.2009.06.003

Miles, J. H. (2011). Autism spectrum disorders—A genetics review. *Genetics in Medicine*, *13*(4), 278–294. https://doi.org/10.1097/GIM.0b013e3181ff67ba

Mishra, A., Singh, S., & Shukla, S. (2018). Physiological and Functional Basis of Dopamine Receptors and Their Role in Neurogenesis: Possible Implication for Parkinson's disease. *Journal of Experimental Neuroscience*, *12*, 1179069518779829. https://doi.org/10.1177/1179069518779829

Missale, C., Nash, S. R., Robinson, S. W., Jaber, M., & Caron, M. G. (1998). Dopamine Receptors: From Structure to Function. *Physiological Reviews*, *78*(1), 189–225. https://doi.org/10.1152/physrev.1998.78.1.189

Missler, M., Zhang, W., Rohlmann, A., Kattenstroth, G., Hammer, R. E., Gottmann, K., & Südhof, T. C. (2003). α-Neurexins couple Ca2+ channels to synaptic vesicle exocytosis. *Nature*, *423*(6943), Article 6943. https://doi.org/10.1038/nature01755

Moberg, P. J., & Turetsky, B. I. (2003). Scent of a disorder: Olfactory functioning in schizophrenia. *Current Psychiatry Reports*, *5*(4), 311–319. https://doi.org/10.1007/s11920-003-0061-x

Mombaerts, P. (2006). Axonal Wiring in the Mouse Olfactory System. *Annual Review of Cell and Developmental Biology*, *22*(1), 713–737. https://doi.org/10.1146/annurev.cellbio.21.012804.093915

Moore, R. Y., & Bloom, F. E. (1978). Central Catecholamine Neuron Systems: Anatomy and Physiology of the Dopamine Systems. *Annual Review of Neuroscience*, *1*(1), 129–169. https://doi.org/10.1146/annurev.ne.01.030178.001021

Mosharov, E. V., Larsen, K. E., Kanter, E., Phillips, K. A., Wilson, K., Schmitz, Y., Krantz, D. E., Kobayashi, K., Edwards, R. H., & Sulzer, D. (2009). Interplay between cytosolic dopamine, calcium, and alpha-synuclein causes selective death of substantia nigra neurons. *Neuron*, *62*(2), 218–229. https://doi.org/10.1016/j.neuron.2009.01.033

Mouly, A.-M., & Sullivan, R. (2010). Memory and Plasticity in the Olfactory System: From Infancy to Adulthood. In A. Menini (Ed.), *The Neurobiology of Olfaction*. CRC Press/Taylor & Francis. http://www.ncbi.nlm.nih.gov/books/NBK55967/

Moy, S. S., Nadler, J. J., Young, N. B., Perez, A., Holloway, L. P., Barbaro, R. P., Barbaro, J. R., West, L. M., Threadgill, D. W., Lauder, J. M., Magnuson, T. R., & Crawley, J. N. (2007). Mouse Behavioral Tasks Relevant to Autism: Phenotypes of Ten Inbred Strains. *Behavioural Brain Research*, *176*(1), 4–20. https://doi.org/10.1016/j.bbr.2006.07.030

Mpaka, D. M., Okitundu, D. L. E.-A., Ndjukendi, A. O., N'situ, A. M., Kinsala, S. Y., Mukau, J. E., Ngoma, V. M., Kashala-Abotnes, E., Ma-Miezi-Mampunza, S., Vogels, A., & Steyaert, J. (2016). Prevalence and comorbidities of autism among children referred to the outpatient clinics for neurodevelopmental disorders. *The Pan African Medical Journal*, *25*, 82. https://doi.org/10.11604/pamj.2016.25.82.4151

Murata, K., Kanno, M., Ieki, N., Mori, K., & Yamaguchi, M. (2015). Mapping of Learned Odor-Induced Motivated Behaviors in the Mouse Olfactory Tubercle. *Journal of Neuroscience*, *35*(29), 10581–10599. https://doi.org/10.1523/JNEUROSCI.0073-15.2015

Murofushi, W., Mori, K., Murata, K., & Yamaguchi, M. (2018). Functional development of olfactory tubercle domains during weaning period in mice. *Scientific Reports*, *8*(1), Article 1. https://doi.org/10.1038/s41598-018-31604-1

Neville, K. R., & Haberly, L. B. (2004). Olfactory Cortex. In G. M. Shepherd (Ed.), *The Synaptic Organization of the Brain*. Oxford University Press. https://doi.org/10.1093/acprof:oso/9780195159561.003.0010

Nigrosh, B. J., Slotnick, B. M., & Nevin, J. A. (1975). Olfactory discrimination, reversal learning, and stimulus control in rats. *Journal of Comparative and Physiological Psychology*, *89*(4), 285–294. https://doi.org/10.1037/h0076821

Nordenbæk, C., Jørgensen, M., Kyvik, K. O., & Bilenberg, N. (2014). A Danish population-based twin study on autism spectrum disorders. *European Child & Adolescent Psychiatry*, *23*(1), 35–43. https://doi.org/10.1007/s00787-013-0419-5

O'Leary, T. P., Stover, K. R., Mantolino, H. M., Darvesh, S., & Brown, R. E. (2020). Intact olfactory memory in the 5xFAD mouse model of Alzheimer's disease from 3 to 15 months of age. *Behavioural Brain Research*, *393*, 112731. https://doi.org/10.1016/j.bbr.2020.112731

Osinga, T. E., Links, T. P., Dullaart, R. P. F., Pacak, K., van der Horst-Schrivers, A. N. A., Kerstens, M. N., & Kema, I. P. (2017). Emerging role of dopamine in neovascularization of pheochromocytoma and paraganglioma. *The FASEB Journal*, *31*(6), 2226–2240. https://doi.org/10.1096/fj.201601131R

Pessiglione, M., Seymour, B., Flandin, G., Dolan, R. J., & Frith, C. D. (2006). Dopamine-dependent prediction errors underpin reward-seeking behaviour in humans. *Nature*, *442*(7106), 1042–1045. https://doi.org/10.1038/nature05051

Pfaffl, M. W. (2001). A new mathematical model for relative quantification in real-time RT–PCR. *Nucleic Acids Research*, *29*(9), e45. https://doi.org/10.1093/nar/29.9.e45

R Core Team (2023). R: A Language and Environment for Statistical Computing. R Foundation for Statistical Computing, Vienna, Austria. https://www.R-project.org

Radyushkin, K., Hammerschmidt, K., Boretius, S., Varoqueaux, F., El-Kordi, A., Ronnenberg, A., Winter, D., Frahm, J., Fischer, J., Brose, N., & Ehrenreich, H. (2009). Neuroligin-3-deficient mice: Model of a monogenic heritable form of autism with an olfactory deficit. *Genes, Brain and Behavior*, *8*(4), 416–425. https://doi.org/10.1111/j.1601-183X.2009.00487.x

Rahayel, S., Frasnelli, J., & Joubert, S. (2012). The effect of Alzheimer's disease and Parkinson's disease on olfaction: A meta-analysis. *Behavioural Brain Research*, *231*(1), 60–74. https://doi.org/10.1016/j.bbr.2012.02.047

Richmond, M. A., Yee, B. K., Pouzet, B., Veenman, L., Rawlins, J. N. P., Feldon, J., & Bannerman, D. M. (1999). Dissociating context and space within the hippocampus: Effects of complete, dorsal, and ventral excitotoxic hippocampal lesions on conditioned freezing and spatial learning. *Behavioral Neuroscience*, *113*(6), 1189–1203. https://doi.org/10.1037/0735-7044.113.6.1189

Rosenfeld, J. A., Ballif, B. C., Torchia, B. S., Sahoo, T., Ravnan, J. B., Schultz, R., Lamb, A., Bejjani, B. A., & Shaffer, L. G. (2010). Copy number variations associated with autism spectrum disorders contribute to a spectrum of neurodevelopmental disorders. *Genetics in Medicine: Official Journal of the American College of Medical Genetics*, *12*(11), 694–702. https://doi.org/10.1097/GIM.0b013e3181f0c5f3

Sandin, S., Lichtenstein, P., Kuja-Halkola, R., Hultman, C., Larsson, H., & Reichenberg, A. (2017). The Heritability of Autism Spectrum Disorder. *JAMA*, *318*(12), 1182–1184. https://doi.org/10.1001/jama.2017.12141

Sandin, S., Lichtenstein, P., Kuja-Halkola, R., Larsson, H., Hultman, C. M., & Reichenberg, A. (2014). The familial risk of autism. *JAMA*, *311*(17), 1770–1777. https://doi.org/10.1001/jama.2014.4144

Sarafoleanu, C., Mella, C., Georgescu, M., & Perederco, C. (2009). The importance of the olfactory sense in the human behavior and evolution. *Journal of Medicine and Life*, *2*(2), 196–198. https://www-ncbi-nlm-nih-gov.ezproxy.library.dal.ca/pmc/articles/PMC3018978/

Savchenko, A., Müller, C., Lubec, J., Leo, D., Korz, V., Afjehi-Sadat, L., Malikovic, J., Sialana, F. J., Lubec, G., & Sukhanov, I. (2022). The Lack of Dopamine Transporter Is Associated With Conditional Associative Learning Impairments and Striatal Proteomic Changes. *Frontiers in Psychiatry*, *13*. https://doi.org/10.3389/fpsyt.2022.799433

Schellinck, H. M., Forestell, C. A., & LoLordo, V. M. (2001). A Simple and Reliable Test of Olfactory Learning and Memory in Mice. *Chemical Senses*, *26*(6), 663–672. https://doi.org/10.1093/chemse/26.6.663

Schreiner, D., Nguyen, T.-M., Russo, G., Heber, S., Patrignani, A., Ahrné, E., & Scheiffele, P. (2014). Targeted combinatorial alternative splicing generates brain region-specific repertoires of neurexins. *Neuron*, *84*(2), 386–398. https://doi.org/10.1016/j.neuron.2014.09.011

Schultz, W. (2016). Dopamine reward prediction error coding. *Dialogues in Clinical Neuroscience*, *18*(1), 23–32. https://doi.org/10.31887/DCNS.2016.18.1/wschultz

Sesack, S. R., Aoki, C., & Pickel, V. M. (1994). Ultrastructural localization of D2 receptor-like immunoreactivity in midbrain dopamine neurons and their striatal targets. *Journal of Neuroscience*, *14*(1), 88–106. https://doi.org/10.1523/JNEUROSCI.14-01-00088.1994

Shipley, M. T., & Ennis, M. (1996). Functional organization of olfactory system. *Journal of Neurobiology*, *30*(1), 123–176. https://doi.org/10.1002/(SICI)1097-4695(199605)30:1<123::AID-NEU11>3.0.CO;2-N

Siddiqui, T. J., Pancaroglu, R., Kang, Y., Rooyakkers, A., & Craig, A. M. (2010). LRRTMs and Neuroligins Bind Neurexins with a Differential Code to Cooperate in Glutamate Synapse Development. *The Journal of Neuroscience*, *30*(22), 7495–7506. https://doi.org/10.1523/JNEUROSCI.0470-10.2010

Southwick, J. S., Bigler, E. D., Froehlich, A., DuBray, M. B., Alexander, A. L., Lange, N., & Lainhart, J. E. (2011). Memory Functioning in Children and Adolescents With Autism. *Neuropsychology*, *25*(6), 702–710. https://doi.org/10.1037/a0024935

Squillace, M., Dodero, L., Federici, M., Migliarini, S., Errico, F., Napolitano, F., Krashia, P., Di Maio, A., Galbusera, A., Bifone, A., Scattoni, M. L., Pasqualetti, M., Mercuri, N. B., Usiello, A., & Gozzi, A. (2014). Dysfunctional dopaminergic neurotransmission in asocial BTBR mice. *Translational Psychiatry*, *4*(8), Article 8. https://doi.org/10.1038/tp.2014.69

Sterky, F. H., Trotter, J. H., Lee, S.-J., Recktenwald, C. V., Du, X., Zhou, B., Zhou, P., Schwenk, J., Fakler, B., & Südhof, T. C. (2017). Carbonic anhydrase-related protein CA10 is an evolutionarily conserved pan-neurexin ligand. *Proceedings of the National Academy of Sciences of the United States of America*, *114*(7), E1253–E1262. https://doi.org/10.1073/pnas.1621321114

Südhof, T. C. (2017). Synaptic Neurexin Complexes: A Molecular Code for the Logic of Neural Circuits. *Cell*, *171*(4), 745–769. https://doi.org/10.1016/j.cell.2017.10.024

Sugita, S., Saito, F., Tang, J., Satz, J., Campbell, K., & Südhof, T. C. (2001). A stoichiometric complex of neurexins and dystroglycan in brain. *The Journal of Cell Biology*, *154*(2), 435–445. https://doi.org/10.1083/jcb.200105003

Sweatt, J. D. (2010). Chapter 4—Rodent Behavioral Learning and Memory Models. In J. D. Sweatt (Ed.), *Mechanisms of Memory (Second Edition)* (pp. 76–103). Academic Press. https://doi.org/10.1016/B978-0-12-374951-2.00004-4

Tabuchi, K., & Südhof, T. C. (2002). Structure and evolution of neurexin genes: Insight into the mechanism of alternative splicing. *Genomics*, *79*(6), 849–859. https://doi.org/10.1006/geno.2002.6780

Takahashi, L. K. (2014). Olfactory systems and neural circuits that modulate predator odor fear. *Frontiers in Behavioral Neuroscience*, *8*, 72. https://doi.org/10.3389/fnbeh.2014.00072

Tillerson, J. L., Caudle, W. M., Parent, J. M., Gong, C., Schallert, T., & Miller, G. W. (2006). Olfactory discrimination deficits in mice lacking the dopamine transporter or the D2 dopamine receptor. *Behavioural Brain Research*, *172*(1), 97–105. https://doi.org/10.1016/j.bbr.2006.04.025

Treloar, H. B., Feinstein, P., Mombaerts, P., & Greer, C. A. (2002). Specificity of glomerular targeting by olfactory sensory axons. *The Journal of Neuroscience: The Official Journal of the Society for Neuroscience*, *22*(7), 2469–2477. https://doi.org/10.1523/JNEUROSCI.22-07-02469.2002

Tromp, A., Mowry, B., & Giacomotto, J. (2021). Neurexins in autism and schizophrenia—A review of patient mutations, mouse models and potential future directions. *Molecular Psychiatry*, *26*(3), Article 3. https://doi.org/10.1038/s41380-020-00944-8

Trotter, J. H., Wang, C. Y., Zhou, P., Nakahara, G., & Südhof, T. C. (2023). A combinatorial code of neurexin-3 alternative splicing controls inhibitory synapses via a trans-synaptic dystroglycan signaling loop. *Nature Communications*, *14*(1), Article 1. https://doi.org/10.1038/s41467-023-36872-8

Ullrich, B., Ushkaryov, Y. A., & Südhof, T. C. (1995). Cartography of neurexins: More than 1000 isoforms generated by alternative splicing and expressed in distinct subsets of neurons. *Neuron*, *14*(3), 497–507. https://doi.org/10.1016/0896-6273(95)90306-2

Ungerstedt, U. (1971). Stereotaxic Mapping of the Monoamine Pathways in the Rat Brain*. *Acta Physiologica Scandinavica*, *82*(S367), 1–48. https://doi.org/10.1111/j.1365-201X.1971.tb10998.x

Ushkaryov, Y. A., Petrenko, A. G., Geppert, M., & Südhof, T. C. (1992). Neurexins: Synaptic Cell Surface Proteins Related to the α-Latrotoxin Receptor and Laminin. *Science*, *257*(5066), 50–56. https://doi.org/10.1126/science.1621094

Vanderwolf, C. H. (1992). Hippocampal activity, olfaction, and sniffing: An olfactory input to the dentate gyrus. *Brain Research*, *593*(2), 197–208. https://doi.org/10.1016/0006-8993(92)91308-2

Vandesompele, J., De Preter, K., Pattyn, F., Poppe, B., Van Roy, N., De Paepe, A., & Speleman, F. (2002). Accurate normalization of real-time quantitative RT-PCR data by geometric averaging of multiple internal control genes. *Genome Biology*, *3*(7), research0034.1-research0034.11. https://doi.org/10.1186/gb-2002-3-7-research0034

Wesson, D. W. (2013). Sniffing Behavior Communicates Social Hierarchy. *Current Biology*, *23*(7), 575–580. https://doi.org/10.1016/j.cub.2013.02.012

Wilson, D. A., & Sullivan, R. M. (1995). The D2 antagonist spiperone mimics the effects of olfactory deprivation on mitral/tufted cell odor response patterns. *Journal of Neuroscience*, *15*(8), 5574–5581. https://doi.org/10.1523/JNEUROSCI.15-08-05574.1995

Xu, M., Minagawa, Y., Kumazaki, H., Okada, K., & Naoi, N. (2020). Prefrontal Responses to Odors in Individuals With Autism Spectrum Disorders: Functional NIRS Measurement Combined With a Fragrance Pulse Ejection System. *Frontiers in Human Neuroscience*, *14*. https://doi.org/10.3389/fnhum.2020.523456

Yamaguchi, M. (2017). Functional Sub-Circuits of the Olfactory System Viewed from the Olfactory Bulb and the Olfactory Tubercle. *Frontiers in Neuroanatomy*, *11*. https://doi.org/10.3389/fnana.2017.00033

Yang, M., & Crawley, J. N. (2009). Simple behavioral assessment of mouse olfaction. *Current Protocols in Neuroscience*, Chapter 8, Unit–8.24. https://doi.org/10.1002/0471142301.ns0824s48

Yoon, T., & Otto, T. (2007). Differential contributions of dorsal vs. Ventral hippocampus to auditory trace fear conditioning. *Neurobiology of Learning and Memory*, *87*(4), 464–475. https://doi.org/10.1016/j.nlm.2006.12.006

Yung, K. K. L., Bolam, J. P., Smith, A. D., Hersch, S. M., Ciliax, B. J., & Levey, A. I. (1995). Immunocytochemical localization of D1 and D2 dopamine receptors in the basal ganglia of the rat: Light and electron microscopy. *Neuroscience*, *65*(3), 709–730. https://doi.org/10.1016/0306-4522(94)00536-E

Zhang, Z., Zhang, H., Wen, P., Zhu, X., Wang, L., Liu, Q., Wang, J., He, X., Wang, H., & Xu, F. (2017). Whole-Brain Mapping of the Inputs and Outputs of the Medial Part of the Olfactory Tubercle. *Frontiers in Neural Circuits*, *11*. https://doi.org/10.3389/fncir.2017.00052

APPENDIX A: SUPPLEMENTAL TABLES AND FIGURES

Supplemental Table 1. Shapiro-Wilk normality test statistics for all analyzed variables.

Variable	**Shapiro-Wilk normality test**
Training total digging duration	W(73) = 0.791, p <0.001
Training average digging duration	W(73) = 0.796, p < 0.001
Training digging latency	W(73) = 0.887, p < 0.001
Training sugar consumption	W(41) = 0.969, p = 0.2961
Memory test digging duration	W(73) = 0.5165, p < 0.001
Memory test digging latency	W(73) = 0.698, p < 0.001
Olfactory bulb DAT relative expression	W(63) = 0.962, p = 0.044
Olfactory bulb DRD1 relative expression	W(63) = 0.624, p < 0.001
Olfactory bulb DRD2 relative expression	W(63) = 0.876, p < 0.001
Olfactory tubercle DAT relative expression	W(58) = 0.736, p < 0.001
Olfactory tubercle DRD1 relative expression	W(62)= 0.905, p < 0.001
Olfactory tubercle DRD2 relative expression	W(62) = 0.947, p = 0.0079
Hippocampus DAT relative expression	W(53)= 0.766, p < 0.001
Hippocampus DRD1 relative expression	W(61) = 0.770, p < 0.001
Hippocampus DRD2 relative expression	W(60) = 0.920, p < 0.001

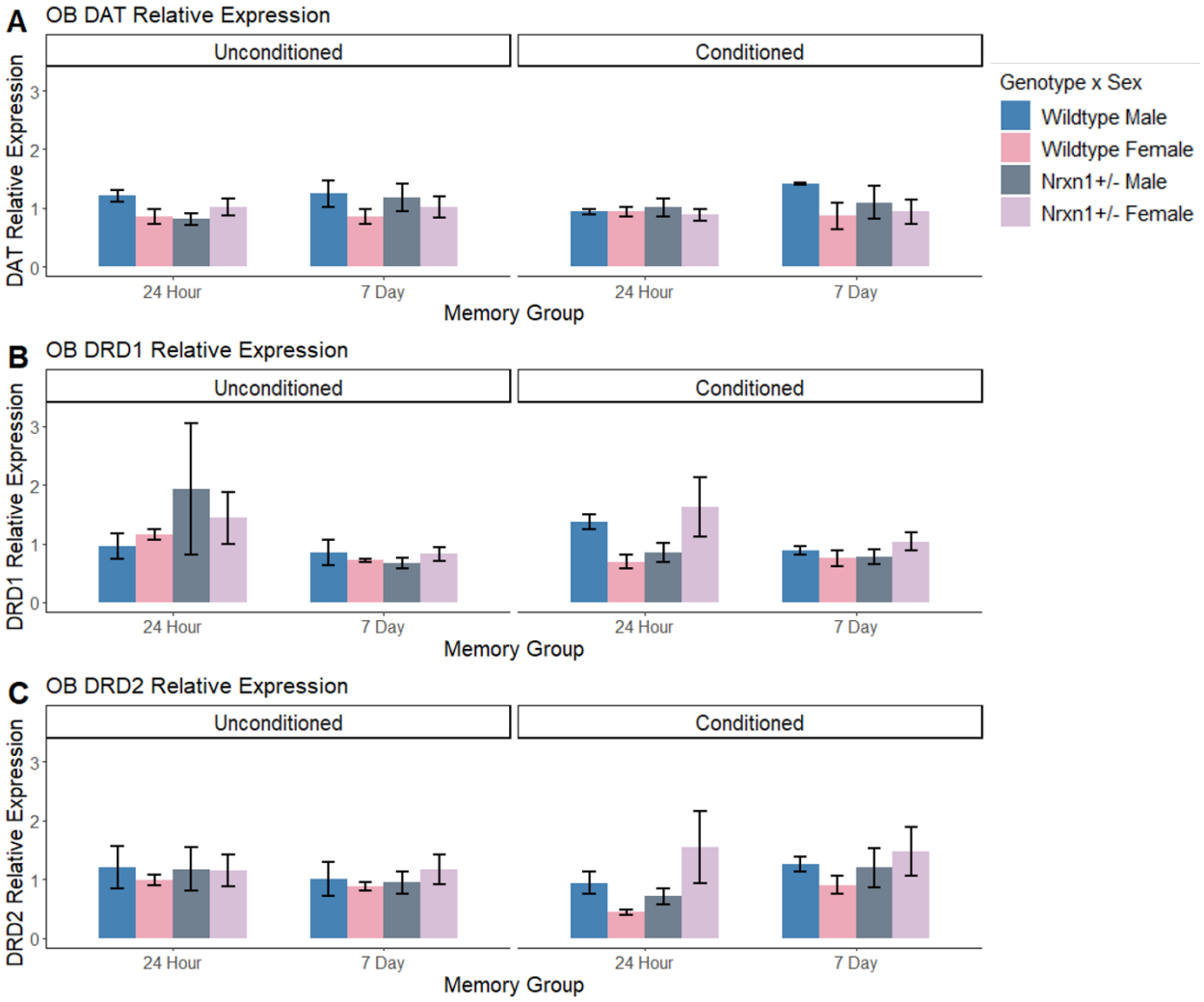

Supplemental Figure 1: Relative expression of target genes in the olfactory bulb of conditioned and unconditioned mice, in the 24-hour and 7-day memory test, divided by genotypes and sexes. **(A)** *DAT*, **(B)** *DRD1*, and **(C)** *DRD2*. None of these comparisons were significant (p >=0.13).

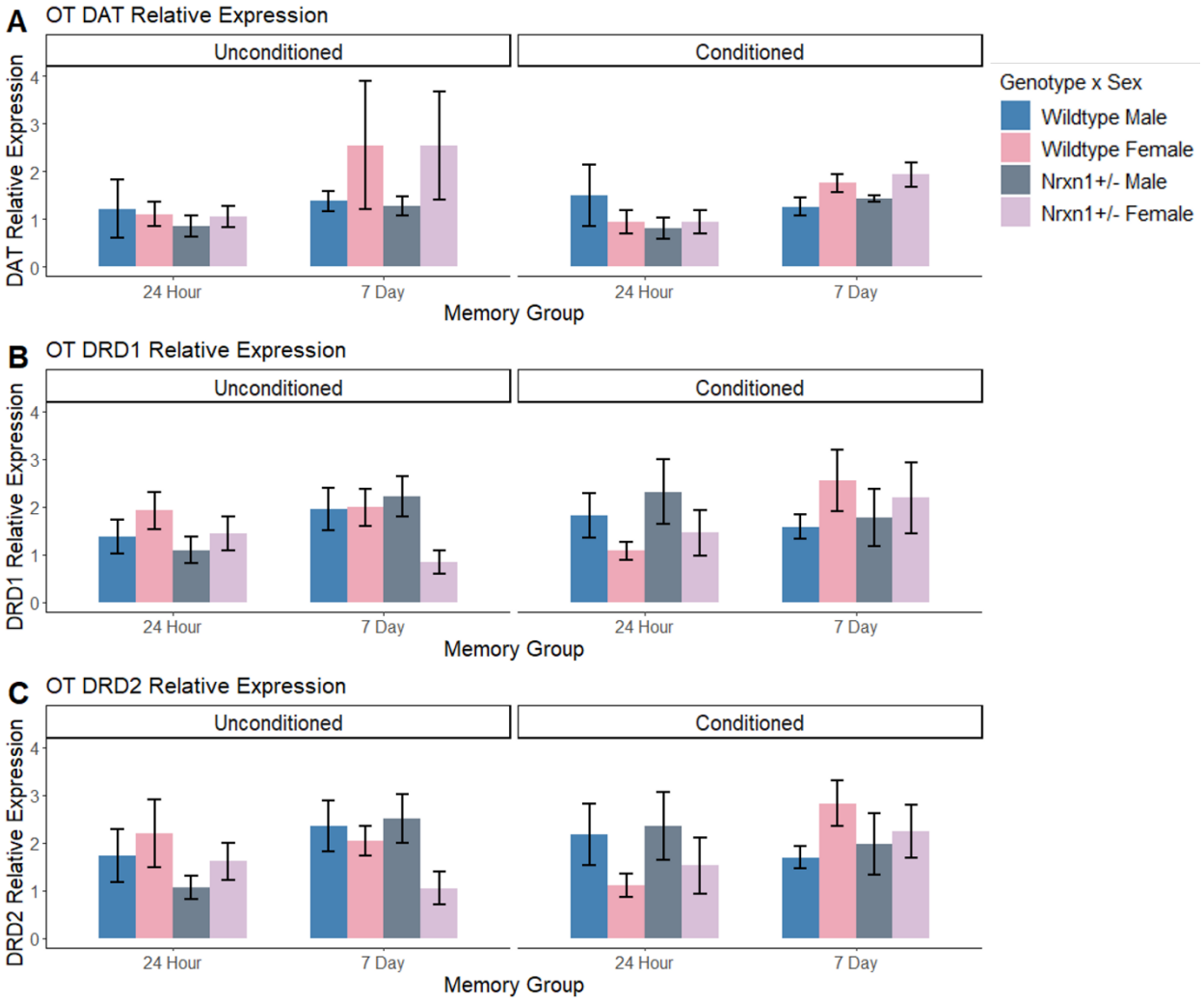

Supplemental Figure 2: Relative expression of target genes in the olfactory tubercle of conditioned and unconditioned mice, in the 24-hour and 7-day memory test, divided by genotypes and sexes. **(A)** *DAT*, **(B)** *DRD1*, and **(C)** *DRD2*. None of these comparisons were significant (p >=0.29).

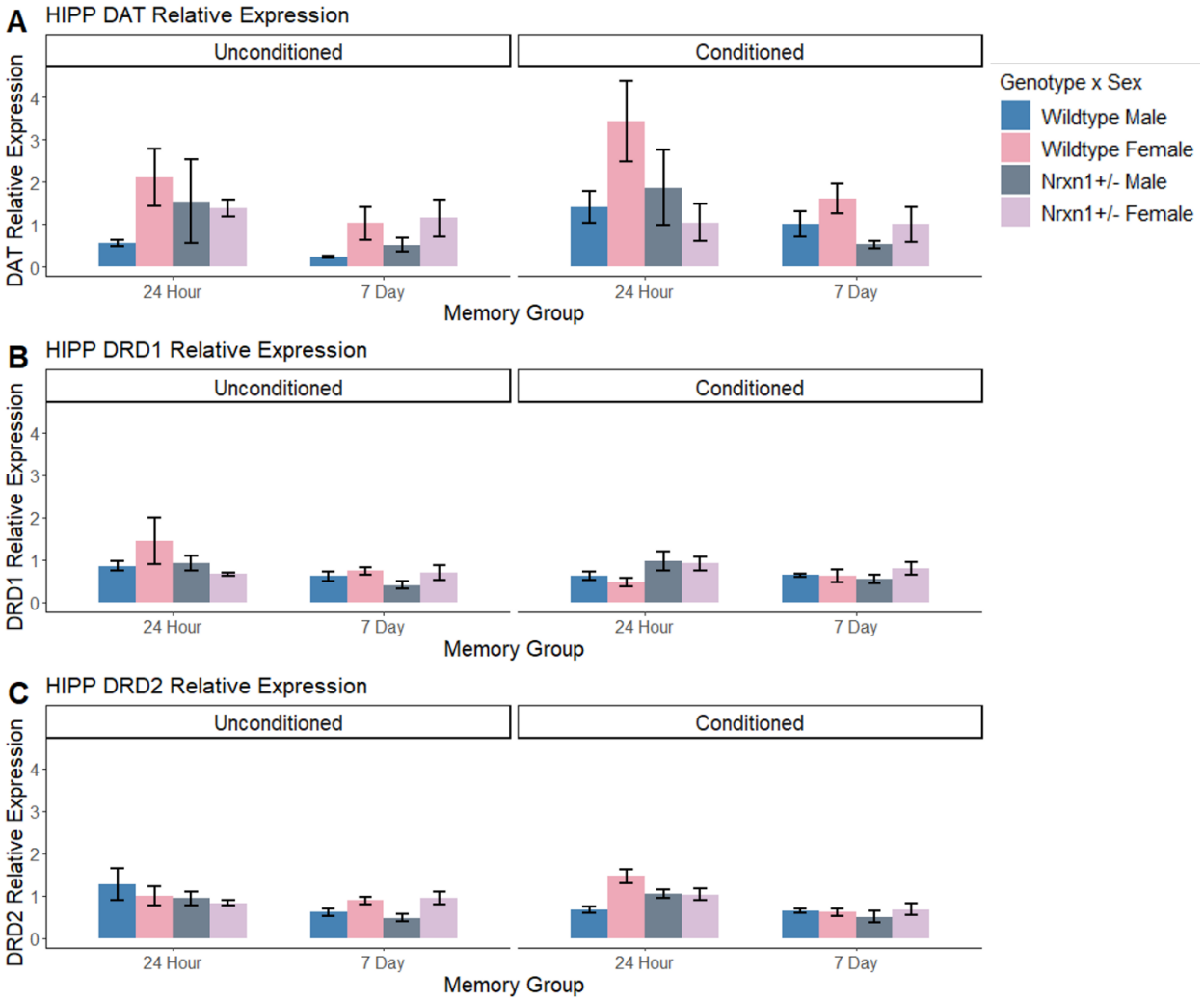

Supplemental Figure 3: Relative expression of target genes in the hippocampus of conditioned and unconditioned mice, in the 24-hour and 7-day memory test, divided by genotypes and sexes. **(A)** *DAT*, **(B)** *DRD1*, and **(C)** *DRD2*. None of these comparisons were significant (p >=0.093).